DEVELOPMENT OF HUMAN AND RAT PTC MONOLAYERS AS IN VITRO MODELS OF NEPHROTOXICITY

Ahmad Obaid

Thesis submitted for the degree of

Doctor of Philosophy

Institute for Cell and Molecular Biosciences

Newcastle University, UK

October 2019

Abstract

Nephrotoxicity is a serious side effect of many drugs due to the kidney being one of the major sites for their excretion. In vitro models of nephrotoxicity are therefore paramount in drug development process, which would be used to detect early stages of drug-induced toxicity. Most current proximal tubule models have their limitation, not only due to the lack of expression of some of the major drugs transporters, but also the lack of species-specific properties. This study investigates the use of human and rat primary proximal tubule cells as in vitro models of nephrotoxicity.

Human and rat proximal tubule cells (PTCs) were isolated and cultured from cortical tissues of the kidney. The cells form highly polarised monolayers that were exposed to polymyxin B, gentamicin and cisplatin – all well-known nephrotoxins. Cell viability and LDH-based cell death were measured, alongside the production of renal toxicity biomarkers, KIM-1, NGAL and clusterin.

As expected, cell viability of the monolayers after polymyxin B, gentamicin and cisplatin challenge deceased. The proportion of cells alive was dependent on the concentration and period of exposure of the nephrotoxin. For example, the cell viability of rat PTCs treated with gentamicin for 48h decreased by 41% than control cells ($P < 0.01$). Similarly, human PTCs treated with cisplatin showed a significant decrease (39%, $P < 0.01$) in cell viability when compared with non-treated cells. This relationship was also observed in LDH-based cell viability. Higher levels of KIM-1, NGAL and clusterin secretion were detected when human and rat PTCs were treated with nephrotoxins. All three biomarkers were predominately secreted across the apical membrane of the PTCs monolayers. For instance, KIM-1 level across the apical membrane was 5.25±1.01 ng/ml after polymyxin B treatment for just 24h, which was significantly higher than across the basolateral membrane at 0.81±0.31 ng/ml. The levels of biomarkers secretion were also found to be dependent on concentrations of nephrotoxin and period of exposure. For example, rat PTCs treated with 250 μg/ml polymyxin B for 24h produced 9.8±1.2 ng/ml of KIM-1, which increased to 25.8±2.5 ng/ml with 48h challenge, an increase of more than 2-fold ($P <0.01$).

The mechanisms of toxicity were also investigated by pre-treating the PTCs with supposedly nephron-protectant, rosuvastatin, cilastatin and cimetidine, prior to nephrotoxin exposure. While 50 μM rosuvastatin did not change the cell viability nor KIM-1 expression levels in human and rat PTCs, the pre-treatment of rosuvastatin with polymyxin B increased cell viability by 15 % when compared to polymyxin-B only treatment. Similarly rat PTCs treated with 250 μg/ml gentamicin and 40 μM cilastatin for 48h showed KIM-1 at levels of 28.8±0.27 ng/ml, compared with 28.7±0.5 ng/ml in cells treated with only gentamicin, giving a decrease of 29 % ($P < 0.001$). Another instance showed human PTCs treated with 250 μg/ml polymyxin B and 50 μM rosuvastatin for 24h produced clusterin at significantly lower level than cells treated with polymyxin B alone (42.3±12.2 ng/ml and 95.6±18.1 ng/ml, $P < 0.001$, respectively). These data suggest mechanisms of the aminoglycoside uptake could be via megalin/cubilin receptors, which were inhibited by rosuvastatin and cilastatin.

Another goal of this project was to investigate the influence of cisplatin treatment on p53, caspase 3, caspase 8 and caspase 9 in human and rat PTCs. These factors are important in the induction of apoptosis and would provide mechanistic data of nephrotoxicity. The activity and mRNA levels of the caspases in PTCs were increased after cisplatin treatment. For example, human PTCs treated with cisplatin, mRNA level of caspase 3 appeared to be increased significantly ($P< 0.01$) with the treatment of cisplatin (3.51±0.34%) compared to control. The co-treatment of cimetidine with cisplatin did decrease caspase 3 mRNA levels significantly to (2.45±0.32, $P< 0.05$) when compared only cisplatin treatment. These data revealed the mechanism of how cisplatin may cause nephtoxocitiy in these PTCs.

Taken together, these data show the utility of human and rat PTCs as in vitro models for the study of nephrotoxicity, and their potential in elucidating the mechanisms of action of polymyxin-B, gentamicin and cisplatin induced toxicity.

Acknowledgements

I would like to thank my PhD supervisors Dr Colin Brown and Dr Git Chung, for their help, ideas, excellent support, encouragement and guidance during my PhD.

Many thanks to the funding of this project, Umm Al-Qura University in Kingdom of Saudi Arabia. I am really grateful for their continuous help and support through my study.

Thanks are also due to the members of the Epithelial Research Group, who have contributed immensely to my personal and professional time at Newcastle University. The group has been a source of friendship as well as advice and collaboration.

A Special thanks to my parents and my brothers and sisters for all their sacrifices on behalf of me. Finally, I would like to thank my wife, Rehab Maghrabi, for her love, support and patience and thanks to my daughters Meral and Mayar for making my PhD journey full of love and beauty.

Table of Contents

List of Figures

List of Tables

1 Introduction

1.1 The kidney

The kidney is an organ that carries out several important functions, such as the clearance of metabolites and drugs. A pair is located towards the back of the abdomen of many mammals and the tissue can be divided into three regions; the cortex, the medulla, and the renal pelvis. The anatomy of a human kidney can be seen in Figure 1.1. The functional unit of the kidney is the nephron [1], each beginning with the glomerulus, which carries out the infiltration of the blood [2], and continues as tubule where reabsorption and active secretion occurs. The tubules of the nephron and their contents then open up to the bladder via the collecting duct, where waste product is stored temporally before expelled [3].

The importance of the kidney in drug clearance is illustrated in a study which identified that, out of a sample of 330 clinically relevant drug molecules, around 30 % undergo renal clearance [4]. With such high proportion of drugs cleared by the kidneys, and the increase in use of prescription drugs, it is not surprising that the incidence of chronic and acute kidney injury are spiking [5, 6].

The process of renal clearance is a result of three mechanisms: glomerular filtration, tubular secretion and tubular reabsorption. Filtration is the movement of fluid from blood into the lumen of the nephron. Reabsorption is the process of moving substances in the filtrate from lumen of the tubule back into the blood. Secretion removes selected molecules from the bold and adds them to the filtrate in the tubule lumen [7]. Secretion is a more selective process that usually uses membrane proteins to move molecules across the tubule epithelium. It is considered a two-step process consisting of uptake of the molecule across the basolateral membrane into the cell followed by exit across the apical membrane [8]. This uptake process is often mediated by the solute carrier (SLC) transporter superfamily, of which members include organic cation transporters (OCT) and organic cation transporters (OAT). The efflux of molecules across the apical membrane of proximal tubule cells is typically mediated by the ATP binding cassette (ABC) superfamily of transporters, such as breast cancer resistance protein (BCRP), multidrug resistance protein 1 (MDR1), and multidrug-resistance associated protein, although SLC transporters may also be involved.

These transporters undoubtedly play an important role in the clearance of drugs. However, they also contribute to the accumulation of the drugs in the proximal tubule, which can lead to nephrotoxicity [9, 10]. Indeed, approximately 20% of nephrotoxicity incident is induced by drugs, and some potent medicine such as those used in chemotherapy or cancer treatment medicine has been limited due to their nephrotoxic effects [11, 12].

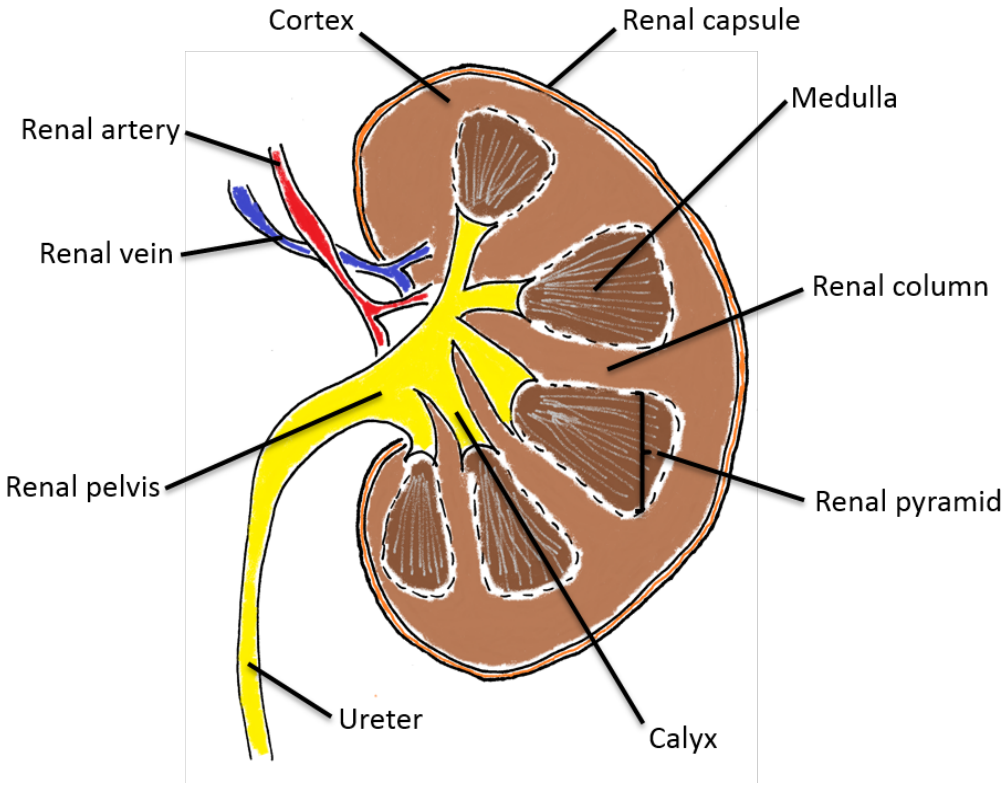

Figure 1.1: Anatomy of the human kidney.

On the surface of a bisected human kidney the cortex and medulla are distinct. The pyramids' apexes have little openings leading into the calyzes of the renal pelvis which drains the urine that is produced through the ureter into the bladder. For rat, only single renal pyramids are found in the medulla of their kidneys.

1.2 Drug transporters

The renal proximal tubule plays a vital role in the excretion of a wide range of xenobiotics and endogenous metabolites. Tubular secretion can be regarded as a two-stage process consisting of xenobiotic absorption across the basolateral membrane into the cell followed by exit across the apical membrane[13]. The uptake of molecules from circulation across the basolateral membranes of proximal tubular cells is often mediated by the members of the solute carrier (SLC) superfamily, whereas the efflux of molecules across proximal tubule cells apical membrane is typically mediated by both ABC and SLC transporters. A summary of most of the characterised transporters of human and rat PTCs are shown in Figure 1.2 and Figure 1.3.

1.2.1 MATE

Multidrug and MATE proteins are widely distributed across mammalian tissues[14]. Bacterial MATE transporters were well known as cationic / H^+ or Na^+ exchangers, but mammalian MATE proteins were only described in recent years [15]. There are two highly expressed MATE proteins found in the human kidneys–MATE1 and MATE2-K [14, 16]. MATE2-K is an isoform of MATE2 that is unique to the human kidney. Another MATE2 isoform is found in the brain exclusively and is referred to as MATE2-B[16] . In rat tissues, rat Mate1 is also abundantly expressed, but curiously not in the liver [17, 18]. There is also no Mate2 mRNA detected while rat Mate1 is found in the kidney[19]. Human MATE1, MATE2-K and rat Mate1 are located on the apical membrane of the proximal tubular cells [14, 18]and are therefore considered to be significant toxicity barriers. Human MATE1 and MATE2-K, and rat Mate1 are H+-coupled organic cation transporters found in the proximal tubular cell apical membrane. They can transport a variety of organic cations and share substrate close to OCT including TEA, MPP+, metformin, and cimetidine [20, 21]. These also bear certain organic anions, including estrone sulphate [22].

Affinities of MATE1 and MATE2-K for cationic substrates also vary from those of OCTs. For example, when metformin was introduced to MDCK cells transfected with OCT2 only, metformin accumulation was higher when compared with OCT2 and MATE1 doubly-transfected cells. However, metformin was not saturated in transfected cellsOCT2/MATE1 over a variety of concentrations, indicating efflux capacity by MATE1 [23]. Cimetidine was also shown to be a more active metformin transport receptor by MATE1 compared with OCT2 [24].

This drug interaction with cimetidine may result in metformin uptake in proximal tubular cells, since drug use by OCT2 inhibits MATE less efficiently than efflux throughout the apical membrane. Therefore, OCTs and MATE's in renal proximal tubules are believed to form organic cation transport systems.

1.2.2 MRP

The multidrug resistance-associated protein (MRP) family is another subgroup of the ABC family involved in substrate efflux in the proximal tubule. Members of this family include nine structurally-related (MRP1-9) proteins with a wide distribution [25]. Every member works as lipophilic anion efflux conveyor and is expressed either on the epithelial apical or basolateral membrane[26]. In the drug-resistant lung cancer cell line H69AR, MRP1 was first identified, suggesting that this carrier has a role in drug resistance in cancer cell. MRP1 was found in the basolateral membrane of the distal and collecting tubular cells in the mouse kidney but not in the proximal tubule cells [27]. Subsequently MRP2, MRP3, MRP4 and MRP5 were identified in several cancer cell lines and tissue samples, and many medicines including anticancer and antiviral agents have demonstrated as substrates of MRPs [28].

1.2.3 MDR1

Another member of the ABC superfamily is the multidrug resistance protein 1 (MDR1). It carries a wide variety of substrates including drug molecules and, like BCRP, MDR1 expression in the cells gives multidrug resistance[29]. In humans, one gene encodes MDR1[30, 31], whereas in rats there are two gene isoforms; Mdr1a and Mdr1b[32]. Human MDR1 can be found in different tissues, including the kidney in the apical surface of the proximal tubular cells [33]. Likewise, Mdr1a and b rats are widespread in all tissues.

1.2.4 OCT

Transport in a kidney of the OCT family's organic cations is an important way of removing blood from the urine. Like several OATs, rats Oct1 and Oct2 were initially identified and cloned from rat kidneys prior to the identification of human versions. Human OCT1 is mainly present in liver, while rat Oct1 is omnipresent in both liver and kidney and low in other tissues. In the human kidney, another member of the transport family (OCT3). The basolateral membrane of

the proximal tubules is located in all three transporters[34]. OCT3 is found in the kidney of humans and transport cations; but its role in nephrotoxicity is still unknown[35].

1.2.5 OAT

The main movement for organic anions (OAs) is happening the proximal tubule, which are extracted from the blood and passed into the urine[36]. OAs are secreted in at least two stages in PTCs, namely exogenous substrates (e.g. drugs) and endogenous substrates (e.g. urate)[37]. A well-known group of uptake transporter is that of the organic anion transport (OAT) family, which is focused on basolateral membranes in human proximal tube cells, including OAT1, OAT2 and OAT3[38].

1.2.6 Megalin/Cubilin

Megalin is a transmembrane protein of (600 kDa) from the family of low density lipoprotein receptors[39]. The extracellular domain of megalin consists of four clusters of repeats rich in cysteine, which are thought to be involved in ligand binding, and a variety of ligands have been identified. Megalin contains a single domain of transmembrane (23 amino acids), and the receptor has a cytoplasmic tail of 209 amino acids intracellular C-terminal. Megalin cytoplasmic domain regulates the trafficking of receptors and endocytosis [40]. Megalin is highly expressed on the apical membrane of PTCs.

In particular, it is located in the brush border, endocytic vesicles, dense apical tubules and in lysosomes to some extent[41]. Clinical markers for the endocytic function of megalin are glomerular-filtered low-molecular weight proteins, such as α1-microglobulin, β2-macroglobulin and liver-type fatty acid binding protein[42]. Megalin also mediates the absorption of nephrotoxic substances by PTCs, which lead to the development of chronic kidney disease and acute kidney injury[43].

Cubilin is a large extracellular 460 kDa glycosylated protein composed of 27 C-terminal CUB domains (C1r/C1s complement, and bone morphogenic protein 1), which is thought to be responsible for ligand binding[39].The cubilin N-terminal part consists of eight repeats of the epidermal growth factor and a stretch of 110 amino acids. Cubilin is an extracellular protein and interacts for membrane localization and endocytosis with other membrane proteins[44].

It is believed that the proximal tubule cubilin interacts with megalin and forms a multireceptor complex with the internalization of the complex and bound ligands by megalin driving.

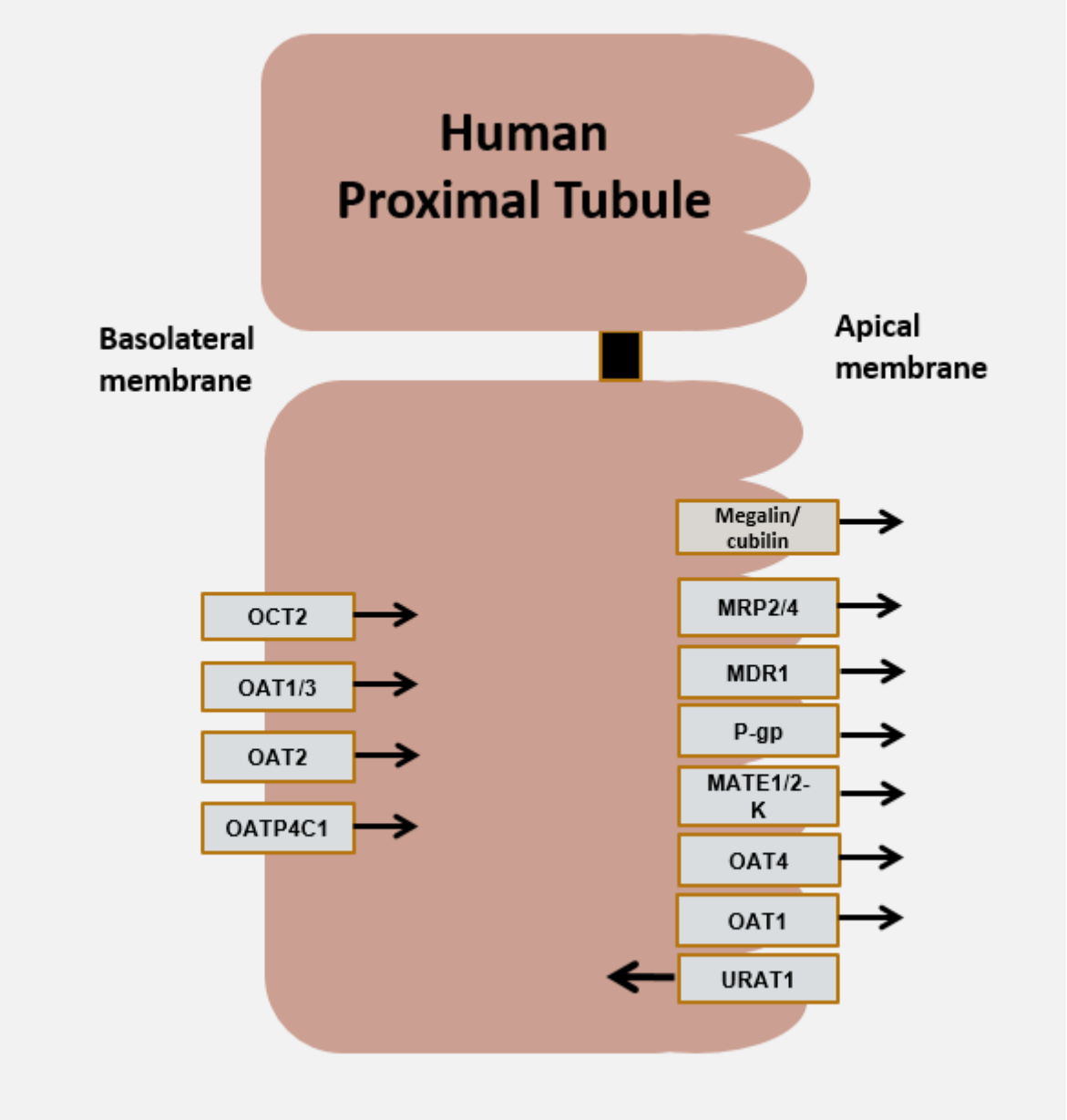

Figure 1.2: A summary of the uptake and efflux transporters expressed within human renal proximal tubule cells.

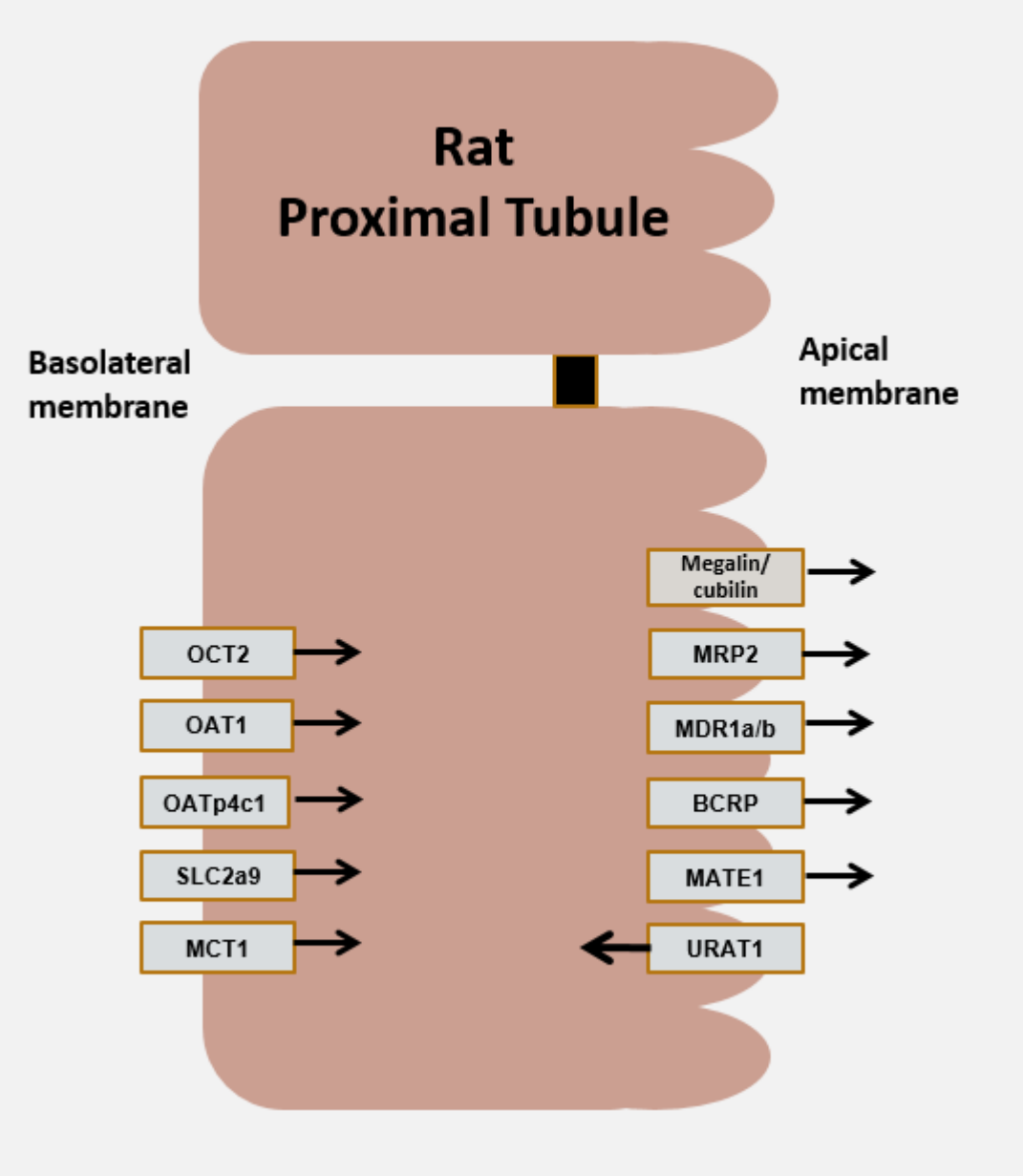

Figure 1.3: A summary of the uptake and efflux transporters expressed within rat renal proximal tubule cells.

1.3 Nephrotoxicity

Nephrotoxicity refers to the continuous accumulation of the toxin concentration inside the kidney, and as a result affects the normal functioning of the kidney renal[7]. While medications generate approximately 20% of nephrotoxicity, older medicine raises the incidence of nephrotoxicity to 66% as the average lifetime increases. It is therefore imperative noting that nephrotoxicity may take place as a result of various forms of drug intake as the excessive accumulation of drugs without creating an effective path for eliminating them may affect the normal functioning of the renal in one way or another. It is worth noting that nephrotoxicity is caused by substances known as the nephrotoxins[7]. The level of the nephrotoxicity advances or worsens with the stage of any form of kidney failure. General nephrotoxicity pathways include changes in glomerular hemodynamics, toxicity of tubular cells, inflammation, crystal nephropathy, rhabdomyolysis, and thrombotic microangiopathy [45]. In concentration and reabsorption by glomerulus, PTCs are exposed to drugs and are affected by drug Toxicity[46]. Drug include one of the major substances that may lead to the occurrence of the nephrotoxicity. For instance, heroine, as well as pamidronate are famous for leading to the glomerulosclerosis focal segmentation.

1.4 Kidney biomarkers

Due to the limitation of serum creatinine, it is important to develop and establish new biomarkers to detect early stages of kidney injuries. A biomarker is a characteristic that is measured and evaluated as an indicator of normal biological or pathogenic processes, or pharmacologic response. Biomarkers should show the relationship and differences between diseases state [10]. An example of a class of kidney injury biomarkers is the urinary enzymes. These enzymes are normally found in the tubular epithelial cells and released into urine during cellular stress, which may be an indication of nephrotoxicity. Thus, enzyme detection in the urine provides valuable information not only to the site of tubular injury (proximal or distal tubule) but also the severity of injury [45]. These enzymes include alanine aminopeptidase, alkaline phosphatase, α-glutathione-S-transferase, γ-glutamyl transpeptidase, π-glutathione-S-transferase, and N-acetyl-D-glucosaminidase [12]. Alongside the enzymes, high molecular weight protein also can be detected in urine, which is a sign of damaged glomerulus and can be construed as kidney injury [45].

1.4.1 KIM-1

Kidney injury molecule-1(KIM-1 also named TIM-1 and HAVCR-1) is a glycoprotein (104 kDa) cell membrane type I, which is highly preserved in rodents, dogs, primates and humans[47]. KIM-1 is also a receptor of phosphatidylserine found in renal epithelial cells, which recognizes apoptotic cells and enables phagocytosis to clear them[48]. In normal kidney tissue, KIM-1 is not detectable, but is inducible by ischemic and toxic insult[49]. KIM-1 expresses in high amounts in the apical membrane of surviving proximal tubule epithelial cells and is detectable in the urine[50]. KIM-1 mRNA is up-regulated during proximal tubular injury and the ectodomain of KIM-1 protein (90 kDa) is transferred from the membrane of the brush border into the urine[51]. Many studies have shown that patients with subclinical AKI show an increase in urinary KIM-1 levels depending on time. However, the clinical relevance of changes in subclinical AKI in KIM-1 is not entirely clear[48].

1.4.2 NGAL

The NGAL gene encodes a small protein (25 kDa) linked to gelatinase from human neutrophils and a lipocalin superfamily member with different immunological functions[52]. It is expressed in inflammatory responses, but it is also expressed in different tissue epithelial cells[53]. NGAL was significantly induced in the mice's kidneys in a transcriptomic study to identify ischemia-related genes[53]. Plasma NGAL was found to be an accurate marker of AKI in human patients undergoing cardiac surgery[54]. Usually, urinary NGAL is expressed in low concentrations, but renal tubular epithelial injury induces its expression[55]. Further work has shown that NGAL is up- regulated and enriched in proliferating mouse proximal tubule cells after ischemia[56]. Recently, the secretion of NGAL protein in the urine has gained interest in the use of AKI as a biomarker[55]. In patients already affected by chronic nephropathies, NGAL may eventually have prognostic value in predicting not only acute but also chronic deterioration in renal function[57].

1.4.3 Clusterin

Clusterin is also another glycoprotein that is useful in the assessment of nephrotoxicity. Clusterin was first isolated from rat testes fluid by Blaschuk, Burdzy, and Fritz in 1983. It is found in the proximal convoluted tubule, as well as towards the end of the distal convoluted tubule. As such, it can be used as an important biomarker as it can be detected in the patients'

urine, especially those suffering from acute injury of their kidneys. Clusterin had been measured using radioimmunoassay, and it's had been correlated with the increase of serum creatinine in a gentamicin-induced renal injury model in rats [58], although in another study clusterin mRNA and protein level did not rise until day 5 of treatment with cisplatin in some renal models [59].

1.4.4 Cystatin C

Cystatin C (Cys C) is one of the all nuclear cells within the cystine proteinase inhibitor family. Cystatin C was proposed as an alternative filtration marker to creatinine, a small non-glycosylated 13 kDa basic protein. All nuclear cells and proximal tubule cells secrete CysC and 98% of this protein is absorbed by renal tubules. Cys C has been reported as an early kidney injury marker. Cys C has no influence on muscle mass or diet and can thus better correlate than creatinine to GFR measured. It is believed that Cys C is less affected by age, sex and race than creatinine.

1.5 Nephrotoxins drugs

Nephrotoxic drugs are kidney-harming compounds that could cause renal damage. In this study 3 nephrotoxins drugs used (gentamicin, polymyxin B and cisplatin).

1.5.1 Cisplatin

Cisplatin, an effective chemotherapeutic drug, used in the treatment of many solid tumors, such as testicular, ovaries, esophageal, head and throat, and bladder tumors[60]. Because of its side effects, especially nephrotoxicity, it has limited use in medical practice[61]. About 25 % -40% of patients in clinical practice have renal dysfunction following cisplatin treatment[62].The mechanisms involved in cisplatin are still unclear, cellular damages, renal tubular cell apoptosis, vascular dysfunction, inflammatory response and oxidative damage may be causing them[60]. The first animal study report of nephrotoxicity in 1971 showed histopathological changes of acute necrosis and azotemia. In 14% to 100% of the cumulative doses, early clinical usage cisplatin saw dose-related acute renal failure in 14% to 100% of the patients[63]. Cisplatin clearance occurs primarily in the kidney through both glomerular and tubular filtration. Cisplatin concentration in the kidney exceeds its plasma concentration, indicating that the drug is accumulated in renal cells[64]. Two different transporters have been

identified in recent years, namely copper transporter 1 (Ctr1) and organic cation transporter 2 (OCT2), as responsible for the active transport of cisplatin to mammalian cells[65]. Downregulation of Ctr1 in kidney cells attenuates the accumulation and subsequent toxicity of the cisplatin which indicates that Ctr1 partially at least mediates the accumulation of the cisplatin to the kidney cells[66]. However, it has not been studied whether Ctr1 plays a role in cisplatin - induced nephrotoxicity in vivo. OCT2 is mainly located in renal proximal tubular cells, as opposed to the universal expression of Ctr1. Initially the transport of other OCT2 substrate into kidney cells was suppressed by cisplatin[67]. Some OCT2 gene mutations are associated with a reduced risk of nephrotoxicity caused by cisplatin in patients [68].

1.5.2 Polymyxin B

Polymyxin B were discovered 1950s from Paenibacillus polymyxa (Bacillus polymyxa), however their toxicity has restricted their use[69]. Polymyxin B was prescribed for life-threatening gram-negative bacterial infections on its own or in combination with other antimicrobials[70]. Polymyxin B is classified as an antibiotic cyclic lipopeptide and includes a decapeptide sequence containing a polycationic heptapeptide ring and a fatty acyl tail. Polymyxin B amphipathic chemistry for antibacterial activity is essential[71]. The nephrotoxic effects of polymyxin B include mechanisms that kill bacteria through lipid an interactions, disrupting the Ca2+ and Mg2 + bridges, which destabilize the molecules of lipopolysaccharide in the bacterial membrane[70]. The nephrotoxicity of polymyxin B therefore appears to be due to effects on the content of D-amino and fatty acid components that increase membrane permeability and cation influx[69]. Recent in vitro and in vivo studies showed at least three main pathways of apoptosis — mitochondrial, endoplasmic reticulum and death receptor— which play key roles in polymyxin B induced nephrotoxicity[72]. A study showed, 73 patients used polymyxin B, almost 60% developed acute renal injury (AKI). The acute tubular necrosis or tubular epithelial cell apoptosis has been characterized by polymyxin B nephrotoxicity[70]. In vitro, polymyxin B intake into proximal tubular epithelial cells was demonstrated to be saturable and showed a strong affinity to megalin, a low- density lipoprotein receptor, expressed on the proximal tubules apical membrane. Therefore, megalin is assumed to play an important role in the absorption of polymyxin B into renal tubular cells; the identification

of an effective antagonist off megalin will be a new direction in preventing polymyxin B nephrotoxicity [73].

1.5.3 Gentamicin

Gentamicin is a widely used and highly effective antibiotic of aminoglycosides[74]. It is usually used to treat patients with gram-negative bacterial infections[75]. Gentamicin effectively links to prokaryotic ribosomes and mistranslates the inhibition of protein synthesis leading to bacterial death[74]. The clinical use of gentamicin is limited because of it is serious complications such as nephrotoxicity and ototoxicity. Gentamicin nephrotoxicity clinical symptoms are renal tubular injury and glomerular filtration dysfunction[76]. Approximately 10-25% of patients with a single dose of gentamicin show signs of nephrotoxicity. Gentamicin causes tubular damage by necrosis of tubular epithelial cells, mainly in the proximal tubule, and changes in the function of the main cellular components involved in water transport and solutes[76]. Treatment of animals with gentamicin is associated with apoptosis and tubular epithelial cell necrosis. The increased accumulation of gentamicin in proximal tubules is associated with the expression of protein and cation (megalin and cubilin complex) transport molecules in apical membrane of the proximal tubules[75]. This complex is known to be responsible for the transportation of gentamicin by endocytosis[75]. The glomerular filtration actively eliminates gentamicin. Approximately 3 to 5% of the entered gentamicin is actively reabsorbed in proximal tubules and cause necrosis of the proximal tubules segmentS1-S2[77]. The accumulation of undigested phospholipids in lysosomes is closely linked to genetically modified nephrotoxicity. Gentamicin acts directly and indirectly on mitochondria in cytoplasm and activates the intrinsic apoptosis pathway, breaks the respiratory chain, reduces the synthesis of ATP and leads to oxidative stress by creating superoxide anion and hydroxyl radical, which leads to cell death. The indirect mitochondrial effect is mediated by increased levels of protein X (Bax) associated with Bcl-2 by inhibiting proteasomal degradation. In vitro studies have shown that the main aspect of gentamicin cytotoxicity is its cytoplasm concentration, not the accumulation of lysosomes as previously thought[75].

1.6 Limitation of current clinical methods to measure nephrotoxicity

Current clinical method to access renal function or nephrotoxicity is to measure the creatinine levels in the serum and/or urine. Creatinine is a waste product from the body that comes from

muscle activity. It is normally removed from blood by kidneys, but when kidney function decreases, the creatinine level in the blood increases. The Glomerular Filtrate Rate (GFR) is another important assessment method of the level of effectiveness of the kidney in filtering the blood [1]. The blood urea nitrogen (BUN) level is also deemed another important method for measuring the level of waste in the blood. Higher level of BUN is a clear indication of low level of functioning of the kidney while the reverse means the vice versa [78], as the kidney is expected to regulate the amount of nitrogen or urea in the blood.

Whilst serum creatinine level and BUN are established methods to measure renal function, they are limited in providing early signs of chronic kidney diseases. For instance, the level of creatinine production is corresponding to body weight, and it reduces with age and is slower in females than in males, meaning there is no physiologically normal level to be used as a baseline [79]. Kidney damage can be found with small rise or no change in serum creatinine because of the instability of the normal response to protein change; tubular secretion of creatinine rises after a protein meal healthy people, but not in patients with renal diseases [80]. Also, Tomlanovich et al. found heart transplant patients receiving cyclosporine (CsA), a known nephrotoxin had their creatinine level increased only after GFR has become depressed below normal values by two thirds or more [81].

1.7 Project aims

There is a pressing challenge for the pharmaceutical industry to develop less nephrotoxic drugs in recent years. However, assessment of nephrotoxicity remains difficult and usually detected late in the development pipeline due to lack of good pre-clinical models. Therefore, it is important to find a model that can be more physiologically relevant in terms of drug handling and nephrotoxicity. Most models of transporters in the kidney have been used are from human and animal cells. However, they have several limitations, one of which is that they lose the expression of many inherent renal transporters. For example, HK-2 proximal tubule cells do not express SLC22 transporters (e.g. OAT1, OAT3, and OCT2) at the mRNA level, which are ubiquitous in the proximal tubule. Similarly, ABCG1 (BCRP) is also not detected. This suggests HK-2 cells are limited in vitro model of drug transporter expression in the human proximal tubule [82]. In contrast, primary PTCs has been shown to be a good renal model for xenobiotic handling, due to the cells maintaining their full complement of endogenous renal transporters

at the protein levels (reference). The cells appear to be more physiologically relevant and better indicator of what happens in vivo. The renal PT is therefore could be an ideal in vitro model for nephrotoxicity tests.

With that in mind, the purpose of this study is to characterise and validate primary proximal tubule cells from human and rat kidney as in vitro models for drug safety and nephrotoxicity studies. Proximal tubule cells will be isolated from human and rat kidneys as outlined in Brown et al. (2008), and characterise the cells in the presence of various nephrotoxins. Firstly, to ensure the models retain their differentiated functions, the treated monolayers will be assessed at the mRNA and functional expression levels for important transporters of the ABC and SLC families. Secondly, the expression of several nephrotoxicity biomarkers (KIM-1, NGAL and clusterin), along with cell viability, will be measured in the models when they are exposed to the nephrotoxins to determine their use in predicting nephrotoxicity. In addition to the above mentioned, it is also necessary to highlight the differences in human and rat proximal tubular cells on renal drug handling, which could be useful in extrapolating inter-species data.

2 Materials and Methods

2.1 Materials

Cell culture reagents used in this project included high-glucose Dulbecco's modified eagles medium (HG-DMEM), Ham's F-12 nutrient mixture, Roswell Park Memorial Institute (RPMI)-1640 medium, foetal calf serum (FCS), penicillin, streptomycin, L-glutamine, trypsin with 0.02% ethylenediaminetetraacetic acid (EDTA), collagen, Dulbecco's phosphate-buffered saline (PBS) and mouse epidermal growth factor (EGF) purchased from Sigma-Aldrich (UK). Percoll was bought from GE Healthcare Life Sciences (UK), type 2 collagenase from Worthington Biochemicals (USA), and 10X Hanks' balanced salt solution (HBSS) from Invitrogen (USA). Renal epithelial cell growth medium (REGM) SingleQuot kit supplements and growth factors (containing insulin, hydrocortisone, gentamycin amphotericin-B (GA) - 1000, adrenaline, tri-iodothyronine (T3), transferrin, FCS and human EGF) were procured from Lonza (Switzerland).

Cells were grown on various cell culture vessels bought from Corning (UK). These included 24-well Transwell® permeable insert cell culture plates (with a surface area of 0.33 cm^2 per insert and polycarbonate filter pore size of 0.4 µm), plastic 96-well plates (0.33 cm^2 surface area), plastic 12-well plates (3.8 cm^2 surface area), T25 flasks (surface area 25 cm^2) and T75 flasks (surface area 75 cm^2).

Direct-zol RNA MiniPrep kit by Zymo Research Ltd, USA was used to isolate total cell RNA. Moloney murine leukaemia virus (M-MLV) reverse transcriptase, M-MLV 5x reaction buffer, RNasin, magnesium chloride, deoxyribonucleotide triphosphate (dNTP) mix, 5x Green GoTaq® reaction buffer, GoTaq polymerase, and pGem-T-easy cloning vector kit (consisting of T4 DNA ligase, pGem®-T vector, 2x ligation buffers) were procured from Promega (UK). Random hexamers were obtained from GE Healthcare Life Sciences, and MiniElute PCR purification kit from Qiagen. Agarose, EDTA, boric acid, ethidium bromide were bought from Sigma Aldrich, UK. Bespoke primers were ordered from IDT DNA (Belgium).

2.2 Isolation of proximal tubule cells

Human primary proximal tubule cells (PTCs) were isolated from healthy, transplant quality human kidneys with at least a glomerular filtration rate of 60 ml/min, supplied by a UK licensed Tissue Bank with full ethical approval for commercial use for drug development and safety

screening. Rat PTCs were isolated from kidneys of 8 to 12-week-old male Sprague-Dawley rats after they had been humanely euthanised. All cell culture work was performed in a class II vertical laminar flow hood to ensure sterility. All kidneys were first decapsulated before thin cortical slices were taken with a sharp scalpel. This process was repeated until the medulla was reached, and the cortical slices finely chopped to around 1 mm^3 pieces. 25 ml of isolation medium was used to suspend every 1 g of minced tissue. The composition of the isolation medium can be found in Table 1. Type 2 collagenase (activity of ≈300 units/mg, working concentration of 1 µg/ml) was added to the suspension to initiate the digestion of the tissue. The suspension was kept shaken for 2 hours at 37 °C before cell separation. To separate the cells, the suspension was passed through a 40 µm nylon sieve to remove undigested material and then centrifuged gently at 240 relative centrifugal force (RCF) for 10 minutes. In this and all subsequent centrifugation steps the temperature was maintained at 4 ˚C. The resulting cell pellet was resuspended in fresh isolation medium before the cells were pelleted again by centrifugation (this is considered the wash step). The cell pellet was then loosened and gently resuspended again in fresh isolation medium.

Supplements	Final concentration
RPMI-1640 Medium	-
FCS	5 %
Penicillin/Streptomycin	200 units/mL, 200 µg/mL respectively.

Table 1: Composition of isolation medium used in the isolation of human and rat PTC.

To isolate the proximal tubule cells, the cell suspension was loaded on top of discontinuous Percoll gradients with densities of 1.04 g/ml and 1.07 g/ml, and centrifuged at 1500 RCF for 25 minutes. After centrifugation, PTCs at the intersection of the gradients were aspirated and washed as previously described. The cells were resuspended in warm renal epithelial growth medium (REGM). The compositions of human and rat REGM are shown in Table. The cell yield was estimated using Cellometer Auto T4 Cell Counter (Nexcelom Bioscience LLC, USA) after

passing the cell suspension through a large bore needle three times to separate aggregated cells.

Isolated cells were seeded on to 24-well Transwell inserts (surface area of 0.33 cm2), at a density of 75,000 cells in 200 µl of REGM per insert, and the inserts submerged in 700 µl of REGM. PTCs were also seeded on to 24-well cell culture plates at 18,000 cells per well with 500 µl of REGM, 96-well cell culture plates at 7200 cells per well with 200 µl of REGM, and T25 cell culture flasks at a density of 1.875 million cells in 5 ml of REGM. The medium was refreshed after 24 hours of initial seeding, and thereafter every two days. PTCs were maintained in a humidified incubator at 37 ˚C with 5 % CO2 and 95 % air.

Monolayers were then used for experiment as and when they achieve confluency as determined by their TEER values. This usually was around 5-6 days after culture for rat, and 6-7 days for human. The monolayers used within these days did not show donor to donor variations in previous studies.

Ingredient	Amount
DMEM/Ham's F-12 (1:1)	500 mL
Supplements	
L-Glutamine	2.5 mL
Mouse EGF	0.5 mL
Insulin	0.5mL
Hydrocortisone	0.5 mL
GA	0.5 mL
FCS	2.5 mL
Adrenaline	0.5 mL
T3	0.5 mL
Transferrin	0.5 mL
Penicillin/Streptomycin	2.5 mL

Table 2: The composition of rat REGM.

2.3 Transepithelial electrical resistance (TEER)

Confluency of the cells was determined by visual inspection of the cell culture flask under a phase contrast microscope. Growing PTCs on uncoated Transwell plates improve the differentiated status with an expression of a variety of functional drugs transporters. A study showed improved protein expression and functionality of many drug transporters when primary human PTCs were grown on Transwell filter plates. The polycarbonate philtre is calculated to allow the cells to be polarised and bathed in a medium from the apical and basolateral sides, to replicate the physiology of the in vivo cells and thus to maintain their differentiated state. In our project, PTCs growth was monitored by microscopic examination and also TEERs value was measured as well. In other studies, to characterize PTCs, examination of alkaline phosphatase activity (the proximal tubule brush border enzyme) and AGT mRNA expression was used to proof of growing PTCs [83]. The transepithelial electrical resistance (TEER) was used as an indicator of monolayer confluency on the Transwell inserts. The monolayer resistance, which comprises the resistance of the filter and cell monolayer, was

measured using an electric voltohmmeter (EVOM, World Precision Instruments, UK). The TEER of the monolayers, with the unit of Ω.cm2, was calculated by subtracting the base resistance created by the filter submerged in culture medium (90 Ω) and then multiplying it by the surface area (0.33 cm^2) of the filter. Only monolayers with TEERs greater than 80 $\Omega.cm^2$ were used in experiments.

2.4 CellTiter 96® AQueous One Solution Cell Proliferation Assay (MTS)

We used cellTiter 96® AQueous One solution cell proliferation assay to quantify the live cells (Promega, Madison, WI, USA; #G3582). The MTS tetrazolium compound is reduced by cells to a coloured formazan product that is soluble in the tissue culture medium. This conversion is carried out by NADPH or NADH in metabolically active cells produced by dehydrogenase enzymes. Human and rat PTCs were treated with different nephrotoxins to quantify the cell viability. Confluent PTCs seeded onto 96-well plates were cultured with a concentration of the nephrotoxins in the REGM for a period of 24 or 48 hours. Spent media were collected and the cells were washed with warmed modified-Krebs buffer three times before equilibrated with 100 µl of modified-Krebs buffer for 30 minutes. The composition of the modified-Krebs buffer used is shown in Table 3. After equilibration of the cells to the buffer, 20 µl of MTS was added and the plates covered to prevent photo-bleaching of the compounds. The entire set-up was maintained at 37 °C by placing the plates on thermostat-controlled heated platforms. The change in colour of MTS was monitored spectrophotometrically by taking absorbance readings at 490 nm using a microplate reader (BMG Labtech, Germany).

Salt	Concentration (mM)
NaCl	140
KCl	5.4
MgSO4	1.2
NaH2PO4	0.3
KH2PO4	0.3
Glucose	5
CaCl2	2
HEPES	10
Tris Base	ad hoc to pH 7.4

Table 3: Composition of modified-Krebs buffer.

2.5 CellTiter-Glo® Luminescent Cell Viability Assay

Cell viability was measured using CellTiter-Glo Luminescent Cell Viability Kit (Promega, Madison, WI, USA; #G7570) by measurement of intracellular adenosine triphosphate (ATP), an indicator of metabolically active cells. Human and rat PTCs were treated with nephrotoxins for 24h and 48h. Cells were cultured in white 96-well plate to decrease luminescence loss. We added equal volume of CellTiter-Glo® Reagent to the volume of cell culture medium present in each well (50µl of reagent to 50µl of medium). Incubated for 10 min at room temperature. The luminescence signal were recorded using a microplate reader (BMG Labtech, Germany).

2.6 Lactate dehydrogenase (LDH) Cytotoxicity Assay

The amount of LDH released from human and rat PTCs after nephrotoxins treatment were quantify damaged cells as a biomarker for cellular cytotoxicity by using Pierce™ LDH Cytotoxicity Assay Kit (Thermo fisher,IL, USA;TG267605). Release of LDH in the cell culture medium, it reduces NAD+ to NADH and H+ through the oxidation of lactate to pyruvate. Later, the catalyst (diaphorase) then transfers H/H+ from NADH + H+ to the tetrazolium salt INT to form the red colored formazan salt. According to the kit protocol (absorbance at 450 nm, background absorbance at the reference wavelength of 600 nm). The average absorbance

values of the control and samples, each in 3 repeats, were calculated by subtraction of the background absorbance from the measured absorbance. The cytotoxicity (% of LDH release) was calculated as: (treated cells – mean of lysis control cells) × 100.

2.7 Enzyme-Linked Immunosorbent Assay (ELISA)

The amount of KIM-1 and NGAL produced by rat PTCs after nephrotoxins treatments were quantified. In addition, the amount of KIM-1, NGAL and clusterin were quantified after treated human PTCs with different nephrotoxins. The spent media collected from the above section were used in KIM-1, NGAL and clusterin ELISA kits sourced from R&D Systems, USA. The protocol for the assay was followed as recommended by the manufacturer. A 96 well plate was coated with a 1/100 solution of capture antibody. The plate was incubated overnight at room temperature (RT). The contents of the plate were discarded and wells were washed three times using 200µl wash buffer per well (0.05% Tween 20 in 1X phosphate buffer solution (PBS), pH 7.2-7.4). Then blocked with 1.0% bovine serum albumin (BSA) solution in 1X PBS for one hour at RT. The plate contents was aspirated and washed three, 100µl of standards diluted in 100µl of PBS or 100µl of cell culture media were added in duplicate. The plate was incubated for two hours at RT and the washing stage was repeated. 100µl of detection antibody was added to each well and the plate was incubated for two hours at RT. After another washing step was done, 100µl of streptavidin horseradish peroxidase (HRP) diluted in 1.0% BSA was added to each well and incubated for 20 minutes out of direct light at RT. A substrate solution (1:1 mixture of reagent A (H202) and reagent B (tetramethylbenzidine)) was added to each well (100µl) and the plate was incubated away from direct light for a further 20 minutes at RT. The addition of 50µl stop solution (2N H2 SO4) was required for each well for 20 minutes. The optical density (OD) of the contents was determined was taken using a microplate reader (BMG Labtech, Germany) set at 540 nm. The biomarkers levels were normalised to amount of live cells based on MTS data.

2.8 Caspase-Glo 3/7 assay.

The Caspase-Glo 3/7 assay reagent (Promega, Madison, WI) was used for caspase 3/7 measurement in treated human PTCs with different nephrotoxins. The kit provides a proluminescent caspase-3/7 substrate, which contains the tetrapeptide sequence DEVD, in

addition to a luciferase and a cell-lysing agent. The addition of the Caspase-Glo 3/7 reagent directly to the cells well results in cell lysis, followed by caspase cleavage of the DEVD substrate, and the generation of luminescence. The level of luminescence is proportional to the amount of caspase activity in the PTCs after nephrotoxins treatment and apoptotic renal cell death. Luminescence readings were recorded with a microplate reader (BMG Labtech, Germany).

2.9 Quantification of RNA

Key drug transporters were detected at the mRNA level in human and rat PTC monolayers by using endpoint PCR. In addition, the effects of cisplatin on caspas3, caspase8, caspase9 and p53in human and rat PTCs were assessed at the mRNA level by using qPCR. Nephrotoxins treated PTCs, were washed with PBS before lysed with TRI-reagent and cell total RNA extracted using column-based Direct-zol RNA MiniPrep kit by Zymo Research Ltd, USA. The manufacturer's protocol was followed to ensure maximum yield. RNA yield was quantified using NanoDrop (Thermofisher, UK), which also provided the A260/280 and A260/230 ratios. Only samples with ratios of 1.8-2.2 were used for downstream applications.

Prior to the start of endpoint PCR and qPCR, the RNA samples were reversed transcribed to cDNA. Briefly, this involved incubating 1 µg of cell total RNA with of 0.5 mg/ml random hexamers to a total volume of 13 µl at 65 for 5 minutes to ensure denaturing of RNA and annealing of primers. A reaction mixture of 12 µl comprising MMLT-RT at 200 units/µl, reaction buffer, 2 mM dNTPs and RNasin at 40 units/µl, were added to the RNA samples and incubated at 42 ˚C for 2 hours followed by 10 minutes at 90 ˚C for 3 minutes.

Endpoint PCRs were carried out for genes of interest using GoTaq DNA polymerase (Promega, UK). A typical endpoint PCR consisted of 0.25 µl GoTaq DNA polymerase at activity of 5 units/µl, 2 µl 2 mM dNTPs, 0.5 µM of each primer of the gene of interest, 4 µl of 5X Green GoTaq buffer, 1.5 µl of cDNA template and molecular grade water to make up to a volume of 20 µl. The amplification protocol was as follows: 95 ˚C for 2 minutes, 35 cycles of 95 ˚C for 30 seconds, Ta ˚C for 30 seconds and 72 ˚C degree for 30 seconds, then an end stage of 72 ˚C for 10 minutes. The PCR products were separated by size on a 1.5% agarose gel and visualized with safe view

and an UV-transilluminator and verified by sequence analyses. The sequences of the primers are listed in Table 4.

Gene	Accession Number	Sequences	Annealing Temperature	Amplicon Size (bp)
Human Megalin	NM_004525.2	F: ATT GAT GGC ACA GGA AGA GA R: GCT AGC CTC ATG ACA CTG AT	57	134
Human Cubilin	NM_001081.3	F:TGA AGG TGT GGG CAG GAA C R:GAG ACT GGA AGA CGG CAG TG	57	120
Human OCT2	NM_003058.3	F:ACC TGG TGA TCT ACA ATG GCT R:TGA GGA ACA GAT GTG GAC GC	58	145
Human OAT1	NM_004790.4	F:ACCAGTCCATTGTCCGAACC R:TGTCTGCCGGATCATTGTGG	56	116
Human MRP2	NM_000392.4	F: CAC CAT CAT GGA CAG TGACAA GG R: CCG CAC TCT ATA ATC TTC CCG	60	60
Human PGP1	NM_018850.2	F:TTCACTTCAGTTACCCTC R:GTCTGCCCACTCTGCACCTTC	58	76
Rat Megalin	NM_030827.1	F:CTACACAGTTTCGGTGCCCT R:CAGTTTAACACACAGCCCGC	57	109
Rat Cubilin	NM_053332.2	F:TGGAGATTCGAGACGGTCCT R:GTCCAGATCCGACTGTGTGG	57	179
Rat OCT2	NM_031584.2	F:ATC CCT GAT GAT CTA CAG TGG R:CAA GAT TCC TGA TGT ATG TGG	57	127
Rat OAT1	NM_017224.2	F:ATG CTG TGG TTT GCC ACT AGC R:AAC TTG GCA GGC AGG TCC AC	59	119
Rat Mdr1a/b	NM81855.1	F:GTC AAG GAA GCC AAT GCC R:AAG GAT CTT GGG GTT GCG GAC	59	147
Rat MRP2	NM_012833.2	F:GTT CTC GTC CTG GAA GAA GC R:TTC AGC AGC TGA GGA TTC AG	57	170

Table 4: Sequences of primers used in endpoint PCR for the amplification of human and rat PTCs drug transporters.

2.10 Quantitative PCR

The effects of cisplatin on caspas3, caspase8, caspase9 and p53in human and rat PTCs were assessed at the mRNA level by using qPCR. Diluted cDNA produced earlier was mixed with SYBR-green Master Mix, 10 µM primer mix of gene of interest and molecular grade water to a volume of 10 µl in a well of a 96-well format qPCR plate. PCR has run in a Roche LightCycler 480 (Roche, UK) with the following protocol: 95 ˚C for 10 minutes, 45 cycles of 95 ˚C for 10 seconds, Ta ˚C for 20 seconds and 72 ˚C for 10 seconds, followed by melt curve step (cooling to 65 ˚C followed by heating to 97 ˚C), and a cooling step. Ta represents the annealing temperature of the primers used in the reaction. The primers for the genes of interest were designed using the Primer-Blast tool on the National Centre for Biotechnology Information website (www.ncbi.nlm.nih.gov). Either forward or reverse primer is intron spanning. The primer sequences are summarised in Table 5.

The PCR cycle and its corresponding fluorescence from each sample were logged by the software LightCycler 480 (version 1.5, Roche, UK). The software calculated the fluorescence baseline during the first 15 cycles of the PCR to create a common starting fluorescence intensity for all the samples. A threshold level of fluorescence intensity was also defined by an algorithm where it was significantly above the background fluorescence but still within the linear phase of amplification. The cycle at which a sample produces fluorescence intensity that crosses the threshold is termed the threshold cycle (Ct), and is correlated to the starting concentration of the cDNA template; the greater the amount of starting cDNA, the earlier the Ct. As such, for the purpose of analysis, samples that produced Ct of 35 and above were disregarded.

Gene	Accession Number	Sequences	Annealing Temperature	Amplicon Size (bp)
Human caspase 3	NM_004346.3	F:ACTCCACAGCACCTGGTTAT R:TCTGTTGCCACCTTTCGGTT	58	148
Human caspase 8	NM_001080125.1	F:AAGGAGGAGATGGAAAGGGAAC R: AGAGCATGACCCTGTAGGCA	59	70
Human Caspase 9	NM_032996.3	F: CAAGAAAATGGTGCTGGCTT R: TCCATCTGTGCCGTAGACAG	58	139
Human P53	NM_001126118.1	F: CTGAGGTTGGCTCTGACTGTA R: AGCTGTTCCGTCCCAGTAGA	59	141
Rat Caspase 3	NM_012922.2	F: GAGCTGGACTGCGGTATTGA R: TAGTAACCGGGTGCGGTAGA	59	113
Rat caspase 8	NM_012922.2	F: TCTGTTTTGGATGAGGTGACCA R: CCCCGAGGTTTGCTCTTCAT	59	116
Rat caspase 9	NM_031632.1	F: AGATGGATGCTCTGTGTCCA R: AGTGAAGGCCACCTCAAAGC	58	145
Rat P53	NM_030989.3	F: GGGAGTGCAAAGAGAGCACTG R: CAGCTCTCGGAACATCTCGAA	60	129

Table 5: Sequences of primers used in qPCR for the amplification of human and rat PTCs caspase3, 8, 9 and p53.

2.11 Transport of Albumin–fluorescein isothiocyanate conjugate (FITC)-albumin

Human and rat PTCs cultured on 24-well Transwell filter support were used to investigate the functional expression of megalin and cubilin using FITC-albumin as the fluorescence substrate probe. Culture medium was first aspirated from the insert wells and washed three times with warm modified-Krebs buffer. The inserts were then placed in a clean 24-well plate and we added 200µl of modified-Krebs buffer to each insert well and 500µl of modified-Krebs were

added to each plate well from the original plate to equilibrate the cells for an hour. For the objective of this experiment, the insert wells are referred to as the apical membrane and the plate wells are referred to as the basolateral membrane. We used a thermostatically controlled heated platform to keep the temperature at 37 ˚C. Experiment was started when apical and basolateral solutions were replaced with 30µg/ml albumin in three wells, 30 µg/ml albumin and 250µg/ml polymyxin B in another three wells and 30 µg/ml albumin plus 50µM of rosuvastatin in three wells too, and incubated for two hours. After that, we washed the inserts and plate wells with cold modified- Krebs buffer. We added 0.01% SDS to lysis the cells in both side (apical and basolateral) and incubated for 30 min and transferred into a clean 96-well plate. The FITC- albumin was measured by using a microplate reader. The raw values are expressed as absorbance unit (AU).

2.12 Transepithelial flux of creatinine and PAH

The rate of movement of a substrate through a membrane can be measured, and is termed flux. When conducted under certain controlled environments, a flux experiment can be used to determine the mechanisms upon which the substrate moves across the membrane. In this study, the movement of creatinine and PAH from the extracellular environment through the apical or basolateral membranes of human and rat PTC monolayers into the cells and vice versa under a series of conditions over a period of time was conducted. This would allow the identification of the membrane transporters responsible for its movement.

The flux of creatinine and PAH in the apical-to-basolateral direction is referred to as the absorptive flux (J_{A-B}). The movement of creatinine in the opposite direction of basolateral-to-apical is referred to as the secretory flux (J_{B-A}). In addition to the fluxes, the movement of creatinine and PAH from the extracellular environment across either the apical membrane or basolateral membrane into the cells in a fixed period of time was also investigated, and referred to as the uptake of the substrate.

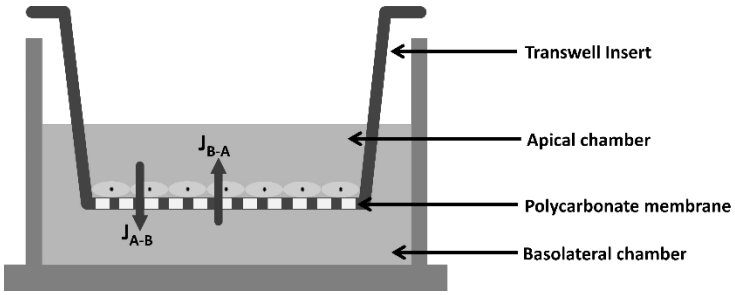

Figure 2.1: Schematics of transepithelial flux of creatinine and PAH by PTC monolayers.

J_{A-B} denotes the movement of a substrate in the absorptive direction of apical to basolateral, whereas J_{B-A} denotes the movement of a substrate in the secretory direction of basolateral to apical. In this instance, the brush-border membrane of the PTC monolayers faces the apical chamber, which is the equivalent of the tubule lumen in vivo, and the basolateral membrane faces the interstitial space/blood.

Culture media were first aspirated from the insert wells before sequential transfer of the inserts into three beakers of around 100 ml warm modified-Krebs buffer. The monolayers were then equilibrated with differential pH across the apical and basolateral membrane. The inserts were placed in a clean 24-well plate, each well containing 1000 µl warm modified-Krebs buffer of pH 7.4, and 200 µl of pH 6.8 was added to the insert's well. For the purpose of this study, the insert wells are referred to as the apical chamber and the plate wells are referred to as the basolateral chamber. The temperature of the whole set up was kept at 37 °C by placing the plates on a thermostat-controlled heated platform.

Prior to the initiation of flux of creatinine and PAH, monolayers were pre-incubated for at least 30 minutes with Krebs buffer containing a specified concentration of the TA or inhibitor in one or both chambers. This was to investigate potential drug-drug interactions of the TA or inhibitors with creatinine. Control monolayers were pre-incubated with Krebs buffer with no inhibitor. Master stocks of all TAs or inhibitors were reconstituted with DMSO. The amount of solvent incorporated into the final working solutions were not more than 0.5 %.

At the end of the pre-incubation period, flux was initiated when the Krebs buffer was aspirated from the apical or basolateral chambers and replaced with equal volume of 10 µM creatinine and PAH. This flux solution also contained the TA/inhibitor at the concentration used during

the pre-incubation step, and mannitol at the same concentration of creatinine. The presence of the inhibitor during creatinine flux ensured sustained interaction of the membrane transporters with the inhibitor. The addition of mannitol at the same time and solution with creatinine allowed the measurement of paracellular flux. The chambers with the flux solutions are referred to as the donor chamber. Radiolabelled creatinine (with ^{14}C isotope) was included in the flux solutions at activity of 0.5 µCi/ml to trace the movement of the substrate. Mannitol movement was traced with ^{3}H isotope at 0.1 µCi/ml.

Sampling of 50 µl from the contralateral chamber (referred to as the receiver chamber) at predetermined time points of 120 minutes after experiment initiation was carried out. After each sampling, equal amount of fresh Krebs with the appropriate pH and substrate was replaced. At the last sampling, the reaction terminated by sequentially transferring the inserts into four beakers of ice-cold Krebs buffer and left to dry. The samples from the receiver chambers were placed into scintillation vials. The filters of the inserts, on which the monolayers were adhered, were then excised out and also transferred to scintillation vials. The filter samples provided the amount of creatinine accumulated at over the 120 minutes flux period, which was indicative of the uptake of the substrates from across either the apical or basolateral membrane of the monolayers.

Radioactivity in all samples was determined by liquid scintillation spectrophotometry after 2 ml of Optiphase Hisafe 2 scintillation solvent (Perkin Elmer, UK) was added. Radioactivity in terms of disintegration per minute was detected using TriCarb 2910 liquid scintillation counter (Perkin Elmer, UK). The liquid scintillation counter was serviced annually, with the last service and calibration performed in August 2018 by Isocount ltd, UK. 5 µl of donor samples at flux initiation were also put through the scintillation counter to be used as the reference. Background activity was counted using a vial containing only 2 ml scintillation fluid and this value was automatically deducted from the counts.

The raw data provided by the liquid scintillation counter were expressed in disintegration per minute (DPM) and was able to distinguish between ^{14}C-labelled and ^{3}H-labelled substrates. To convert the counts to flux or paracellular flux of a substrate (i.e. amount of radiolabeled substrate moving from the donor to the receiving chamber), the following equation was used:

$$\text{Amount of substrate} = \frac{\mathbf{A}_{\text{STD}}}{\text{DPM}_{\text{STD}}} \times \mathbf{3} \times \text{DPM}_{\text{SPL}}$$

where A_{STD} represents the amount of substrate in 5 µl in the donor chamber, DPM_{STD} represents the DPM of the radiolabeled substrate in 5 µl of the dosing solution, and DPM_{SPL} represents the DPM of 50 µl from the receiver chamber. The constant 3 was used to express the result in cm^2 (surface area of a Transwell insert was 0.33 cm^2). All calculations were performed using Microsoft Excel for Office 365. The corrected flux of the substrate was determined by subtracting the mannitol paracellular flux from the calculated flux and expressed as nmol/cm^2/hr or pmol/cm^2/hr.

2.13 Data analysis

All data presented in the results are expressed as mean ± standard error of mean (SEM) of three technical replicates. One-way Analysis of Variance (ANOVA) statistical test was performed to compare significance of difference in data conditions. This test was used because we are comparing between different conditions within the same cells. GraphPad Prism 8.0 (GraphPad software Inc, USA) was used to perform the analysis.

3 Characterising renal proximal tubule cells model

3.1 Introduction

The absence of a decent model of the human proximal tubule has impaired the understanding of kidney drug handling in human. Current in vitro drug screens depend on immortalized renal epithelial cells, which poorly predict in vivo setting. Several studies on characterization of renal epithelial cells lines have also noted that these cells lack drug and metabolic enzyme expressions, fail to maintain microvilli at the brush border or cannot create confluent monolayers with tight junctions, although the cells can be transfected steadily to express missing transporters. The expression of the transporters in these cell lines however does not represent the physiological level of expression of the transporters as they are powered by the transmission machinery and vector promoters.

An alternative is to use primary proximal tubule cells. The protocol most frequently used to isolate fresh proximal tubule cell cultures involves the enzyme dispersion of tubular cells from the kidney cortex, followed by differential sieving (via Percoll gradients centrifugation), and fluorescent surface marker antibody labelling and cell sorting via FACS [8, 84]. Cells are also chosen using cultured growth medium that encourages interest cell growth compared to other cell types after isolation.

The acquisition of tissues from which the primary cells are isolated is a challenge. The supply of human kidney cortex is far a few in between, not least due to the short fall in organ donation and the lengthy waiting list for transplants. It is therefore vital that an effective isolation protocol is carried out to maximize the primary cell yield, when tissues are available. Rat kidneys are more accessible, on the other hand.

This chapter highlights the results from the characterisation of human and rat proximal tubule cells (PTCs). Freshly isolated PTCs are seeded on to Transwell inserts, which allow for the formation of monolayers. Transepithelial electrical resistance (TEER) measurement is used to assess the barrier function and properties of filter-grown PTCs. The expression of several key transporters is investigated using endpoint PCR. The functional expressions of several transporters are investigated by examining creatinine and PAH flux, and also the uptake of FITC-albumin.

3.2 Cell culture and morphology of rat PTCs

PTCs have been isolated from rat kidney cortex and seeded onto multiple platforms of cell culture. Figure 3.1 shows the cells cultured over a 5-day period on a T75 cell culture flask.

The morphology for freshly isolated PTCs of rat showed single cells not more than 40 µm in diameter, although depending on the isolation efficiency, clumps of cells (tubules) were still identifiable. Rat PTCs appeared to adhere within the first 24 hours of seeding, with visible lamellipodia at the cell edges. By day 3, (Figure 3.1C) defined regions of flattened cells in loose contact can be seen. Clusters of cuboidal forms or islets of rounded cells were seen at day 4 and 5 of culture (Figure 3.1D and E). The cells were seen proliferating and the typical morphology of an almost confluent monolayer could be observed.

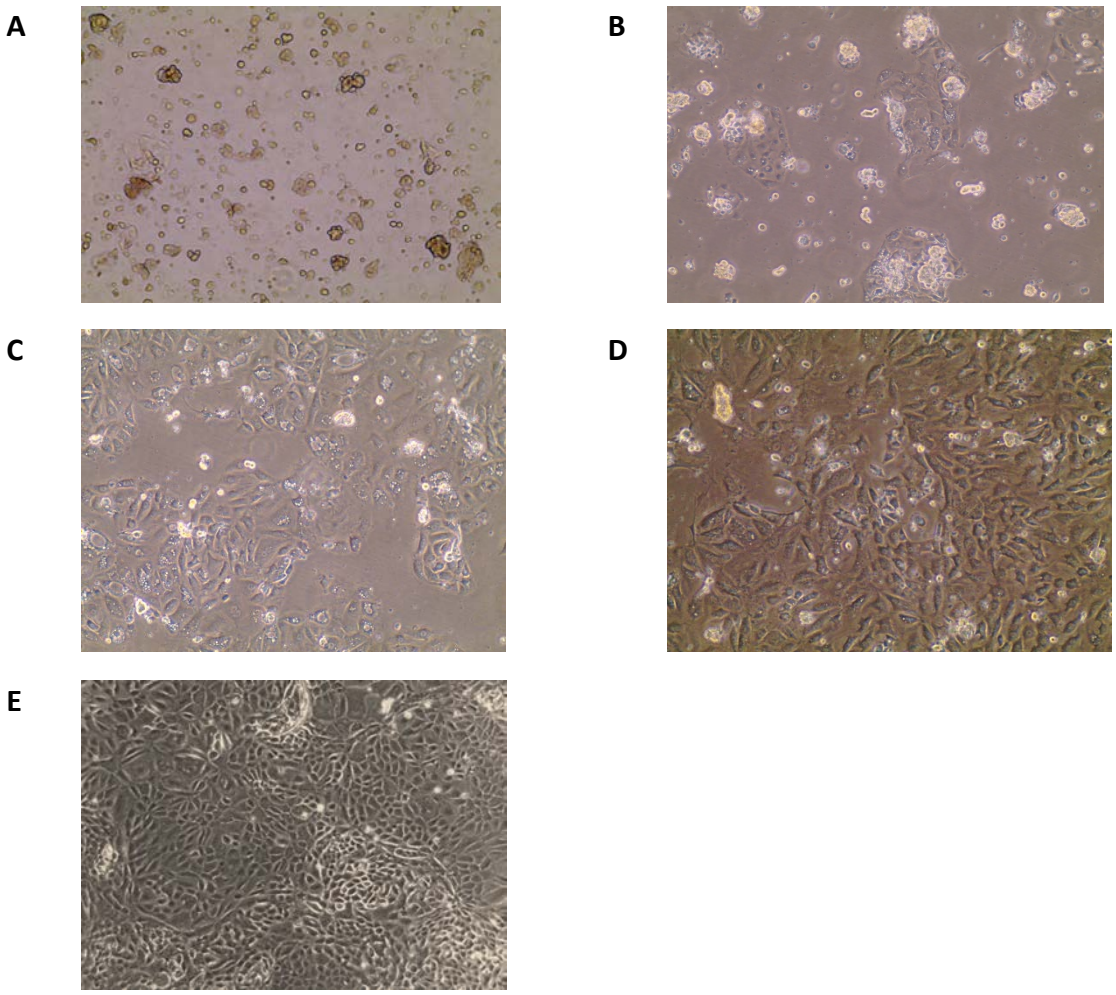

Figure 3.1: Phase contrast images of T75 cell culture flask seeded with rat PTCs over 5 days of culture.

Phase contrast images of rat PTCs seeded onto T75 cell culture flask with initial seeding density of 300,000 cells per ml on (A) day 1, (B) day 2, (C) day 3, (D) day 4, and (E) day 5 of culture. Cells appeared to adhere to the flask within the first 24 hours of seeding, and formed confluent monolayer by day 4/5. *Confluent monolayer of rat PTCs was observed at day 5 of culture. Images were taken with a phase contrast microscope at 200 X magnification. This is a representative of 12 experiments.*

3.3 Cell culture and morphology of human PTCs

PTCs were isolated from human kidney cortex and seeded onto multiple platforms of cell culture. Figure 3.2 shows the cells cultured over a 6-day period on a T75 cell culture flask.

Similar to the rat, the morphology for isolated human PTCs was primarily individual cells with a diameter of not more than 40 µm. Most cells can be recognized with lamellipodia at the edges of the cell within the first 24 hours. On day 4 to 6 of culture, clusters of cuboidal forms or islets of rounded cells were observed. The cells then spread, and it was possible to observe the typical morphology of an almost confluent monolayer.

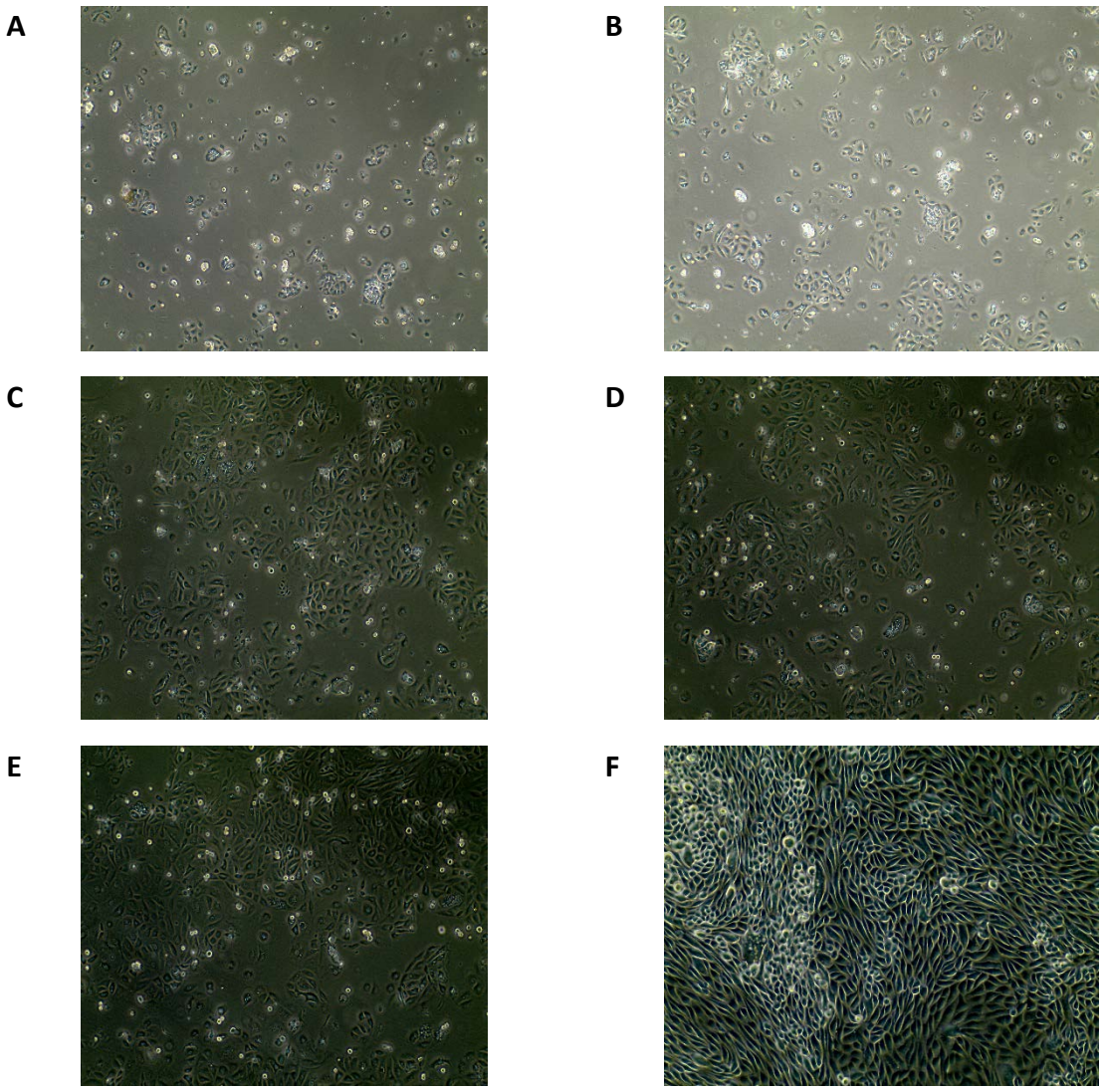

Figure 3.2: Phase contrast images of T75 cell culture flask seeded with human PTCs over 5 days of culture.

Phase contrast images of human PTCs seeded onto T75 cell culture flask with initial seeding density of 300,000 cells per ml on (A) day 1, (B) day 2, (C) day 3, (D) day 4, (E) day 5, and (F) day 6 of culture. Cells appeared to adhere to the flask within the first 24 hours of seeding, and formed confluent monolayer by day 6. Images were taken with a phase contrast microscope at 200 X magnification. This is a representative of 12 experiments.

3.4 Transepithelial electrical resistance of rat PTC monolayers

Isolated rat PTCs were also cultured on Transwell semi permeable filter inserts to recapitulate the formation of a monolayer with distinct apical and basolateral differentiation. The resistance of the monolayers were evaluated throughout the culture period, and the transepithelial electrical resistance calculated (the average basal resistance of the filter inserts was 90 Ω), which are summarised in Figure 3.3.

On day 1 of culture (data not shown) produced negligible TEER. An average TEER of 28.9 ± 7.4 $\Omega.cm^2$ was measured on day 2, however. The TEER rose to 72.7 ± 8.3 $\Omega.cm^2$ on day 3, 96.4 ± 17.3 on day 4 and peaked at 100.9 ± 14.5 $\Omega.cm^2$ on day 5. Thereafter, the TEER declined to 80.9 ± 11.1 on Day 6. The TEER reduced further to 40.8 ± 15.6 $\Omega.cm^2$ and 23.2 ± 5.7 $\Omega.cm^2$ on day 7 and 8, respectively.

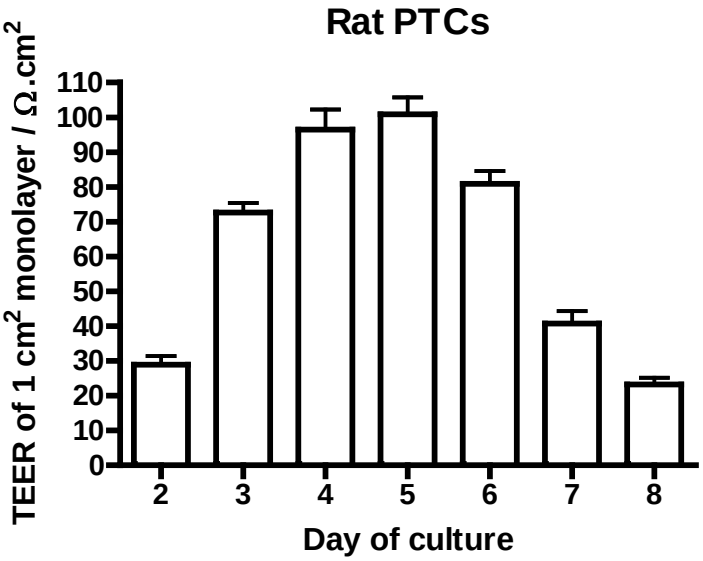

Figure 3.3: TEERs of rat PTC monolayer cultured on Transwell filter support.

The rat PTC monolayers TEER was negligible on day 1, and peaked to 100.8 ± 14.5 Ω.cm^2 on day 5. Thereafter, the TEER reduced to 23.2 ± 5.7 Ω.cm2 on day 8. Each bar represents the mean ± SEM of 9 replicates.

3.5 Transepithelial electrical resistance of human PTC monolayers

Human PTCs were also cultured on Transwell filter inserts to recapitulate monolayer formation. During the culture period, the resistances of the monolayers were measured and TEERs calculated. Figure 3.4 shows the TEERs of the human PTC monolayers over their culture period.

The resistance on day 1 of culture was negligible (the outcome not shown), but an average TEER of 42.1 ± 8.2 ± Ω.cm^2 was measured on day 2. The TEER increased to 73.6 ± 10.7 Ω.cm^2 on day 3, and 97.9 ± 11.5 Ω.cm^2 on day 4, and 126.3 ± 14.2 Ω.cm^2 on day 5. The TEER was 136.3 ± 16.7 on Day 6, with the highest TEERs observed at 139.8 ± 20.1 Ω.cm^2 and 137.7 ± 17.9 Ω.cm^2 on day 7 and 8, respectively. In contrast to the rat PTC monolayers, subsequent days of culture did not see a significant decrease in TEERs. For example, on day 9 and 10, the TEER was 139.55 ± 15.39 Ω.cm^2 and 123 ± 17.1 Ω.cm^2, respectively.

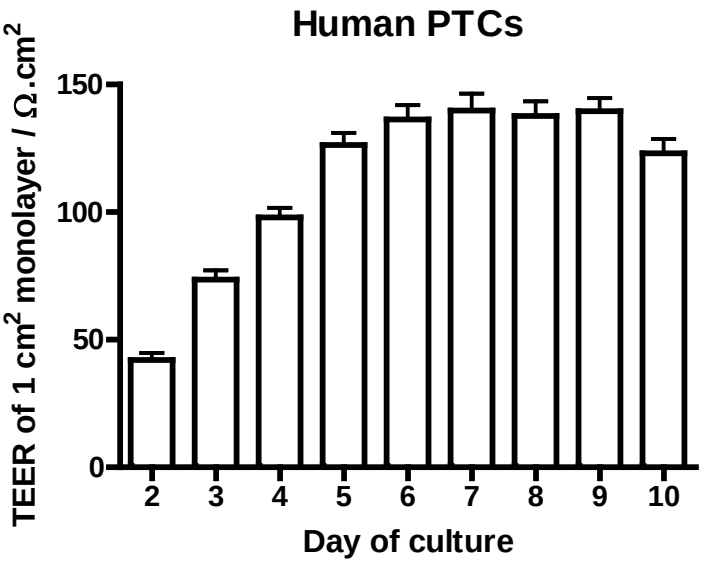

Figure 3.4: TEERs of human PTC monolayer cultured on Transwell filter support.

The resistance of the human PTC monolayers was negligible at day 1 of culture (result not shown). However, an average of 42.1 ± 8.2 ± Ω.cm2 was measured on day 2. The TEER increased to a high of 139.77 ± 20.14 Ω.cm2 on day 7, with no significant change in TEERs over the subsequent days. Each bar represents the mean ± SEM of 9 replicates.

3.6 mRNA expression of small and large molecule transporters in rat and human PTCs

Several key transporters expression at the mRNA level were investigated using endpoint PCR. Total cells RNA from freshly isolated rat and human PTCs were isolated and reverse transcribed before used in end-point PCRs. The PCR products were then visualised on 1.5 % agarose gels stained with ethidium bromide. A negative control was used no confirm there is no contamination in the master mix. Figure 3.5 shows the separation of PCR products on the gels, with clear bands in the lanes where megalin, cubilin, OCT2, OAT1 MRP2 and MDR1 primers were used. This signified the expression of these key transporters in the PTCs of rat and human. The amplicon size of all primers are found in Table 4.

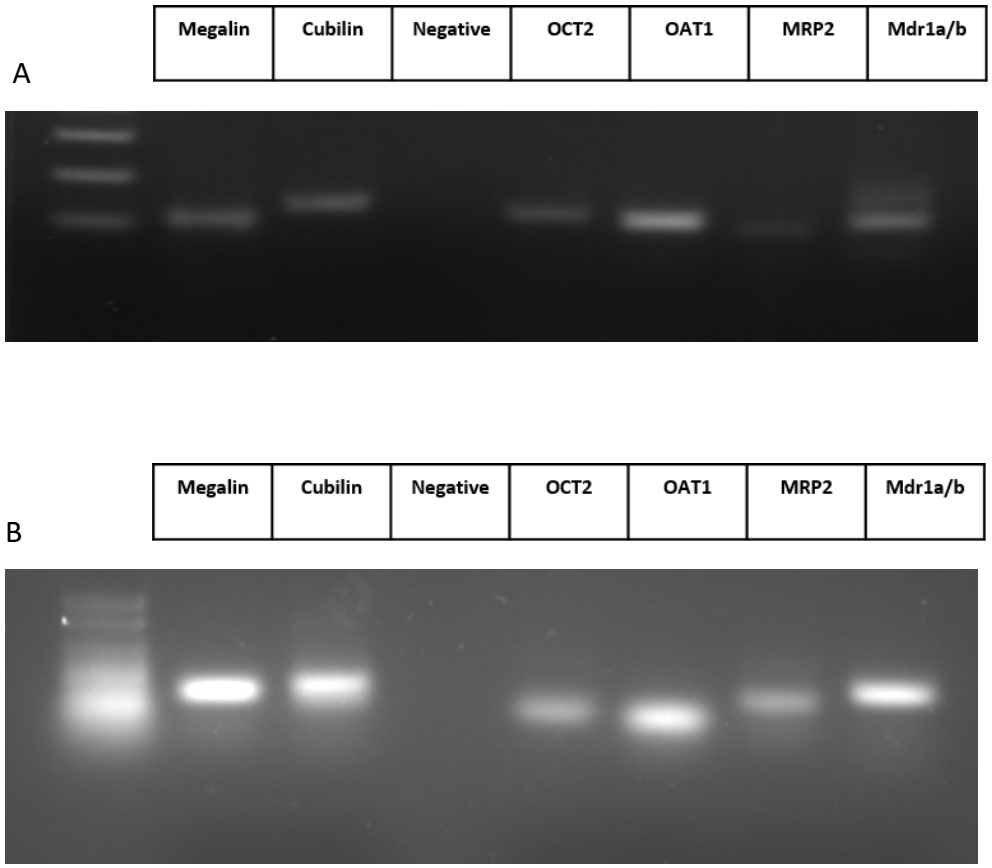

Figure 3.5: 1.5 % agarose gel showing separation of PCR products.

Clear bands in the agarose gel from (A) rat and (B) human PTC samples demonstrated the expression of megalin, cubilin, OCT2, OAT1, MRP2 and MDR1 in the PTCs.

3.7 FITC-albumin concentration range uptake by human and rat PTCs

The functional expressions of megalin and cubilin in rat and human PTCs were investigated using FITC-albumin as the fluorescence substrate probe. It will show the importance of these surface receptors in the PTCs as they provide the mechanism of movement of larger molecules in the kidney. Rat and human PTC monolayers were incubated with a range of concentrations of FITC-albumin (10, 30, 60 and 90 μg/ml) for a period of 1, 2, 4 or 5 hours. Figure 3.6 shows the uptake of FITC-albumin over this time period. The uptake of FITC-albumin had been normalised to the amount of protein (relative number of cells).

The cells waited to be confluence and incubated with albumin and polymyxin B at the same time. For rat the experiment started at day 5 and human at day 7. Both rat and human PTC monolayers showed a concentration dependent uptake of FITC-albumin – uptake of FITC-albumin increased in greater dosing concentration of FITC-albumin. For examples, rat PTC monolayers saw an uptake of 73,662.1 ± 7,597.1 AU with 10 μg/ml dosing concentration of albumin but increased to 128,890.7 ± 17,532.7 AU with 60 μg/ml dosing concentration the 2-hour time point.

Interestingly, both rat and human PTC monolayers did not exhibit a time dependent increase in FITC-albumin uptake. Uptake was significantly higher at the 2 hour time point when FITC-albumin dosing concentration was above 60 μg/ml for rat PTC monolayers, and when FITC-albumin dosing concentration was above 30 μg/ml for human PTC monolayers.

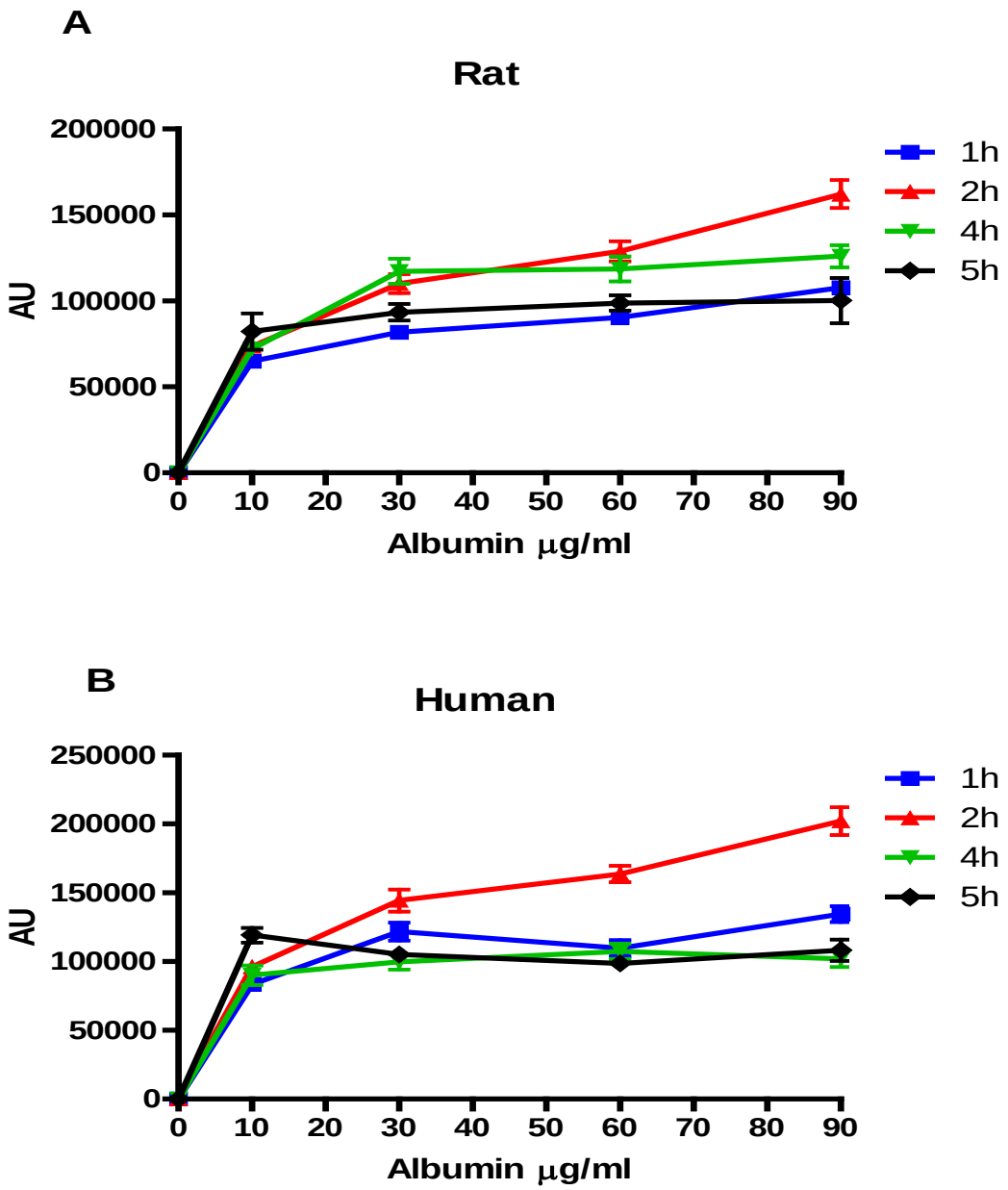

Figure 3.6: Uptake of FITC albumin by rat and human PTC monolayers.

Albumin uptake by (A) rat PTC monolayers and (B) human PTC monolayers were measured over time and dosing concentrations, normalised to protein concentrations. Both species saw concentration dependent uptake of albumin. Interesting, uptake was not time-dependent, as both species saw significantly more uptake at 2-hour time point than any other periods. Graphs are representatives of three independent experiments (N = 3). Each point represents the mean ± S.E.M of the 3 experiments. AU is absorbance unit.

3.8 FITC-albumin uptake by rat and human PTC monolayers in the presence of polymyxin B or rosuvastatin

The uptake of FITC-albumin by rat and human PTCs in presence of 250 μg/ml polymyxin B or 50 μM rosuvastatin was investigated, to demonstrate the potential interaction of large molecules with megalin/cubilin mediated-uptake (FITC-albumin) in the kidney. Polymyxin B dose was the same dose used for biomarkers levels measurement. Based on previous results (Figure 3.6), the uptake of 50 μg/ml FITC-albumin in the presence of the two large molecules over a period of 2 hours. The uptake of FITC-albumin was normalised to the respective protein concentration, and summarised in Figure 3.7.

In rat PTC monolayers, the amount of FITC-albumin decreased significantly in the presence of polymyxin B, from 633,501.1 ± 82,995.3 to 498,337.9 ± 122,370.7 AU ($P < 0.05$). The presence of rosuvastatin also caused a significant decrease in FITC-albumin uptake to 381,585.8 ± 95,978.1 AU ($P < 0.001$).

Similarly, the amount of FITC-albumin taken up by human PTC monolayers also changed significantly in the presence of polymyxin B, which decreased from 758,277.7 ± 170,859 to 482,451.1 ± 62,023.9 AU ($P <0.001$) when compared to the control alone. The presence of rosuvastatin also caused a significant decrease in FITC-albumin level when compared to the control, which was determined as 429,857.1 ± 84,947.6 AU ($P < 0.001$).

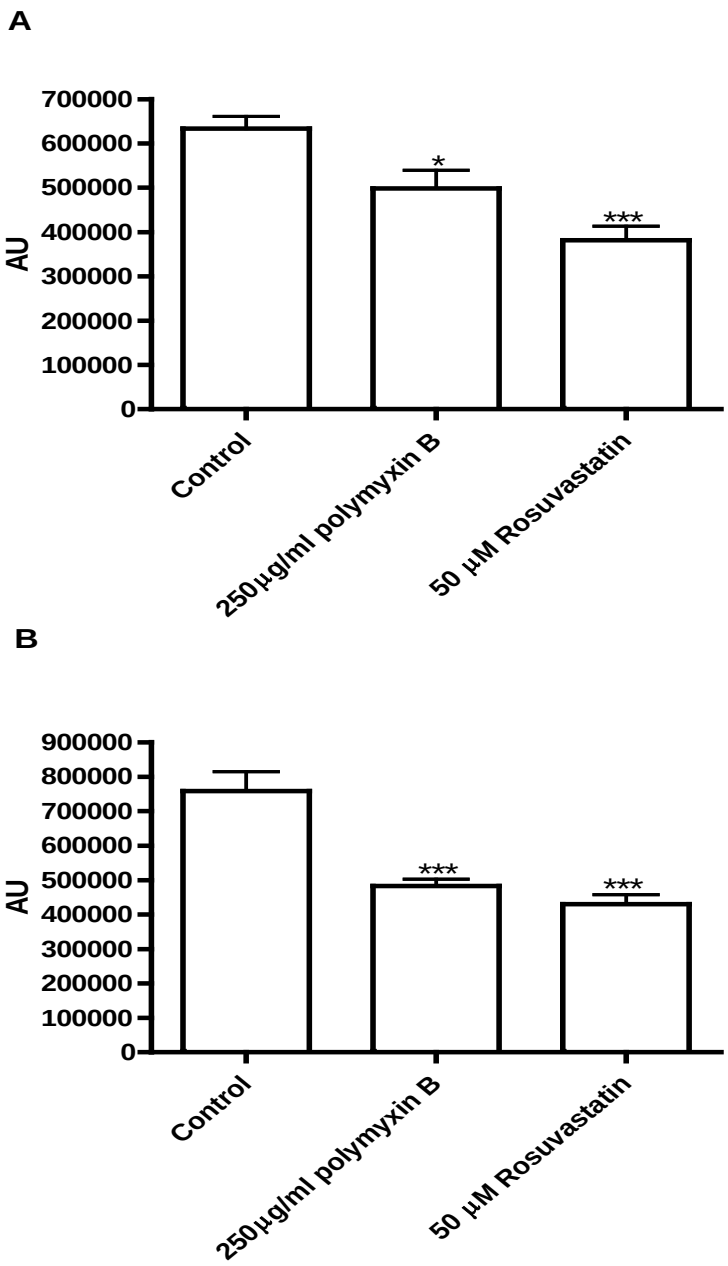

Figure 3.7: Uptake of FITC-albumin by rat and human PTCs in the presence of polymyxin B or rosuvastatin.

*Uptake of albumin by (A) rat PTC monolayers and (B) human PTC monolayers saw significant decrease in the presence of polymyxin B or rosuvastatin. For example, a 20 % decrease in albumin uptake was observed compared to control cells. Each bar represents the mean ± SEM of 3 replicates. One-way ANOVA test was performed to determine statistical significance. * P < 0.5, ** P < 0.1, ***, P < 0.01. AU is absorbance unit.*

3.9 Creatinine uptake by rat and human PTCs monolayers

To investigate the differential functional expression of OCT2 across the apical and basolateral membrane, creatinine uptake was performed using rat and human PTC monolayers. Uptake of creatinine across the apical and basolateral membranes was determined from the amount of intracellular accumulation of creatinine in the PTC monolayers after a period of time, and also in the presence of OCT2 specific inhibitor, dolutegravir. The results are showed in Figure 3.8.

Uptake of creatinine across the basolateral membrane was higher than across the apical membrane in both species of monolayers. For instance, uptake of creatinine by rat PTC monolayers were (1.10 ± 0.19 pmol/cm2/hr) across the basolateral membrane, almost 2 times more than across the apical membrane at 0.56 ± 0.05 pmol/cm2/hr. Similarly, uptake of creatinine by human PTC monolayers were 4.59 ± 0.58 pmol/cm2/hr across the basolateral membrane, a 3 times higher than across the apical membrane at 1.73 ± 0.11 pmol/cm2/hr.

However, monolayers treated with 100 µM dolutegravir saw significantly inhibition of uptake. For example, 60.0 % decrease in uptake across the basolateral membrane (from 4.6 ± 0.3 pmol/cm2/hr to 1.9 ± 0.2 pmol/cm2/hr, $P < 0.01$) when compared to control cells was seen in human PTC monolayers. In rat PTC monolayers, creatinine uptake across the basolateral membrane was also decreased from 1.1 ± 0.1 pmol/cm2/hr to 0.6 ± 0.2 pmol/cm2/hr in the presence of dolutegravir.

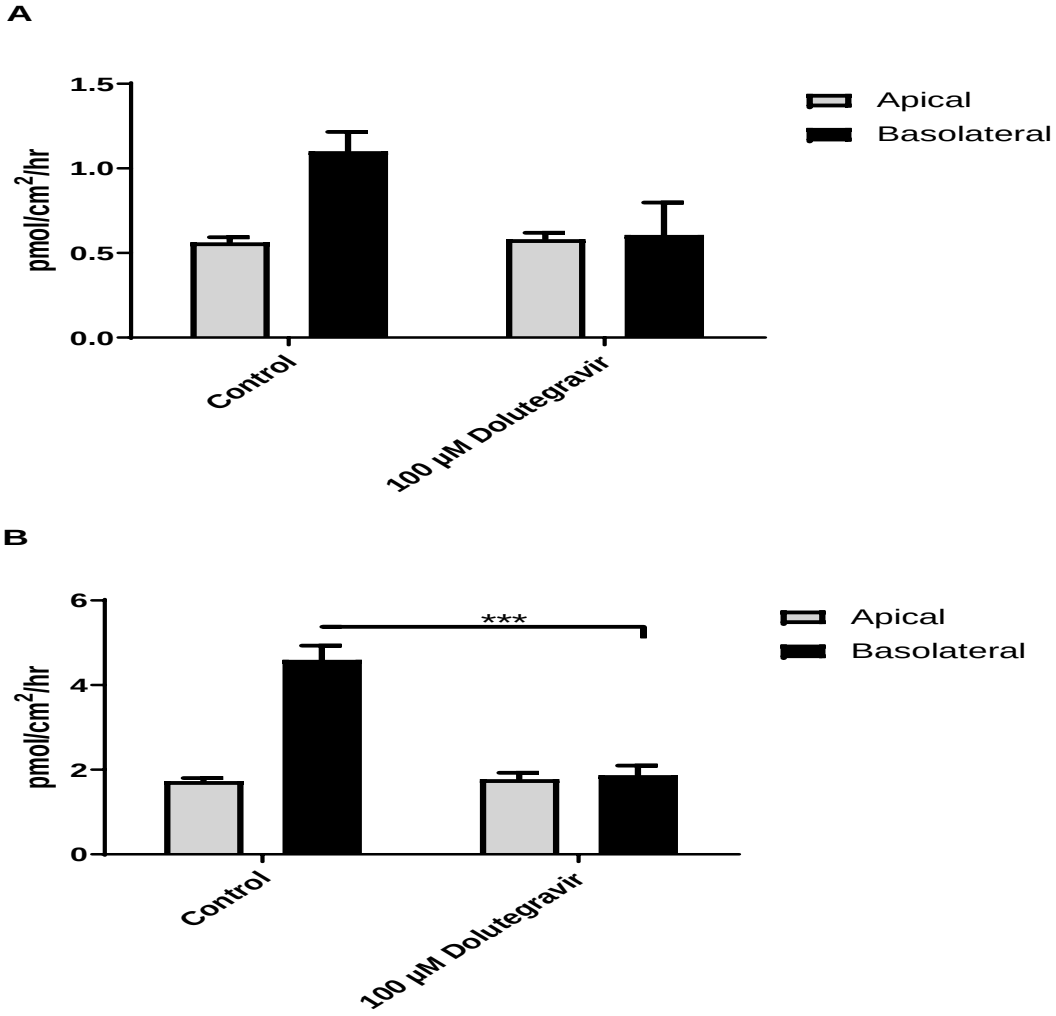

Figure 3.8: Creatinine uptake by rat and human PTC monolayers.

*Apical and basolateral uptake of creatinine by (A) rat and (B) human PTC monolayers, in the presence and absence of 100 µM dolutegravir. Uptake of creatinine were significantly higher across the basolateral membrane then across the apical membrane in both species of monolayers. Basolateral uptake was significantly decreased in the presence of dolutegravir. For instance, human PTC monolayers saw a 60.0 % decrease (4.6 ± 0.3 pmol/cm2/hr to 1.9 ± 0.2 pmol/cm2/hr). Each bar represents the mean ± SEM of 3 replicates. One-way ANOVA test was performed to determine statistical significance. * P < 0.5, ** P < 0.1, ***, P < 0.01.*

3.10 PAH uptake by rat and human PTCs monolayers

To investigate the functional expression of OAT1 in rat and human PTC monolayers, the uptake of PAH by the monolayers were performed. The differences in apical and basolateral PAH uptake magnitudes were also compared to PAH uptake in the presence of OAT1 inhibitor, probenecid. Figure 3.9 shows the results.

As expected, the basolateral uptake of PAH was greater in magnitude across the basolateral membrane of both species of monolayers. For example, uptake of PAH by rat PTC monolayers were (1.69 ± 0.28 pmol/cm2/hr) across the basolateral membrane, and the apical membrane at 1.15 ± 0.39 pmol/cm2/hr. Similarly, uptake of PAH by human PTC monolayers were 7.65 ± 0.82 pmol/cm2/hr across the basolateral membrane, which was 2 times higher than across the apical membrane at 3.04 ± 0.62 pmol/cm2/hr.

PAH uptake measured in the presence of 200 μM probenecid saw significant decrease in uptake across the basolateral membrane of human PTC monolayers, which went from 7.65 ± 0.48 pmol/cm^2/hr to 4.14 ± 0.54 pmol/cm^2/hr ($P < 0.01$). Similarly in rat PTCs, PAH uptake across the basolateral membrane with 200 μM probenecid treatment declined compared to control cells from 1.7 ± 0.2 pmol/cm^2/hr to 1.1 ± 0.1 pmol/cm^2/hr ($P < 0.01$).

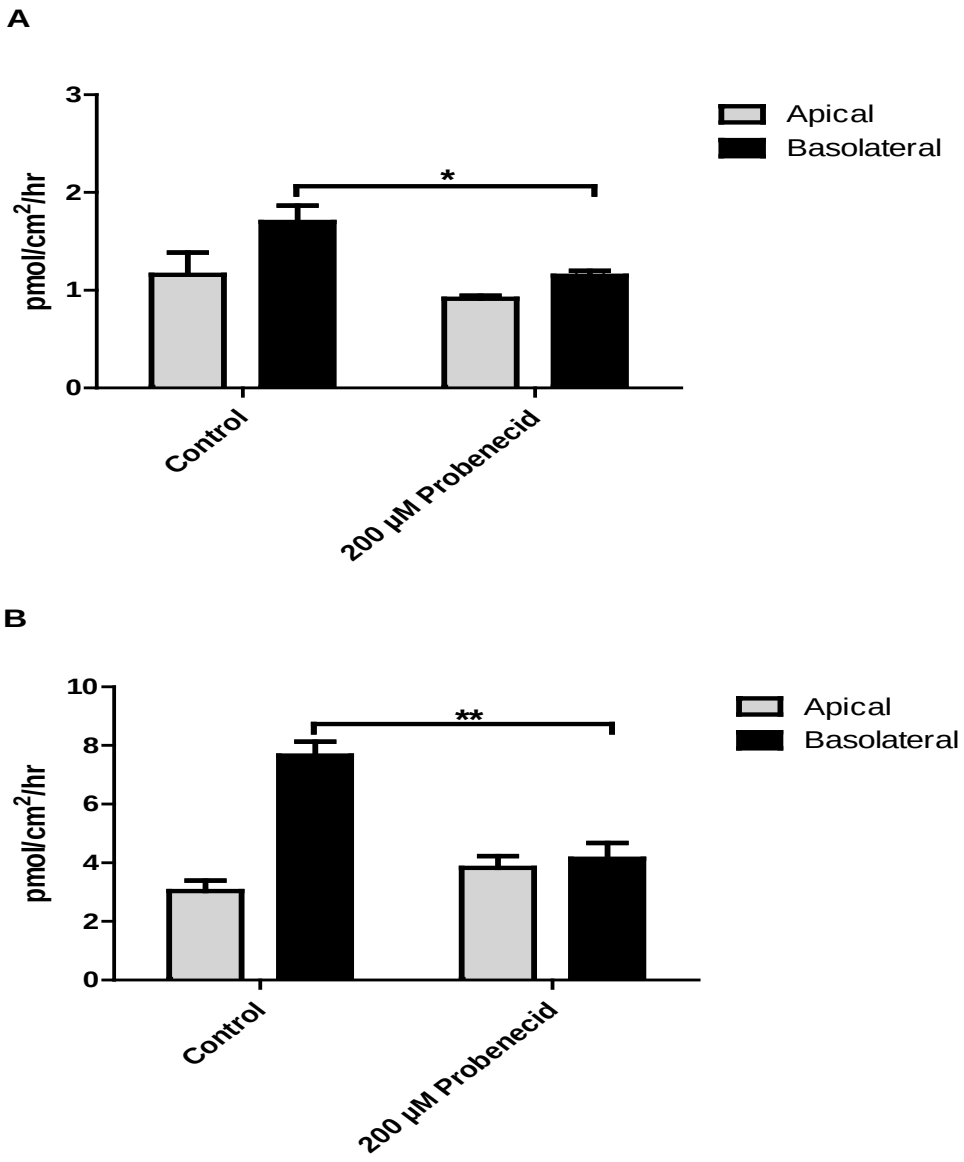

Figure 3.9: PAH uptake by human PTC monolayers in the presence of 200 µM probenecid.

*Apical and basolateral uptake of PAH by (A) rat and (B) human PTC monolayers, in the presence and absence of 200 µM probenecid. Uptake of PAH was significantly higher across the basolateral membrane then across the apical membrane in both species of monolayers. Basolateral uptake was significantly decreased in the presence of probenecid. For instance, human PTC monolayers saw a 40 % decrease in uptake from 7.65 ± 0.48 pmol/cm2/hr to 4.14 ± 0.54 pmol/cm2/hr. Each bar represents the mean ± SEM of 3 replicates. One-way ANOVA test was performed to determine statistical significance. * P < 0.5, ** P < 0.1, ***, P < 0.01.*

3.11 Discussion:

One key property of the primary renal cell model is its ability to express transport proteins located in the basolateral and apical membranes of the cells. This makes the model more physiologically relevant and therefore better in renal handling. In this chapter, human and rat PTCs were cultured on Transwell filter inserts for the initial characterisation of the cells, which focused on expression of a range of key proximal tubule transporters at the mRNA level. This was followed by a study of the functional expression of some transporters expressed in the human and rat proximal tubule.

3.11.1 Measurements of TEERs value

Numerous in vitro models for studying molecular transport across barrier tissues consisting mainly of epithelial and endothelial layers were developed[85]. There is no concern about changing in phenotypic stability over time in culture is because fresh cells were used each time and no passaging is done. In addition, the time of culture is short and the chance of the PTC differentiating to another cell type is low. One of the advantages of growing PTCs on Transwells plates is the ability to allow PTC monolayers to differentiate wth apical and basolateral membranes. However, it requires an effective monitoring technique to determine their cultural quality. The TEERs measurement was in consistent with morphological features of PTCs grown in this project. Primary proximal tubule cells TEER value are between (120–150 $\Omega*cm^2$ in 24-Transwell plates). Low TEER is widely assumed to imply poor growth of PTCs. When PTCs are treated with nephrotoxins drugs, the TEERs value is decreasing because the effect of those drugs to the integrity of the PTCs. The PTCs are leaking and after that die.

3.11.2 mRNA expression of transporters in human and rat PTCs

The mRNA detection of several transporters in human and rat PTCs were examined. The expression of all tested transporters has been identified by endpoint PCRs conducted with a cDNA template that was transcribed from RNA isolated from human and rats PTC cultures. Visualization of the PCR products on the agarose gels showed that in each of the lanes there was only one product. This showed the specificity of the primers used because only the interest gene was amplified. An agarose gel band intensity is a qualitative measure of PCR product quantity. For a quantitative measure of the amount of mRNA level, real-time quantitative PCR is a better technique.

There is consensus that primary tubular cells are better at retention of drug transporter expressions than other renal cell lines [86, 87]. Caki-1 cells, for instance, do not have mRNA from various organic transporters of anion and organic cation, including OAT1, OAT2, OCT1 and OCT2[88]. Rat cell line NRK-52E, and swine cell line LLC-PK1 lack mRNA expression of these transporters as well [89, 90]. In addition, LLC-PK1, which is often used to evaluate renal drug transport, also lack proximal brush-border enzymes compared with those in primary cultured PTCs[86].

It has been demonstrated that the preservation of the differentiated condition of primary cells and incidentally their brush-bound enzyme activity is largely affected by the composition of the culture medium [91, 92]. Furthermore, it has been demonstrated that bathing epithelial cells on both the apical and basolateral sides improves their capacity to stay differentiated, thus repeating in vivo physiology[93]. The data from section 1.6 showed expression of drug transporters in culture primary PTCs. However, the results do not show the location of those drugs transporters and further investigation is needed.

3.11.3 Functional expression of megalin and cubilin using FITC-albumin:

The experiments mentioned had been performed on human and rat PTCs cultured on Transwell filter inserts and demonstrated the functional expression of megalin and cubilin receptors by using albumin-FITC as a tracer substrate. Uptake was also carried out in the presence of polymyxin B and rosuvastatin to identify megalin and cubilin mediated uptake.

The results showed that the uptake of FITC-albumin was concentration dependent, but not time dependent. For instance, in both species of monolayers, 2 hours of incubation appeared to give significantly higher uptake of FITC-albumin than 3 or 4 hours.

The presence of polymyxin B, and to an extend rosuvatstain, decreased the ability of PTCs in albumin uptake. Our data is compatible with another study done with OK cells line, the observation of albumin uptake was noticed after the incubation of OK cells with 3 different statins (rosuvastatin, pravastatin, and simvastatin). In addition, ATP levels was measured and normalised to protein levels. The levels of ATP were stable even with high concentration of statins. That is mean the reduction of albumin uptake was not because the toxicity of the statins[94].

3.11.4 Functional expression of OCT2/MATE1 and OAT1/3 using creatinine and PAH

Creatinine is excreted primarily in urine through glomerular filtration and partially secreted via transport, which, depending on the renal function, account for 10–40 % of the complete creatinine clearance[95]. Creatinine is a substrate for OCT2 and MATE1. Genome-wide association studies show that OCT2 and MATE1 genetic mutations influence the clearance of creatinine [96]. Dolutegravir is an OCT2 clinically appropriate inhibitor that causes serum level increases by inhibition the tubular secretion, and therefore used as an inhibitor of OCT2 in this study [97].

For most anionic drugs, the urinary excretion mechanism includes active tubular secretion and glomerular filtration in the kidney[98]. The main kidney transporters responsible for basolateral uptake of multiple organic anions, including pharmaceuticals and uremic toxins, are regarded to be organic anion carriers OAT1 and OAT3[99]. OAT1 plays a significant part in uptake of hydrophilic and small organic anions such as PAH, 2,4 dichlorophenoxyacetate and acyclic nucleotide phosphonate while OAT3 is more specific in substrate than OAT1 and accepts organic anions and even organic cations (cimetidine) and zwitterion (fexofenadine)[100]. The urinary excretion mechanisms of drugs have been characterized by probenecid. Probenecid is both a powerful inhibitor of OAT1 and OAT3 and probenecid co-administration at a therapeutic dose leads to significant inhibition of OAT1 and OAT3 substrates tubular secretion [101].

Our data showed that creatinine uptake was reduced significantly after incubation with dolutegravir in human PTC, but it didn't change in rat PTC. This may be because creatinine handling by the kidneys is different between human and rat. It has also been shown that OCT2 may not be the only transporter responsible for creatinine uptake in human [102]. Similarly, PAH uptake was reduced in the basolateral membrane after treatment with probenecid but this time the change was notice in both human and rat PTCs.

This chapter has shown the expression of several significant drug transporters by human and rat PTCs at mRNA level. Also, the functional expression and location of some of the transporters on polarized human and rat PTC monolayers. These data highlight the capacity of

human and rat PTCs to reflect proximal tubules in vivo, it would be necessary to investigate their ability as an in vitro template for kidney drug handling.

4 Human Biomarkers

4.1 Introduction

The kidneys are responsible for maintaining circulatory fluid homeostasis and serve as the main organ for xenobiotic elimination and detoxification and receive approximately 25% of all heart blood flow[103]. The nephron with about 1 million nephrons per kidney is the functional filtration unit of the kidney[104]. The nephron has three key functional components, namely the passive blood filtration by the glomeruli and the active absorption and secretion by tubular epithelia. PTCs are enriched by membrane proteins that facilitate and activate the transport of compounds within a cell at significantly higher concentration rates than those observed in circulation[103]. The main driver behind xenobiotic nephropathy, leading to observable acute kidney damage (AKI), was considered to be intracellular accumulation.

The ability to accurately predict toxic kidney damage, for both existing and new pharmaceutical prescription medicines or for risk assessment due to environmental exposures of xenobiotics is a major current challenge[103]. To respond to this concern, new, more sensitive, biomarkers of nephrotoxicity have been identified. One of the biomarkers have been used in this chapter is KIM-1. In 2002, the first KIM-1 human subjects studies were released[105]. The study indicated that a significant enhanced expression of KIM-1 in patients with acute tubular necrosis from renal biopsy samples. Another study detected KIM-1 protein by staining after taking kidney biopsy from 102 patients with different kidney diseases and showed that positive KIM-1 staining was associated with tubulo-interstitial fibrosis and inflammation in dedifferentiated proximal tubular cells[106].

Another biomarker used in this study was NGAL. A study done showed NGAL measurements is an early AKI biomarker in paediatric intensive care environment that can be predicted about 2 days prior to serum creatinine increase [107]. In adult intensive care patient research, measuring plasma NGAL levels were a very useful biomarker for AKI extension within the next 2 days [108].

Clusterin, another biomarker was investigated in this chapter. A study discovered that the expression of clusterin mRNA levels in damaged rat renal tubular epithelial cells of unilateral

ureteral obstruction was considerably enhanced while its urination content decreased simultaneously, indicating clusterin could act as an early biomarker of AKI [109].

One of the nephrotoxic drugs we used is Cisplatin. Cisplatin accumulates in the kidney during glomerular filtration and tubular secretion[110]. Nephrotoxicity caused by cisplatin is dose-dependent and includes kidney cell necrosis, apoptosis and necroptosis [111]. Cisplatin is transported by OCT2 [112] this is why it is a good nephrotoxic molecule to test in our PTCs model.

Another drug used in this study is gentamicin, causing tubular injury by: 1) tubular epithelial cell necrosis, predominantly in the proximal segment, and 2) altering the function of the primary cellular components engaged in water and solute transport [113]. Tubular cytotoxicity is the key element of gentamicin nephrotoxicity. The enhanced accumulation of gentamicin in PTCs is linked to (megalin/cubilin) receptors in the apical membrane of PTCs [114]. These two receptors transports gentamicin by endocytosis. The drug is then transferred into lysosomes, Golgi and endoplasmic reticulum[115].

This study's purpose is therefore to identify and substantiate the use of human primary proximal tubule cells (PTCs), from the kidney, as suitable models in the study of nephrotoxicity and to further the cause of drug related nephrotoxicity. The cells would be isolated from the kidneys, as Brown et al. (2008) described, and subsequently characterised on exposure to different nephrotoxins, namely polymyxin B, gentamicin and cisplatin. These three compounds were chosen as they represent prototypic large (polymyxin B and gentamicin) and small (cisplatin) molecules the kidney would encounter. Measuring the expression of different biomarkers of nephrotoxicity, such as KIM-1, NGAL and clusterin, upon exposure to those nephrotoxins has done.

4.2 Large molecule nephrotoxin – Gentamicin

Before the biomarker expression was quantified by ELISA, human PTCs were treated with gentamicin, a recognized nephrotoxin. Because of the well characterized and related toxicities of gentamicin in vivo, Gentamicin's monolayer PTC impacts are important.

4.2.1 MTS cell viability after treatment in presence of range of concentration of gentamicin

To determine the nephrotoxicity of gentamicin, human PTCs were treated with a range of concentration of gentamicin for 24, 48 and 72 hours. The viability of the human PTCs was determined by measuring the mitochondrial activity using MTS assay. The obtained results are presented Figure 4.1

The results of the MTS assay showed the effect of gentamicin on cell viability in human PTCs. With a rise in gentamicin concentration, cell viability reduced continuously. For example, after 24h treatment with 100 µg/ml gentamicin the cell viability was 23% less than the nonrated cells. The percentage of live cells was less than 50% after 250 µg/ml gentamicin treatment for 24h.

The percentage of live cells decreased with the rise of the gentamicin dose after 48h incubations. For instance, after 300 µg/ml gentamicin the percentage of live cells was 44%. The live was less more than 40% after 400 µg/ml gentamicin treatment.

After 72h treatment with a range of gentamicin concentrations, cell viability decreased significantly. After 100 µg/ml gentamicin treatment, live cells reduced was 71%. In addition, after 500 µg/ml gentamicin incubation the cell viability was only 29%.

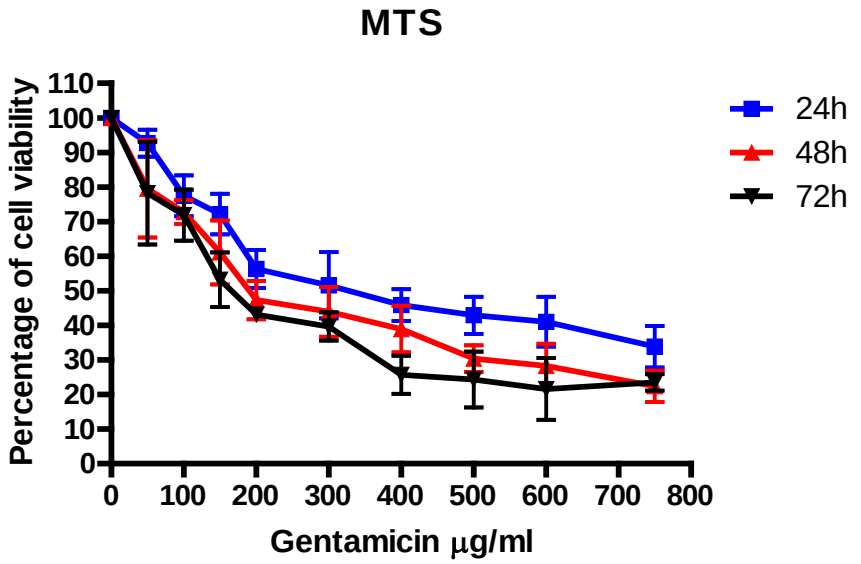

Figure 4.1: Cell viability in human PTCs treated with range concentrations of gentamicin for 24, 48 and 72 hours.

MTS assay was used to measure the cell viability. Gentamicin showed a time and concentrations dependent after 24, 48 and 72 hours treatment. For example, the cell viability after 250 µg/ml gentamicin for 24h was 56.5% and the percentage dropped to 47% after 48h. In addition, cell viability after 300 µg/ml gentamicin treatment for 72h was 39% and after 500 µg/ml gentamicin the cell viability decreased to 21%. Each point represent mean ± S.E.M values of each gentamicin concentration. Each data point is expressed as a percentage of the negative control of no gentamicin treatment.

4.2.2 KIM-1 production after treatment of human PTCs in presence of a range concentration of gentamicin

The effects of a range of gentamicin concentrations on KIM-1 levels produced by human PTCs were investigated. The level of the biomarker was normalised to the cell viability. The results are shown in Figure 4.2**.**

The KIM-1 levels after 24h treatment of gentamicin increased significantly compared to non-treated cells. For instance, the level of KIM-1 production was 24.11±7.21 ng/ml at 250 µg/ml gentamicin, compared with the control 1.60±0.28 ng/ml. The level of KIM-1 increased as the concentration of gentamicin increased up to 600 µg/ml.

The levels of KIM-1 also increased significantly in comparison with the non-treated cells after 48h of gentamicin treatment. The level of KIM-1 was 14.70±2.53 ng/ml after 100 µg/ml gentamicin treatment, and increased further to 55.43±17.72 ng/ml with 300 µg/ml gentamicin treatment.

The KIM-1 levels after 72h treatment of gentamicin increased significantly compared to non-treated cells. For instance, KIM-1 levels were elevated significantly by 250 µg/ml gentamicin concentrations (62.15±14.30 ng/ml). The level of KIM-1 production reached the peak at 500 µg/ml gentamicin treatment to 235.66±12.85 ng/ml.

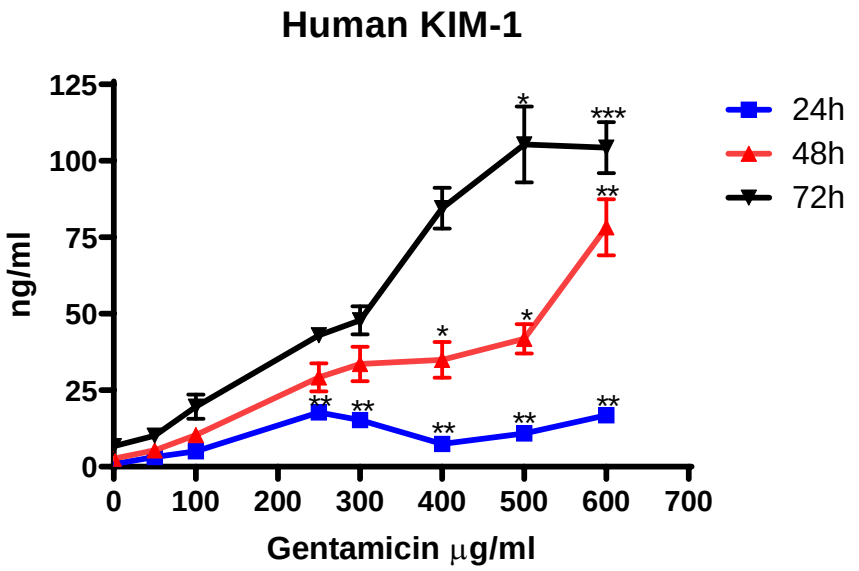

Figure 4.2: Measurement of KIM-1 production by human PTCs treated with gentamicin for 24, 48 and 72 hours.

*Levels were normalised to MTS absorbance value to account for cell numbers after nephrotoxin treatments. Human PTCs were treated with a range of gentamicin concentration (50 to 600 µg/ml). For example, KIM-1 production after 100 µg/ml gentamicin treatment for 24h was 3.1±0.3 ng/ml and after 250 µg/ml the level of KIM-1 increased to 7.6±1.5 ng/ml. The level of KIM-1 after 400 µg/ml gentamicin treatment for 48h was 43.9±10.1 ng/ml and after 72h the level increased to 74.5±26.1 ng/ml. Statistical analysis was conducted using repeated-measures-paired-one-way ANOVA the data are representative of three independent experiments (n=3). Each point mean ± S.E.M values of each group. (*p < 0.05, **p < 0.01, ***p < 0.001).*

4.2.3 NGAL production after treatment of human PTCs in presence of a range concentration of gentamicin

The effects of a range of gentamicin concentrations on NGAL levels produced by human PTCs were investigated. The biomarker levels were normalised to cell viability. The results are showed in Figure 4.3**.**

There was a significant increase in NGAL levels after 24h treatment of gentamicin compared to non-treated cells. NGAL levels were elevated significantly by 50 to 600 µg/ml gentamicin concentrations. The level of NGAL production at 300 µg/ml gentamicin was 65.81±4.89 ng/ml compared with the control 8.45±2.66 ng/ml and then the level of NGAL increased as the concentration of gentamicin increases up to 600 µg/ml.

In comparison to non-treated cells, the levels of NGAL increased significantly after gentamicin treatment for 48h. For example, the level of NGAL after 250 µg/ml gentamicin treatment was 180.49±43.59 ng/ml. The level of NGAL after 400 µg/ml gentamicin treatment was 230.86±60.42 ng/ml.

NGAL concentrations rose considerably relative to non-treated cells after 72 hours of gentamicin treatment. For example, NGAL level was 153.31±29.97 ng/ml after 100 µg/ml gentamicin treatment. The level of NGAL production after 500 µg/ml gentamicin treatment was 709.58±126.68 ng/ml

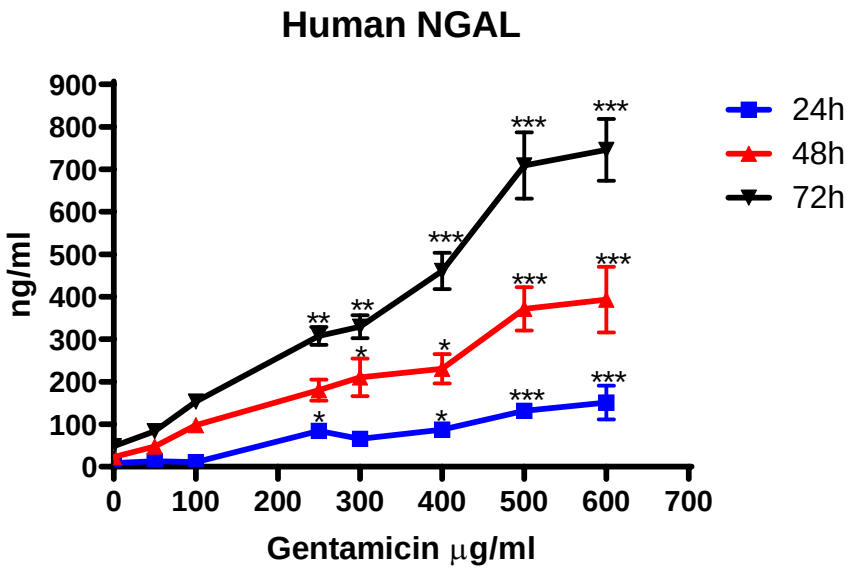

Figure 4.3: Measurement of NGAL production from human PTCs treated with gentamicin for 24, 48 and 72 hours.

*Levels were normalised to MTS absorbance value to account for cell numbers after nephrotoxin treatments. Human PTCs were treated with a range of gentamicin concentration (50 to 600 µg/ml). For example, NGAL production after 300 µg/ml gentamicin treatment for 24h was 65.8±4.7 ng/ml and after 500 µg/ml the level of NGAL increased to 131.4±19.5 ng/ml. The level of NGAL after 250 µg/ml gentamicin treatment for 48h was 180.4±43.5 ng/ml and after 72h the level increased to 307.8±35.7 ng/ml. Statistical analysis was conducted using repeated-measures-paired-one-way ANOVA the data are representative of three independent experiments (n=3). Each point mean ± S.E.M values of each group. (*p < 0.05, **p < 0.01, ***p < 0.001).*

4.2.4 Clusterin production after treatment of human PTCs in presence of a range concentration of gentamicin

The impacts of a range of gentamicin concentrations generated by human PTCs on clusterin levels were studied. The biomarker levels were normalised to cell viability. The results are shown in Figure 4.4.

Clusterin concentrations rose considerably relative to non-treated cells after 24h incubation with range of gentamicin concentrations. The level of clusterin production after 250 µg/ml gentamicin was 53.67±23.58 ng/ml compared with the control 8.85±2.94 ng/ml and then the level of clusterin increased as the concentration of gentamicin increases up to 600 µg/ml.

The levels of clusterin increased significantly in comparison with non-treated cells after 48h of gentamicin treatment. The clusterin levels increased by 50 to 600 µg/ml gentamicin treatment. The highest level of clusterin, compared to control 25.84±1.1 ng/ml, was after 600 µg/ml gentamicin treatment at 380.40±55.44 ng/ml.

After 72h of gentamicin treatment, clusterin levels considerably increased relative to non-treated cells. For instance, the level of clusterin after 100 µg/ml gentamicin treatment to 118.1±23.36 ng/ml compared with the control 82.78±15.93 ng/ml and then the production of clusterin increased as the concentration of gentamicin increases up to 600 µg/ml.

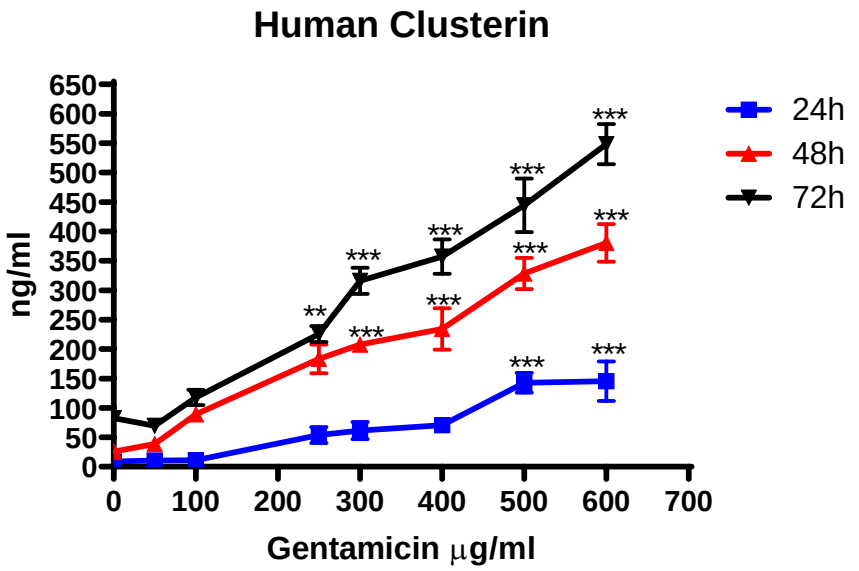

Figure 4.4: Measurement of clusterin production from human PTCs treated with gentamicin for 24, 48 and 72 hours.

*Levels were normalised to MTS absorbance value to account for cell numbers after nephrotoxin treatments. Human PTCs were treated with a range of gentamicin concentrations (50 to 600 µg/ml). For example, clusterin production after exposure to 250 µg/ml gentamicin for 24h was 53.6±23.5 ng/ml and after 500 µg/ml the level of clusterin increased to 142.7±28.8 ng/ml. The level of clusterin after 300 µg/ml gentamicin treatment for 48h was 207.7±19.8 ng/ml and after 72h the level increased to 316.2±38.6 ng/ml. Statistical analysis was conducted using repeated-measures-paired-one-way ANOVA the data are representative of three independent experiments (n=3). Each point mean ± S.E.M values of each group. (*p < 0.05, **p < 0.01, ***p < 0.001).*

4.2.5 MTS and ATP cells viability assays

The cell viability was measured after treatment of human PTCs for 24 and 48 hours with 250 µg/ml gentamicin. The cell viability was also measured in the presence of cilastatin co-treatments. Both CellTiter 96® AQueous Non-Radioactive Cell Proliferation Assay (MTS) and RealTime-Glo™ MT Cell Viability Assay (ATP) were used to assess cell viability. Both the MTS and ATP assays were used to calculate viability from the same plate. The results revealed no significant difference between the two assessment methods. The results are shown in Figure 4.5.

After 24h, the results revealed that cell viability reduced significantly in response to exposure to gentamicin to (65±3.4%, $P < 0.01$) of control. The cilastatin co treatment did not affect the cell viability (95.71±3.44% live cells). The treatment of gentamicin with cilastatin increased the live cells compared to only gentamicin (76.1±3%).

The cell viability was reduced significantly by gentamicin (56.90±5%, $P < 0.01$) after 48h.However, the cell viability did not change with cilastatin (95±3.70%). The cell viability after gentamicin with cilastatin was higher than only gentamicin (74±5.25% viable cells).

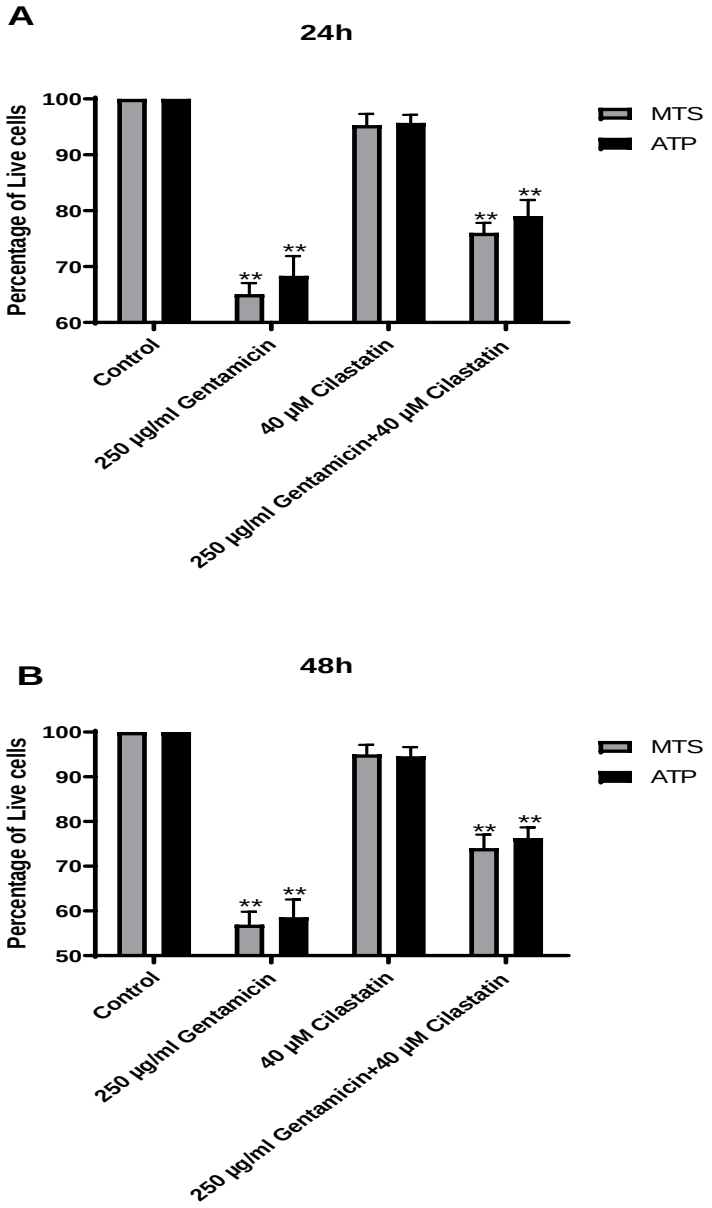

Figure 4.5: Cells Viability of human PTCs after treatment of gentamicin for 24 and 48 hours.

*MTS and ATP assays were used to measure the cell viability. Viability is measured as a percentage of the control. For example, MTS percentage after gentamicin treatment for 24h was 65% and ATP percentage was 68.3%. In addition, the co-treatment of cilastatin with gentamicin for 48h showed, the percentage of MTS was 74.1% and ATP percentage was 76.3%. Statistical analysis was conducted using repeated-measures-paired-one-way ANOVA the data are representative of three independent experiments (n=3). Bars represent mean ± S.E.M values of each group. (*p < 0.05, **p < 0.01, ***p < 0.001).*

4.2.6 Lactate dehydrogenase (LDH) cytotoxic assay

The measurement of cytoplasmic enzymes released by damaged cells is a common method for determining cytotoxicity. Lactate dehydrogenase (LDH) is a stable enzyme found in all cellular systems. In this experiment, we treated human PTCs for 24 and 48 hours with 250 µg/ml gentamicin and LDH was measured. In addition, we measured the LDH after cilastatin co treatment. The results is consistent with cell viability data. Result shown in Figure 4.6

After 24h, the results revealed that LDH increased significantly in response to exposure to gentamicin to 32.28±2.8%. The cilastatin co treatment did not change the LDH (13.74±1.41%). The treatment of gentamicin with cilastatin decreased the LDH compared to only gentamicin (27.38±2.21%).

The LDH was increased significantly by gentamicin (45.58±5.47%) after 48h.However, the LDH did not change with cilastatin (14±1.29%). The LDH after gentamicin with cilastatin was lower than only gentamicin (30.37±5=2.26%).

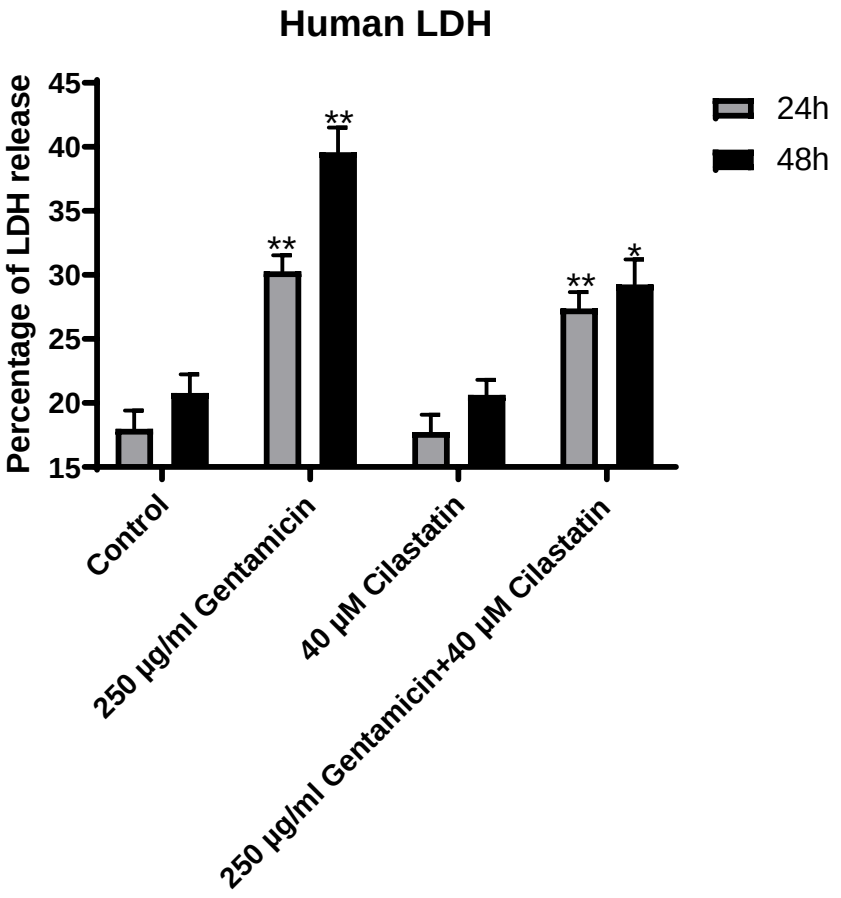

Figure 4.6: LDH of human PTCs after treatment of gentamicin for 24 and 48 hours.

*LDH is measured as a percentage of the control. LDH percentage after gentamicin treatment for 24h was 36.2% and after 48h the percentage increased to 45.5%. In addition, LDH percentage decreased after cilastatin co-treatment with gentamicin for 48h to 30.7% Statistical analysis was conducted using repeated-measures-paired-one-way ANOVA the data are representative of three independent experiments (n=3). Bars represent mean ± S.E.M values of each group. (*p < 0.05, **p < 0.01, ***p < 0.001).*

4.2.7 KIM-1 production after treatment of human PTCs in the presence of gentamicin +/- cilastatin

The amount of KIM-1 produced after treatment of human PTCs for 24 and 48 hours in the presence of gentamicin was measured, and also PTCs co-treated with cilastatin. The concentrations of KIM-1 was normalised to the cell viability as determined from their MTS absorbance, results of which were therefore expressed as ng/ml. The results are shown in Figure 4.7.

With 24h treatment of gentamicin, the amount of KIM-1 in the apical membrane change significantly from the control (12.19±1.93 ng/ml, $P < 0.01$). However, the presence of cilastatin did not change KIM-1 level 4.73±1.05 ng/ml compared to control (4.71±1.11 ng/ml). The co-treatment of gentamicin with cilastatin caused a significant decrease in KIM-1 in the apical membrane (8.16±1.39 ng/ml, $P < 0.0001$) compared to only gentamicin. KIM-1 levels in the basolateral membrane were low compared to apical membrane.

With 48h treatment of gentamicin, the amount of KIM-1 in the apical membrane did change significantly from the control (30.49±5.69 ng/ml, $P < 0.01$). However, when we added cilastatin did not change KIM-1 level 13.45±3.71 ng/ml compared to control 13.32±3.21 ng/ml. The co-treatment of gentamicin with cilastatin caused a significant decrease in KIM-1 in the apical membrane (24.1±5.28 ng/ml, $P < 0.0001$) compare to only gentamicin. KIM-1 levels in the basolateral membrane were low compared to apical membrane.

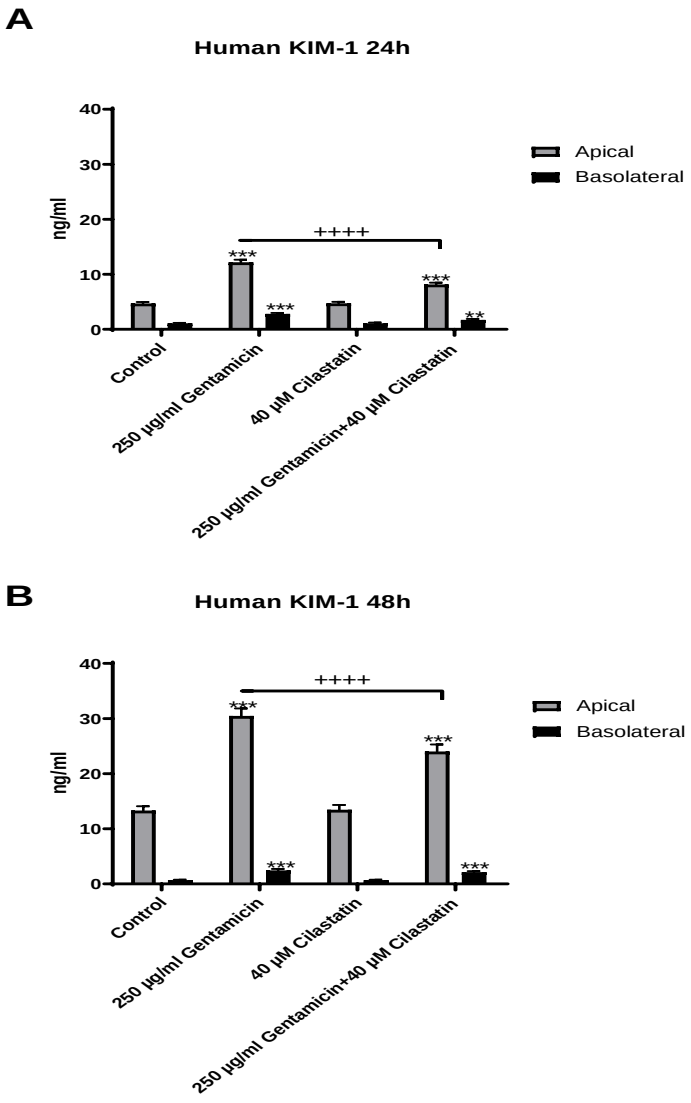

Figure 4.7: The amount of KIM-1 produced after treatment of human PTCs for 24 and 48 hours in presence of gentamicin +/- cilastatin.

*ELISA was used to measure KIM-1 production. For example, KIM-1 production in the apical membrane is significantly higher than basolateral membrane. The amount of KIM-1 in the apical membrane change significantly from the control (12.19±1.93 ng/ml, P < 0.01) after 24h gentamicin treatment. After co-treatment with cilastatin, KIM-1 level decreased to (8.16±1.39 ng/ml, P < 0.0001) compared to only gentamicin. The level of KIM-1 after 48h treatment was more than 1 fold compared to 24h. Statistical analysis was conducted using repeated-measures-paired-one-way ANOVA the data are representative of three independent experiments (n=3). Bars represent mean ± S.E.M values of each group. (*p < 0.05, **p < 0.01, ***p < 0.001, ++++p < 0.0001).*

4.2.8 NGAL production after treatment of human PTCs in the presence of gentamicin +/- cilastatin

NGAL production for 24 and 48 hours in the presence of gentamicin following treatment of human PTCs. In the presence of cilastatin co-treatment, levels of NGAL were also measured. NGAL concentrations had been normalized to cell viability based on the MTS absorption of the PTCs, resulting in ng/ml. The results are shown in Figure 4.8.

With 24h treatment of gentamicin, the amount of NGAL in the apical membrane did increase significantly from the control (230.49±85.20 ng/ml, $P < 0.01$). However, the presence of cilastatin did not change NGAL level 30.39±6.1 ng/ml compared to control 23.72±3.32 ng/ml in the apical membrane. The co-treatment of gentamicin with cilastatin caused a significant decrease in NGAL in the apical membrane (125.79±28.1 ng/ml, $P < 0.0001$) compared to only gentamicin. Compared to apical membrane, NGAL levels in the basolateral membrane were low.

After 48 hour treatment of gentamicin, the amount of NGAL in the apical membrane did increase significantly from the control (439.69±109.81 ng/ml, $P < 0.01$). However, the presence of cilastatin did not change NGAL level 89.18±27.90 ng/ml compared to control 90.43±31.21 ng/ml in the apical membrane. The co-treatment of gentamicin with cilastatin caused a significant decrease in NGAL in the apical membrane (303.32±81.99 ng/ml, $P < 0.0001$) compared to only gentamicin. Compared to apical membrane, NGAL levels in the basolateral membrane were low.

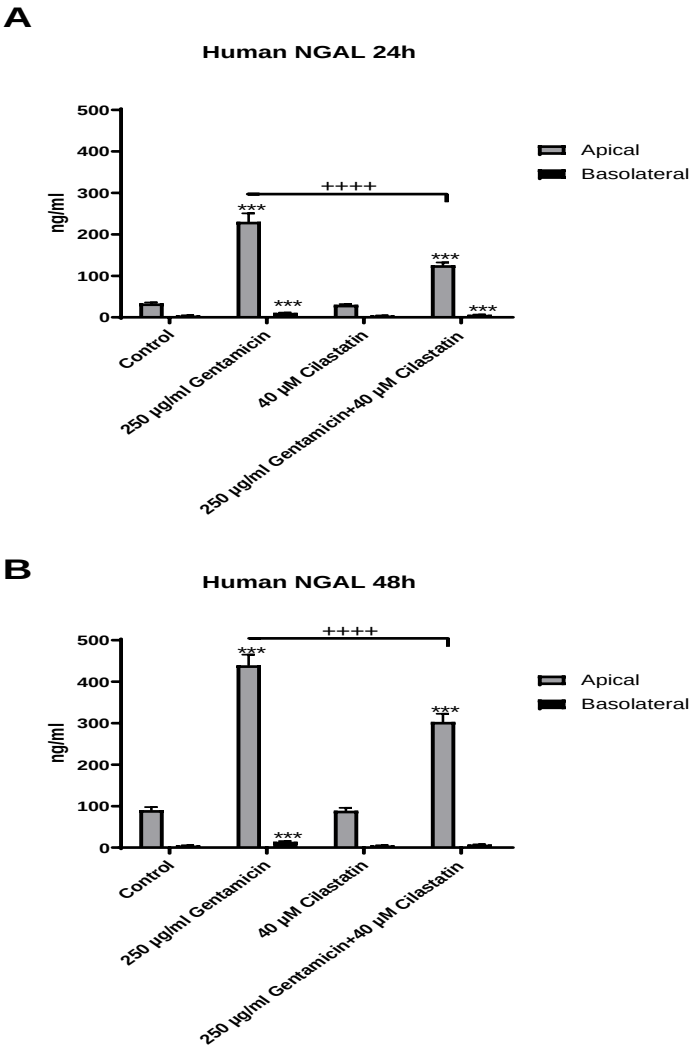

Figure 4.8: The amount of NGAL produced after treatment of human PTCs for24 and 48 hours in presence of gentamicin +/- cilastatin.

*ELISA was used to measure NGAL production. For example, NGAL production in the apical membrane is significantly higher than basolateral membrane. The amount of NGAL in the apical membrane change significantly from the control (230.49±85.20 ng/ml, P < 0.01) after 24h gentamicin treatment. After co-treatment with cilastatin, NGAL level decreased to (125.79±28.1 ng/ml, P < 0.0001) compared to only gentamicin. The level of NGAL after 48h treatment was more than 1 fold compared to 24h. Statistical analysis was conducted using repeated-measures-paired-one-way ANOVA the data are representative of three independent experiments (n=3). Bars represent mean ± S.E.M values of each group. (*p < 0.05, **p < 0.01, ***p < 0.001, ++++p < 0.0001).*

4.2.9 Clusterin production after treatment of human PTCs with gentamicin +/- cilastatin

Clusterin production 24 and 48 hours after treatment of human PTCs in the presence of gentamicin. In the presence of cilastatin co-treatment, levels of clusterin were also measured. Clusterin concentrations had been normalized to cell viability based on the MTS absorption of the PTCs, resulting in ng / ml. The results are shown in Figure 4.9.

With 24h treatment of gentamicin, the amount of clusterin in the apical membrane did increase significantly from the control (277.40±100.63 ng/ml, $P < 0.01$). However, the presence of cilastatin did not change clusterin level 35.52±8.94 ng/ml compared to control 35.87±10.92 ng/ml. The co-treatment of gentamicin with cilastatin caused a significant decrease in clusterin in the apical membrane (135.70±25.03 ng/ml, $P < 0.0001$) compared to only gentamicin. Compared to apical membrane, clusterin levels in the basolateral membrane were low.

With 48h treatment of gentamicin, the amount of clusterin in the apical membrane did change significantly from the control (476.16±143.1 ng/ml, $P < 0.01$). However, when we added cilastatin did not change clusterin level 79.26±12.89 ng/ml compared to control 79.20±23.29 ng/ml. The co-treatment of gentamicin with cilastatin caused a significant decrease in clusterin in the apical membrane (316.75±82.60 ng/ml, $P < 0.0001$) compare to only gentamicin. Clusterin levels in the basolateral membrane were low compared to apical membrane.

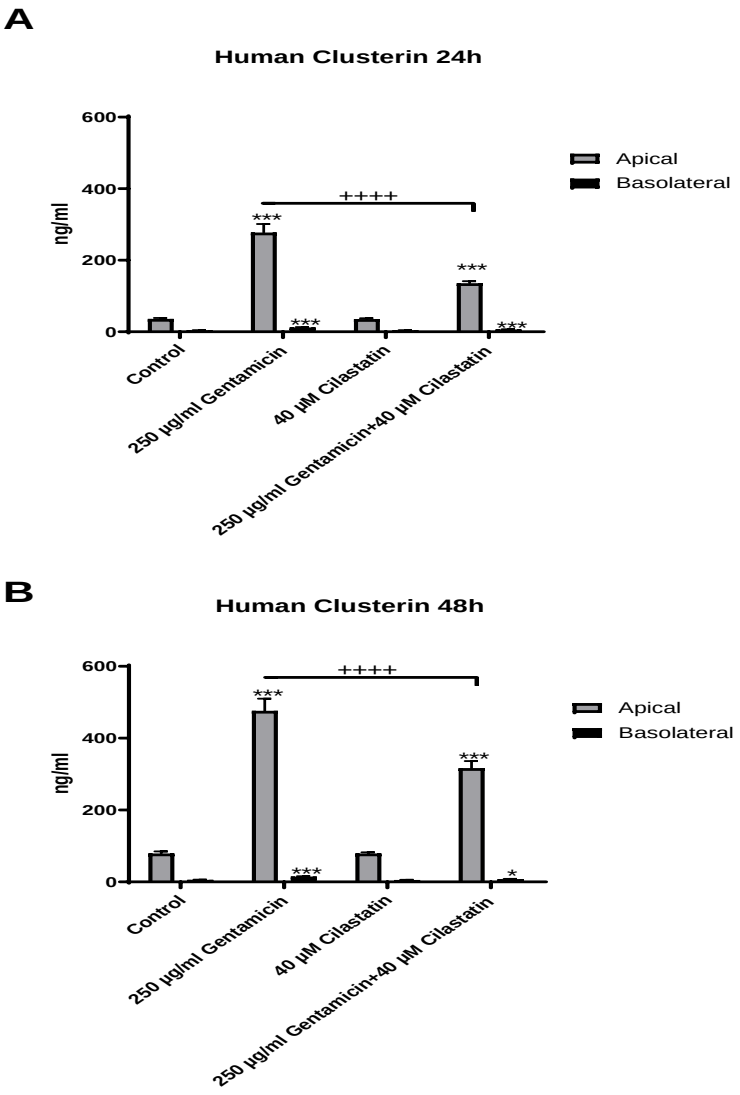

Figure 4.9: The amount of clusterin produced after treatment of human PTCs for 24 and 48 hours in presence of gentamicin +/- cilastatin.

*ELISA was used to measure clusterin production. For example, clusterin production in the apical membrane is significantly higher than basolateral membrane. The amount of clusterin in the apical membrane change significantly from the control (35.87±10.9 to 277.40±100.63 ng/ml, P < 0.01) after 24h gentamicin treatment. After co-treatment with cilastatin, clusterin level decreased to (135.70±25.03 ng/ml, P < 0.0001) compared to only gentamicin. The level of clusterin after 48h treatment was more than doubled compared to 24h. Statistical analysis was conducted using repeated-measures-paired-one-way ANOVA the data are representative of three independent experiments (n=3). Bars represent mean ± S.E.M values of each group. (*p < 0.05, **p < 0.01, ***p < 0.001, ++++p < 0.0001).*

4.3 Large molecule nephrotoxin – Polymyxin B

Human PTCs were treated with polymyxin B before biomarker expression was quantified by using ELISA. The effects of polymyxin B on PTCs were important as the toxicity of polymyxin B was already nephrotoxic in vivo.

4.3.1 MTS cell viability after treatment in presence of range of concentrations of polymyxin B

The cell viability was measured after treatment of human PTCs with a range of concentration of polymyxin B (50 to 600 μg/ml) for 24, 48 and 72 hours. CellTiter 96® AQueous Non-Radioactive Cell Proliferation Assay (MTS) was used to assess cell viability. The MTS absorbance show as a percentage normalised to non-treated cells. The results are shown in Figure 4.10.

The impact of polymyxin B on cell viability in human PTCs was found in the outcome of the MTS assay. The cell viability decreased steadily with an increase in polymyxin B concentration. For example, after 24h treatment with 250 μg/ml polymyxin B the cell viability was 17% less than the nonrated cells. The percentage of live cells was less than 50% after 300 μg/ml polymyxin B treatment.

After 48h incubation with polymyxin B the percentage of live cells decrease as the dose of polymyxin B increase. For instance, at 300 μg/ml polymyxin B the percentage of live cells was 40%. The live was less more than 70% after 400 μg/ml polymyxin B.

There were a major drop in cell viability after 72h treatment with a range of concentration of polymyxin B. after 100 μg/ml polymyxin B treatment, live cells reduced more than 35%. In addition, after 400 μg/ml polymyxin B incubation the cell viability was only 13%.

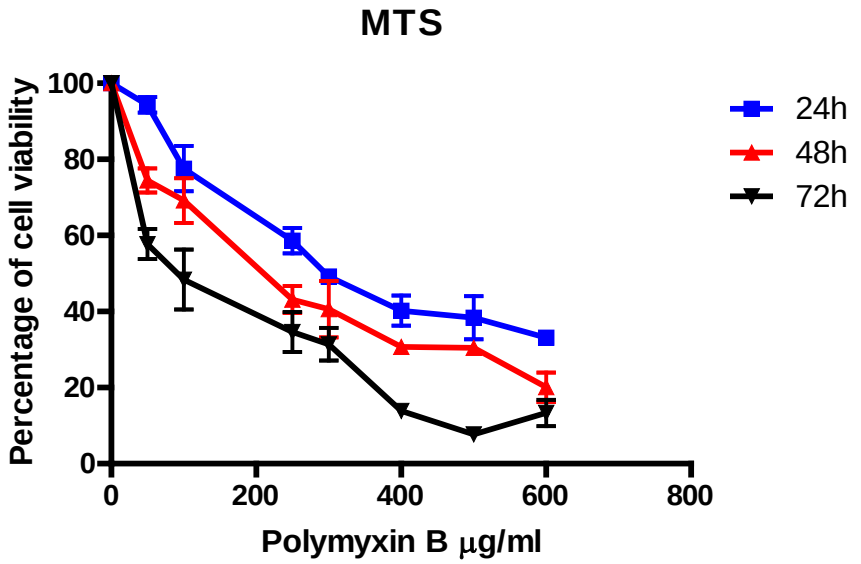

Figure 4.10: Cell viability in human PTCs treated with range concentrations of polymyxin B for 24, 48 and 72 hours.

MTS assay was used to measure the cell viability. Polymyxin B showed a time and concentrations dependent. For example, the cell viability after 250 μg/ml polymyxin B treatment for 24h was 58.6% and the percentage dropped to 43.1% after 48h. In addition, cell viability after 300 μg/ml polymyxin B treatment for 72h was 31.7% and after 500 μg/ml polymyxin B the cell viability decreased to 7.7%. Each point represent mean ± S.E.M values of each polymyxin B concentration.

4.3.2 KIM-1 produced after treatment of human PTCs in presence of a range concentration of polymyxin B

The effect on human PTCs treated with a range concentration of polymyxin B were investigated. The level of KIM-1 was normalised to the cell viability. The results are shown in Figure 4.11**.**

KIM-1 concentrations increased significantly relative to non-treated cells after 24h polymyxin B treatment. KIM-1 levels were elevated significantly and gradually by 50 to 600 µg/ml polymyxin B concentrations. The production of KIM-1 after 250 µg/ml polymyxin B treatment was 24.11±7.21 ng/ml compared with the control 1.59±0.28 ng/ml and then the level of KIM-1 was the same as the concentration of polymyxin B increases up to 600 µg/ml.

KIM-1 concentrations rose considerably after 48h of polymyxin B treatment compared to non-treated cells. The level of KIM-1, compared to control 3.47±0.47 ng / ml, was after 300 µg / ml polymyxin B treatment at 55.43±17.72 ng / ml, and then the KIM-1 level, with the polymyxin B treatment rising up to 600 µg / ml, increased significantly.

The levels of KIM-1 after 72h treatment of polymyxin B increased significantly compared to non-treated cells. For instance, KIM-1 production after 250 µg/ml polymyxin B treatment was 62.15±14.30 ng/ml compared with the control 9.81±1.1 ng/ml and then the level of KIM-1 increased as the concentration of polymyxin B increases up to 600 µg/ml.

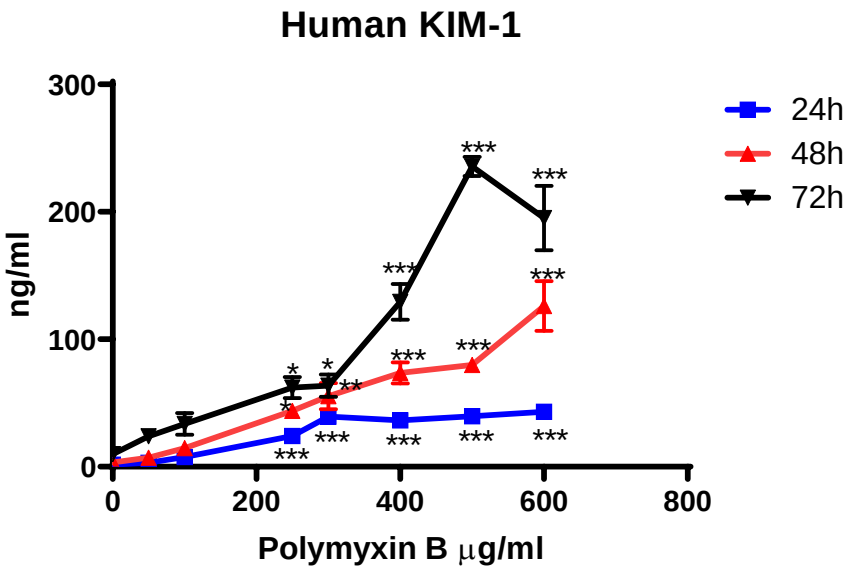

Figure 4.11: Measurement of KIM-1 production from human PTCs treated with range concentrations of polymyxin B for 24, 48 and 72 hours.

*Levels were normalised to MTS absorbance value to account for cell numbers after nephrotoxin treatments. Human PTCs were treated with a range of polymyxin B concentration (50 to 600 µg/ml). The levels of KIM-1 showed, polymyxin B is time and concertation dependent. For example, KIM-1 production after 100 µg/ml polymyxin B treatment for 24h was 7.7±1.7 ng/ml and after 250 µg/ml the level of KIM-1 increased to 24.1±7.2 ng/ml. The level of KIM-1 after 400 µg/ml polymyxin B treatment for 48h was 73.6±14.1 ng/ml and after 72h the level increased to 129.3±24.4 ng/ml. Statistical analysis was conducted using repeated-measures-paired-one-way ANOVA the data are representative of three independent experiments (n=3). Each point mean ± S.E.M values of each group. (*p < 0.05, **p < 0.01, ***p < 0.001).*

4.3.3 NGAL produced after treatment of human PTCs in presence of a range concentration of polymyxin B

The NGAL production after treated human PTCs with a range concentration of polymyxin B were investigated. The concentrations of NGAL was normalised to the cell viability. The results are shown in Figure 4.12**.**

There were a significant increase in NGAL levels after 24h treatment of polymyxin B compared to non-treated cells. NGAL levels were elevated significantly by (50 to 600) µg/ml polymyxin B concentrations. For example, the level of NGAL production was at 100 µg/ml polymyxin B to 16.37±2.96 ng/ml compared with the control 6.1±0.45 ng/ml and then the level of NGAL remained the same as the concentration of polymyxin B increases up to 600 µg/ml.

The levels of NGAL increased significantly in comparison with non-treated cells after 48h of gentamicin treatment. The maximum level of NGAL was after 600 µg / ml polymyxin B treatment 426.18±130.72 ng / ml compared to the control 18.78±3.1 ng / ml.

The NGAL levels after 72h treatment of polymyxin B increased significantly compared to non-treated cells. For example, the level of NGAL production after 250 µg/ml polymyxin B treatment was 306.19±65.39 ng/ml compared with the control 40.95±3.84 ng/ml and then the level of NGAL increased as the concentration of polymyxin B increases up to 600 µg/ml.

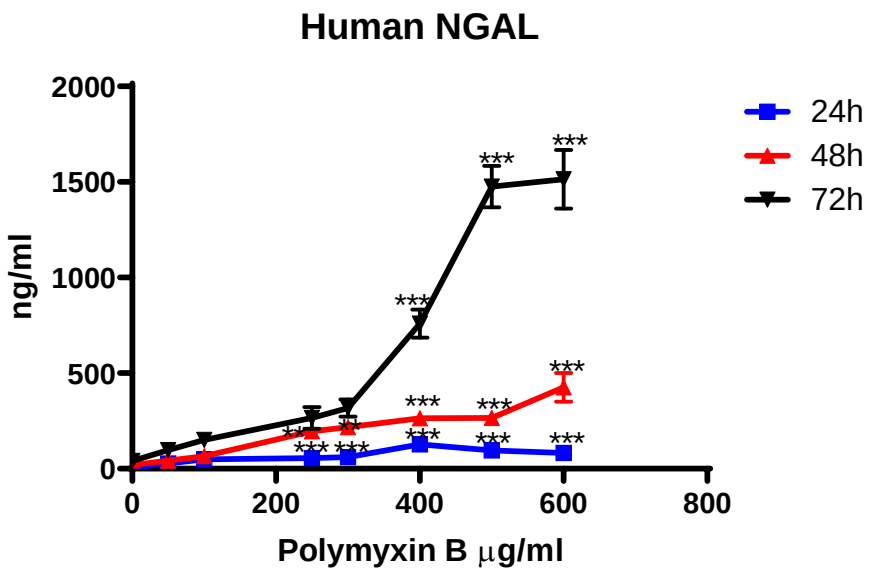

Figure 4.12: Measurement of NGAL production from human PTCs treated with range concentrations of polymyxin B for 24, 48 and 72 hours.

*Levels were normalised to MTS absorbance value to account for cell numbers after nephrotoxin treatments. Human PTCs were treated with a range of polymyxin B concentration (50 to 600 µg/ml). For example, NGAL production after 300 µg/ml polymyxin B treatment for 24h was 50.7±0.3 ng/ml and after 500 µg/ml the level of NGAL increased to 68.7±15.4 ng/ml. The level of NGAL after 250 µg/ml polymyxin B treatment for 48h was 195.32±24.4 ng/ml and after 72h the level increased to 306.1±65.3 ng/ml. Statistical analysis was conducted using repeated-measures-paired-one-way ANOVA the data are representative of three independent experiments (n=3). Each point mean ± S.E.M values of each group. (*p < 0.05, **p < 0.01, ***p < 0.001).*

4.3.4 Clusterin produced after treatment of human PTCs in presence of a range concentration of polymyxin B

The impact of a range of polymyxin B concentrations on clusterin levels produced by human PTCs were investigated. The concentrations of the biomarker was normalised to the cell viability. The results are shown in Figure 4.13.

Clusterin concentrations rose considerably in comparison with non-treated cells concentrations after 24 h polymyxin B incubation. Clusterin levels were increased gradually and significantly by 50 to 600 µg/ml polymyxin B concentrations treatment. The level of clusterin after 300 µg/ml gentamicin treatment was 64.92±5.30 ng/ml compared with the non-treated cells 6.43±0.49 ng/ml and then the level of clusterin remained at stable as the concentration of polymyxin B increases up to 600 µg/ml.

After 48h of polymyxin B incubation, clusterin concentrations significantly increased compared with non-treated cells. The highest production of clusterin, compared to control 26.52±2.82 ng / ml, was after 250 µg / ml polymyxin B treatment at 203.25±30.81 ng / ml, and then the clusterin level, with the polymyxin B rising up to 600 µg / ml, remained almost the same.

The clusterin production after 72h treatment of polymyxin B increased significantly compared to non-treated cells. For instance, clusterin levels were gradually elevated by 50, 100, 250 and 300 µg/ml polymyxin B concentrations. The level of clusterin after 300 µg/ml polymyxin B treatment was 332.53±72.1 ng/ml compared with the control 44.57±1.1 ng/ml.

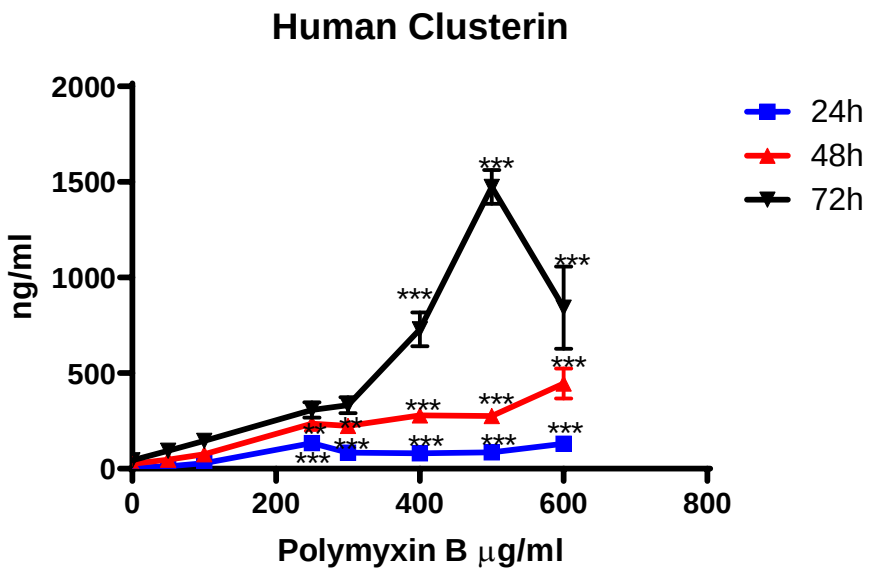

Figure 4.13: Measurement of clusterin production from human PTCs treated with a range of concentrations of polymyxin B for 24, 48 and 72 hours.

*Levels were normalised to MTS absorbance value to account for cell numbers after nephrotoxin treatments. Human PTCs were treated with a range of polymyxin B concentration (50 to 600 µg/ml). For example, clusterin production after 250 µg/ml polymyxin B treatment for 24h was 54.8±2.3 ng/ml and after 500 µg/ml the level of clusterin increased to 85.6±19.7 ng/ml. The level of clusterin after 300 µg/ml polymyxin B treatment for 48h was 223.7±30.8 ng/ml and after 72h the level increased to 307.8±69.4 ng/ml. Statistical analysis was conducted using repeated-measures-paired-one-way ANOVA the data are representative of three independent experiments (n=3). Each point mean ± S.E.M values of each group. (*p < 0.05, **p < 0.01, ***p < 0.001).*

4.3.5 MTS and ATP cell viability assays

After 24 and 48 hours treatment with 250 µg / ml polymyxin B, cell viability was measured. The cell viability was also measured in the presence of rosuvastatin co-treatments. The cell viability from the same plate was assessed using both MTS and ATP assays. The results showed no significant difference between the two methods used for cell viability. The results are shown in Figure 4.14**.**

After 24h of treatment, the results revealed that cell viability decreased significantly in response to exposure to polymyxin B to 74.52±4.88% of control. The rosuvastatin co treatment did not change the cell viability (96.16±2.85% live cells). The treatment of polymyxin B with rosuvastatin increased the live cells compared to only polymyxin B (87.25±4.26%).

The cell viability was reduced significantly by polymyxin B (65.55±8.1%) after 48h of treatment. However, the cell viability did not change with rosuvastatin (94.99±2.94 %). The cell viability after polymyxin B with rosuvastatin was higher than only polymyxin B (77.65±5.17% viable cells).

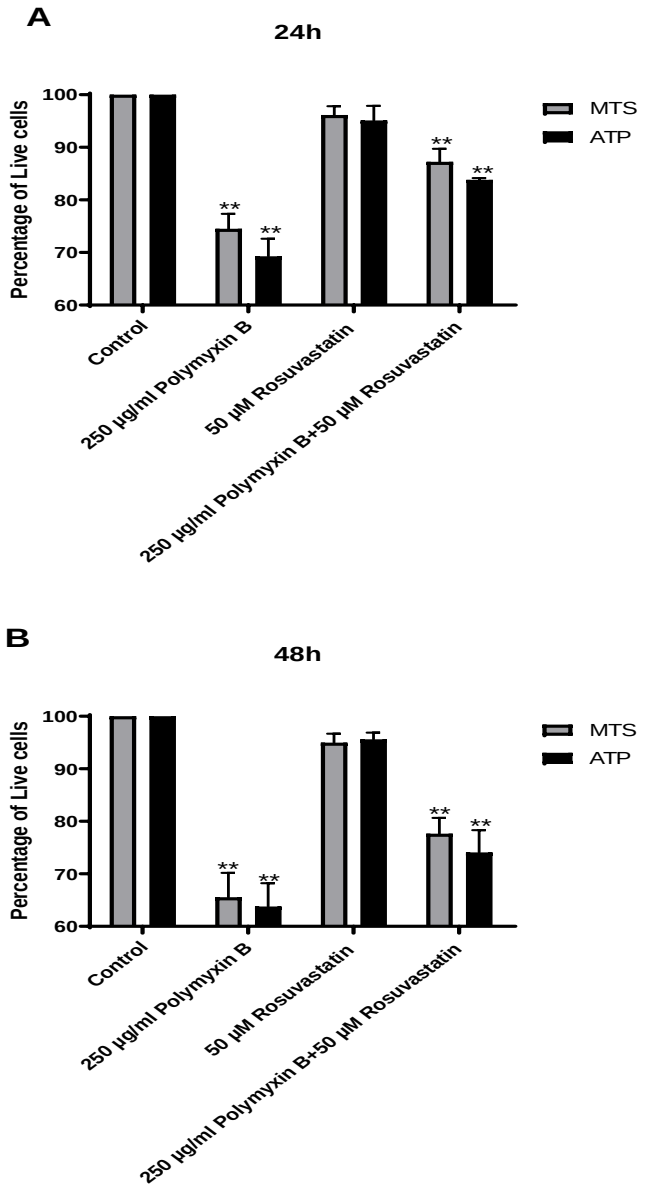

Figure 4.14: Cells Viability of human PTCs after treatment of polymyxin B for 24 and 48 hours.

MTS and ATP assays were used to measure the cell viability. Viability is measured as a percentage of the control. For example, MTS percentage after polymyxin B treatment for 24h was 74.5% and ATP percentage was 69.2%. In addition, the co-treatment of rosuvastatin *with polymyxin B for 48h showed, the percentage of MTS was 77.6% and ATP percentage was 74.1%. Statistical analysis was conducted using repeated-measures-paired-one-way ANOVA the data are representative of three independent experiments (n=3). Bars represent mean ± S.E.M values of each group. (*p < 0.05, **p < 0.01, ***p < 0.001).*

4.3.6 Lactate dehydrogenase (LDH) cytotixicy assay

LDH released by damaged cells was measured. In this experiment, we treated human PTCs for 24 and 48 hours with 250 μg/ml polymyxin B and LDH was measured. In addition, we measured the LDH after rosuvastatin co treatment. The results are consistent with cell viability data. Result is shown in Figure 4.15

After 24h, the results revealed that LDH increased significantly in response to exposure to polymyxin B to 40.62±4.17%. The rosuvastatin co treatment did not change the LDH (12.1±0.27%). The treatment of polymyxin B with cilastatin decreased the LDH compared to only polymyxin B (27.38±2.21%).

The LDH was increased significantly by polymyxin B (47.91±5.1%) after 48h treatment. However, the LDH did not change with rosuvastatin (12.41±0.95%). The LDH after polymyxin B with cilastatin was lower than only polymyxin B (33.01±3.49%).

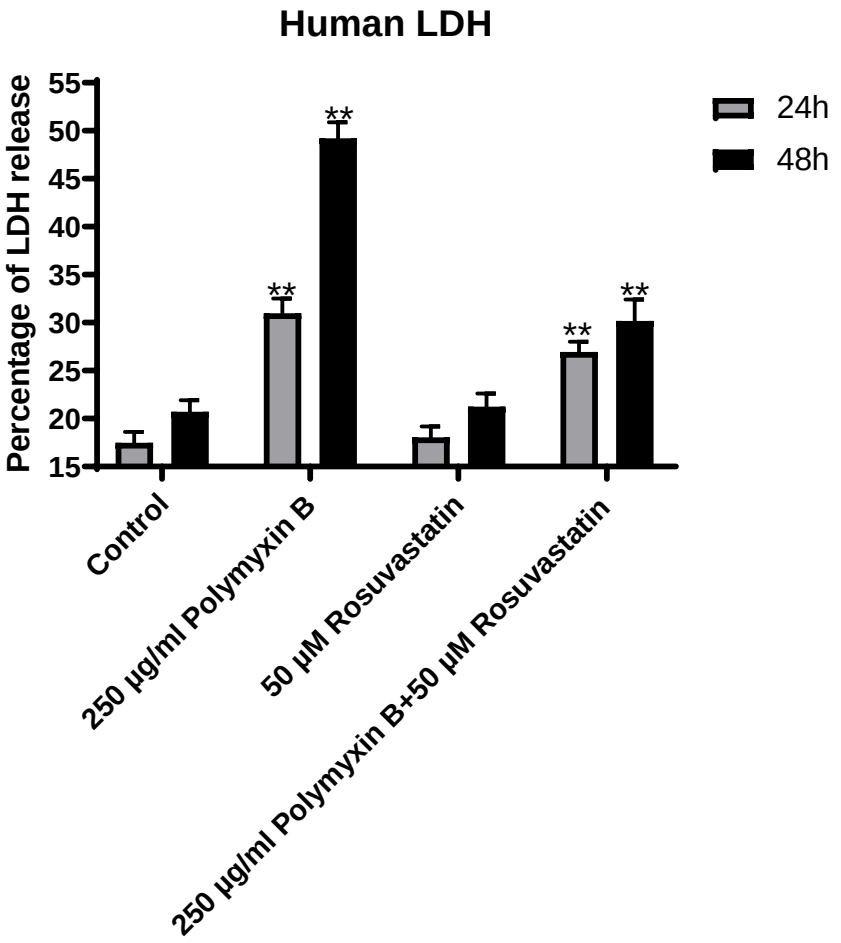

Figure 4.15: LDH of human PTCs after treatment of polymyxin B for 24 and 48 hours.

*LDH is measured as a percentage of the control. LDH percentage after polymyxin B treatment for 24h was 40.6% and after 48h the percentage increased to 47.9%. In addition, LDH percentage decreased after rosuvastatin co-treatment with polymyxin B for 48h to 33.1% Statistical analysis was conducted using repeated-measures-paired-one-way ANOVA the data are representative of three independent experiments (n=3). Bars represent mean ± S.E.M values of each group. (*p < 0.05, **p < 0.01, ***p < 0.001).*

4.3.7 KIM-1 production after treatment of human PTCs in presence of polymyxin B +/- rosuvastatin

The quantity of KIM-1 produced after human PTCs were exposed for 24 and 48 hours with 250 µg / ml polymyxin B were investigated. The levels of KIM-1 was also measured in the presence rosuvastatin co-treatments. The concentrations of KIM-1 was normalised to the cell viability as determined from their MTS absorbance's, expressed as ng/ml. The results are shown in Figure 4.16**.**

After 24h treatment of polymyxin B, the amount of KIM-1 in the apical membrane did change significantly from the control (1.73±0.51 to 5.25±1.01 ng/ml, $P < 0.01$). However, the presence of rosuvastatin did not change KIM-1 level to 1.71±0.55 ng/ml compared to control 1.73±0.51 ng/ml. The co-treatment of polymyxin B with rosuvastatin caused a significant decrease in KIM-1 in the apical membrane (2.44±0.81 ng/ml, $P < 0.0001$) compared to only polymyxin B. In comparison with apical membrane, basolateral membrane levels of KIM-1 were undetectable.

The amount of KIM-1 on the apical membrane changed significantly from the control after 48h of treatment with polymyxin B (20.80±5.08 ng/ml, $P < 0.01$). However, when we added rosuvastatin did not change KIM-1 level 6.98±1.28 ng/ml compared to control 6.77±1.18 ng/ml. The co-treatment of polymyxin B with rosuvastatin caused a significant decline in KIM-1 in the apical membrane (13.01±3.55 ng/ml, $P < 0.0001$) compare to only polymyxin B. In comparison with apical membrane, the basolateral membrane levels of KIM-1 were small.

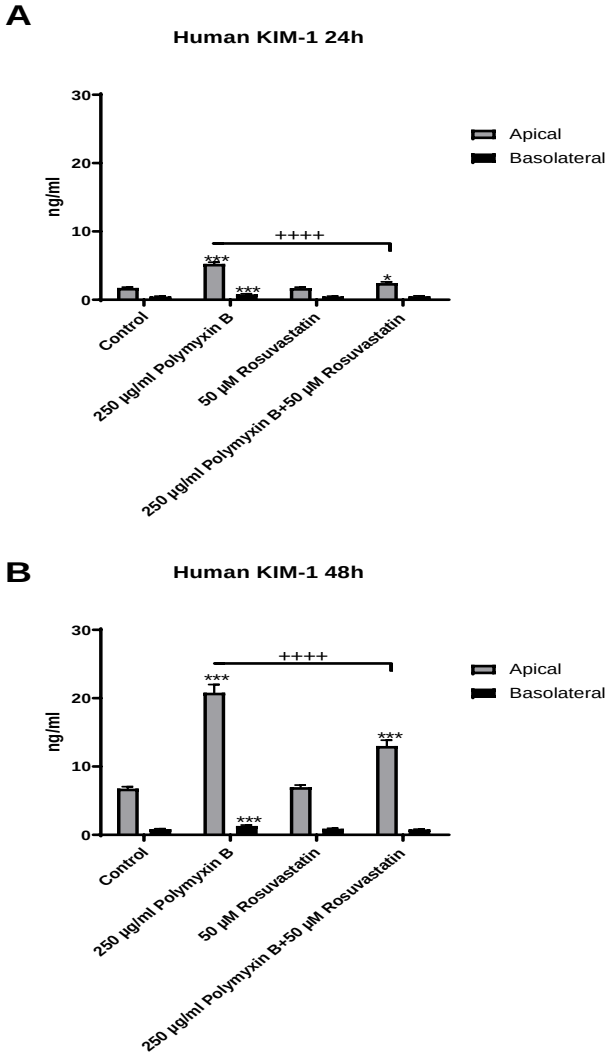

Figure 4.16: The amount of KIM-1 produced after treatment of human PTCs for 24 and 48 hours in presence of polymyxin B +/- rosuvastatin.

*ELISA was used to measure KIM-1 production. For example, KIM-1 production in the apical membrane is significantly higher than basolateral membrane. The amount of KIM-1 in the apical membrane change significantly from the control (5.25±1.01 ng/ml, P < 0.01) after 24h polymyxin B treatment. After co-treatment with rosuvastatin, KIM-1 level decreased to (8.16±1.39 ng/ml, P < 0.0001) compared to only polymyxin B. The level of KIM-1 after 48h treatment was more than 3 fold compared to 24h. Statistical analysis was conducted using repeated-measures-paired-one-way ANOVA the data are representative of three independent experiments (n=3). Bars represent mean ± S.E.M values of each group. (*p < 0.05, **p < 0.01, ***p < 0.001, ++++p < 0.0001).*

4.3.8 NGAL production after treatment of human PTCs in presence of polymyxin B +/- rosuvastatin

NGAL production for 24 and 48 hours in the presence of 250 µg/ml polymyxin B following treatment of human PTCs. In the presence of rosuvastatin co-treatment, levels of NGAL were also measured. NGAL concentrations had been normalized to cell viability based on the MTS absorption of the human PTCs, resulting in ng / ml. Figure 4.17 shows the results.

In 24h treatment of polymyxin B, the amount of NGAL in the apical membrane did increased significantly from the control (70.16±18.28 ng/ml, $P < 0.01$). However, the presence of rosuvastatin did not change NGAL level 20.52±5.60 ng/ml compared to control 20.41±5.56 ng/ml. The co-treatment of polymyxin B with rosuvastatin caused a significant decrease in NGAL in the apical membrane (43.75±15.54 ng/ml, $P < 0.0001$) compared to only polymyxin B. NGAL concentrations in the basolateral membrane were very low compared to apical membrane.

After 48h treatment of polymyxin B, the amount of NGAL in the apical membrane did increase significantly from the control (178.28±49.36 ng/ml, $P < 0.01$). However, the presence of rosuvastatin did not change NGAL level 38.83±15.78 ng/ml compared to control 38.72±14.58 ng/ml. The co-treatment of polymyxin B with rosuvastatin caused a significant decrease in NGAL in the apical membrane (108.20±9.45 ng/ml, $P < 0.0001$) compared to only polymyxin B. Compared to apical membrane, NGAL levels in the basolateral membrane were low.

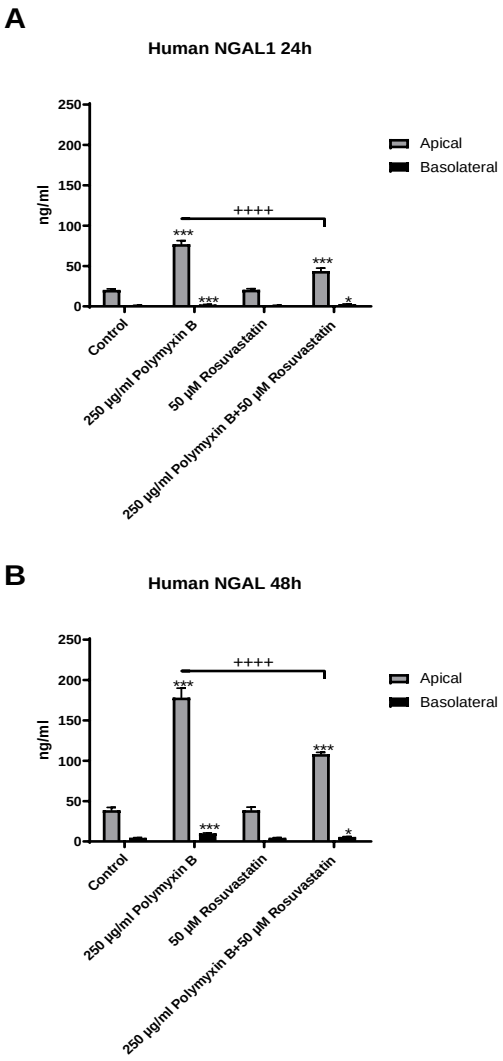

Figure 4.17: The amount of NGAL produced after treatment of human PTCs for 24 and 48 hours in presence of polymyxin B +/- rosuvastatin.

*ELISA was used to measure NGAL production. For example, NGAL production in the apical membrane is significantly higher than basolateral membrane. The amount of NGAL in the apical membrane change significantly from the control (70.16±18.28 ng/ml, P < 0.01) after 24h polymyxin B treatment. After co-treatment with rosuvastatin, NGAL level decreased to (43.75±15.54 ng/ml, P < 0.0001) compared to only polymyxin B. The level of NGAL after 48h treatment was more than 2 fold compared to 24h. Statistical analysis was conducted using repeated-measures-paired-one-way ANOVA the data are representative of three independent experiments (n=3). Bars represent mean ± S.E.M values of each group. (*p < 0.05, **p < 0.01, ***p < 0.001, ++++p < 0.0001).*

4.3.9 Clusterin production after treatment of human PTCs for in presence of polymyxin B +/- rosuvastatin

Clusterin production in the presence of 250 µg / ml of polymyxin B was measured after 24 and 48 hours of human PTC treatment using ELISA. Clusterin levels were also measured in the presence of rosuvastatin co-treatment. Levels of clusterin were normalized to cell viability based on the PTCs ' MTS absorption, resulting in ng / ml. The results are shown in Figure 4.18**.**

After 24h treatment of polymyxin B, the amount of clusterin in the apical membrane did increase significantly from the control (95.63±18.11 ng/ml, $P < 0.01$). However, the presence of rosuvastatin did not change clusterin level 19.22±5.29 ng/ml compared to control 19.28±8.64 ng/ml. The co-treatment of polymyxin B with rosuvastatin caused a significant decrease in clusterin in the apical membrane (42.42±12.12 ng/ml, $P < 0.0001$) compared to only polymyxin B. The levels of clusterin in the basolateral membrane were low compared to the apical membrane.

After 48h of polymyxin B treatment, the amount of clusterin in the apical membrane changed significantly from control (411.27±147.69 ng/ml, $P < 0.01$). However, when we added rosuvastatin did not change clusterin level 76.25±10.72 ng/ml compared to control 76.88±12.14 ng/ml. The co-treatment of polymyxin B with rosuvastatin caused a significant decrease in clusterin in the apical membrane (240.29±78.68 ng/ml, $P < 0.0001$) compare to only polymyxin B. Clusterin levels in the basolateral membrane were low compared to apical membrane.

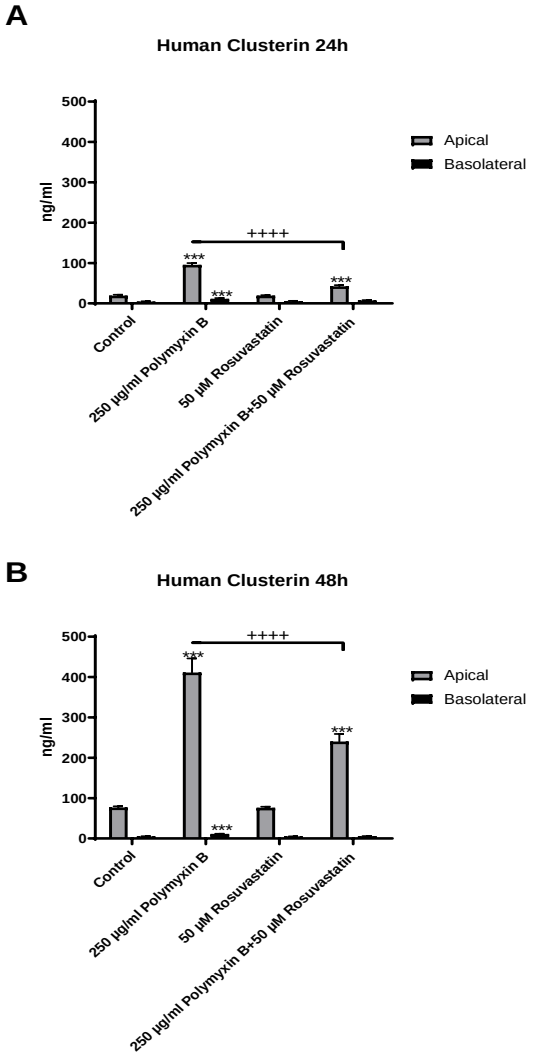

Figure 4.18: The amount of clusterin produced after treatment of human PTCs for 24 and 48 hours in presence of polymyxin B +/- rosuvastatin.

*ELISA was used to measure clusterin production. For example, clusterin production in the apical membrane is significantly higher than basolateral membrane. The amount of clusterin in the apical membrane change significantly from the control (95.63±18.11 ng/ml, P < 0.01) after 24h polymyxin B treatment. After co-treatment with rosuvastatin, clusterin level decreased to (42.42±12.12 ng/ml, P < 0.0001) compared to only polymyxin B. The level of clusterin after 48h treatment was more than 3 fold compared to 24h. Statistical analysis was conducted using repeated-measures-paired-one-way ANOVA the data are representative of three independent experiments (n=3). Bars represent mean ± S.E.M values of each group. (*p < 0.05, **p < 0.01, ***p < 0.001, ++++p < 0.0001).*

4.4 Small molecule nephrotoxin – Cisplatin

Before quantifying the expression of biomarkers using ELISA, human PTCs were treated with cisplatin, a known nephrotoxin. The uptake of cisplatin in human PTC is regulated by OCT2 transporter in the basolateral membrane. The effects of cisplatin on human PTC monolayers were important as toxicity induced by cisplatin is already well characterized and can be compared in vivo.

4.4.1 MTS cell viability after treatment in presence of range of concentrations of cisplatin

After cisplatin concentration ranges (5 to 40 µM) were used for 24, 48 and 72 hours for human PTCs, the cell viability was measured. MTS assay was used to assess cell viability. The MTS absorbance show as a percentage normalised to non-treated cells. The results are shown in Figure 4.19.

The findings from MTS assay show the impact of cisplatin on human PTCs. With the rise in cisplatin concentration, cell viability reduced significantly. For example, after 24h treatment with 20 µM cisplatin the cell viability was 67.83% compared to non-treated cells. The percentage of live cells was less than 30% after 30 µM cisplatin treatment.

After 48h, the cisplatin dose decreases the percentage of live cells. For instance, at 25 µM cisplatin the percentage of live cells was 59%. The live cells was less than 55% after 35 µM cisplatin.

There was a major decrease in cell viability after 72h treatment with a range of concentration of cisplatin. After 15 µM cisplatin treatment, live cells reduced more than 30%. In addition, after 40 µM cisplatin incubation the cell viability was only 11%.

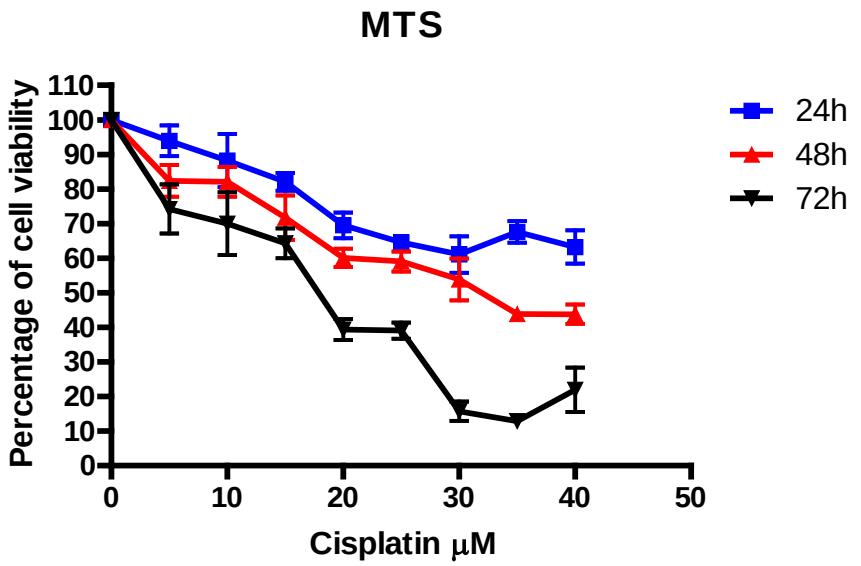

Figure 4.19: Cell viability in human PTCs treated with range concentrations of cisplatin for 24, 48 and 72 hours.

MTS assay was used to measure the cell viability. Cisplatin showed a time and concentrations dependent after 24, 48 and 72 hours treatment. For example, the cell viability after 25 μM cisplatin for 24h was 64.5% and the percentage dropped to 59.1% after 48h. In addition, cell viability after 10 μM cisplatin treatment for 72h was 80.8% and after 20 μg/ml cisplatin the cell viability decreased to 39.3%. Each point represent mean ± S.E.M values of each cisplatin concentration.

4.4.2 KIM-1 production after treatment of human PTCs in presence of a range concentration of cisplatin

The effects of a range of cisplatin concentrations on KIM-1 levels produced by human PTCs were explored. The concentrations of the biomarker was normalised to the cell viability. The results are shown in Figure 4.20.

KIM-1 concentrations rose considerably after 24h of cisplatin treatment compared to non-treated cells. For instance, the level of KIM-1 production at 20 µM cisplatin to 58.11±9.92 ng/ml compared with the control 2.40±0.83 ng/ml and then the level of KIM-1 increased as the concentration of cisplatin increases up to 40 µM.

The levels of KIM-1 increased significantly in comparison with non-treated cells after 48h of cisplatin treatment. The KIM-1 levels have been considerably increased by 5 to 30 µM cisplatin treatment. Compared to control 4.21±0.39 ng / ml, the peak level of KIM-1 was at 83.41±9.94 ng / ml after 30 µM cisplatin treatment, and then the KIM-1 level increased, with cisplatin levels rising to 40 µM.

The KIM-1 levels increased significantly compared to non-treated cells after 72h of cisplatin treatment. For instance, KIM-1 levels were elevated significantly by 5, 10, 15 and 20 µM cisplatin concentrations. The level of KIM-1 production reached the peak at 20 µM cisplatin treatment to 98.62±10.74 ng/ml compared with the control 19.1±5.13 ng/ml and then the level of KIM-1 was increased as the concentration of cisplatin increases up to 40 µM.

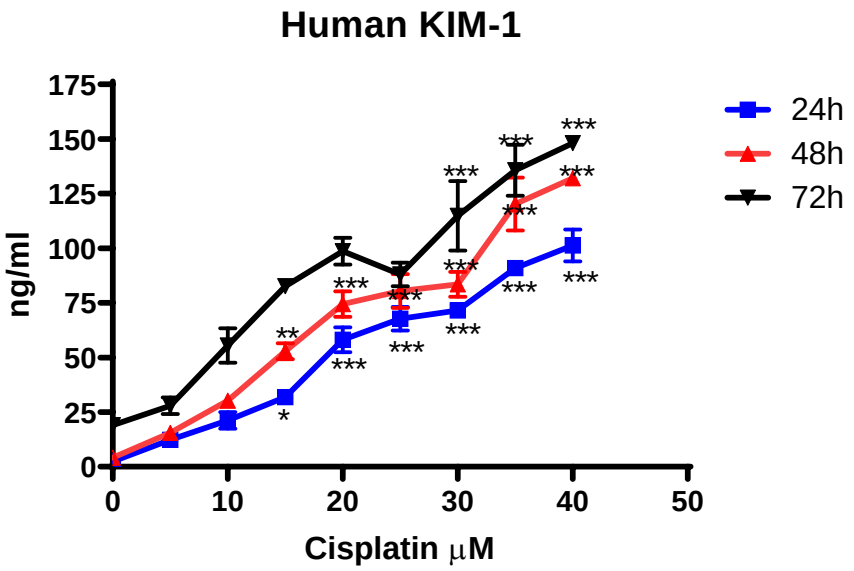

Figure 4.20: Measurement of KIM-1 production from human PTCs treated with range concentrations of cisplatin for 24, 48 and 72 hours.

*Levels of KIM-1 were normalised to MTS absorbance value to account for cell numbers after nephrotoxin treatments. Human PTCs were treated with a range of cisplatin concentration (5 to 40 µM). For example, KIM-1 production after 10 µM cisplatin treatment for 24h was 4.5±0.7 ng/ml and after 25 µM the level of KIM-1 increased to 7.8±1.1 ng/ml. The level of KIM-1 after 30 µM cisplatin treatment for 48h was 26.7±7.7 ng/ml and after 72h the level increased to 114.8±27.6 ng/ml. Statistical analysis was conducted using repeated-measures-paired-one-way ANOVA the data are representative of three independent experiments (n=3). Each point mean ± S.E.M values of each group. (*p < 0.05, **p < 0.01, ***p < 0.001).*

4.4.3 NGAL production after treatment of human PTCs in presence of a range concentration of cisplatin

After treatment of human PTCs with a range of cisplatin concentrations, NGAL production was explored. NGAL concentrations were normalized to the viability of the cell. The results are shown in Figure 4.21**.**

NGAL concentrations have increased significantly relative to non-treated cells after 24h cisplatin treatment. NGAL levels were elevated significantly by (5 to 30) µM cisplatin concentrations. The highest level of KIM-1 production was at 30 µM cisplatin to 345.60±93.1 ng/ml compared with the control 30.22±5.86 ng/ml and then the level of NGAL decreased as the concentration of cisplatin increases up to 40 µM.

NGAL levels increased significantly after 48h of cisplatin treatment compared to non-treated cells. The NGAL levels increased by 5 to 35 µM cisplatin. The level of NGAL reached the peak after 35 µM cisplatin treatment 460.23±137.88 ng / ml compared to the control 45.45±11.38 ng / ml.

The NGAL levels increased significantly in comparison with non-treated cells after 72h of cisplatin treatment. For example, the level of NGAL production at 25 µM cisplatin treatment was 412.78±143.1 ng/ml compared with the control 83.16±17.40 ng/ml and then the level of NGAL increased as the concentration of cisplatin increases up to 40 µM.

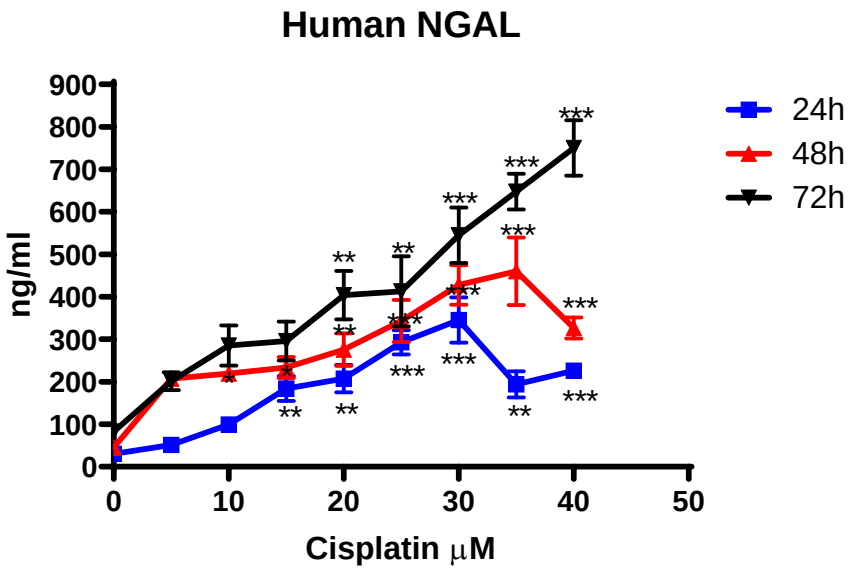

Figure 4.21: Measurement of NGAL production from human PTCs treated with range concentrations of cisplatin for 24, 48 and 72 hours.

*Levels of NGAL were normalised to MTS absorbance value to account for cell numbers after nephrotoxin treatments. Human PTCs were treated with a range of cisplatin concentration (5 to 40 µM). For example, NGAL production after 20 µM cisplatin treatment for 24h was 207.1±56.1 ng/ml and after 30 µM the level of NGAL increased to 345.6±93.1. The level of NGAL after 25 µM cisplatin treatment for 48h was 343.3±24.4 ng/ml and after 72h the level increased to 412.7±143.1 ng/ml. Statistical analysis was conducted using repeated-measures-paired-one-way ANOVA the data are representative of three independent experiments (n=3). Each point mean ± S.E.M values of each group. (*p < 0.05, **p < 0.01, ***p < 0.001).*

4.4.4 Clusterin production after treatment of human PTCs in presence of a range concentration of cisplatin

The effects of a range of cisplatin concentrations on clusterin levels produced by human PTCs were investigated. The concentrations of the biomarker was normalised to the cell viability. The results are shown in Figure 4.22**.**

The level of clusterin considerably increased relative to non-treated cells after 24h cisplatin treatment. The level of clusterin reached the peak at 15 µM cisplatin to 211.23±17.75 ng/ml compared with the control 26.56±10.22 ng/ml and then the level of clusterin decreased slightly as the concentration of cisplatin increases up to 40 µM.

The levels of clusterin increased significantly in comparison with non-treated cells after 48h of cisplatin treatment. The clusterin levels increased by 5 to 25 µM cisplatin treatment. The highest clusterin level compared to 37.63±10.83 ng / ml was at 274.97±56.20 ng / ml after 25 µM cisplatin treatment, and then the clusterin level slightly decreased with a cisplatin level of up to 40 µM.

The clusterin production after 72h treatment of cisplatin increased significantly compared to non-treated cells. For instance, clusterin levels were gradually elevated by 5 to 25 µM cisplatin concentrations. Clusterin production peaked at 25 µM cisplatin to 356.53±59.95 ng / ml in comparison with the 72.98±13.41 ng / ml control, and then the clusterin production rose with a cisplatin concentration increased up to 40 µM.

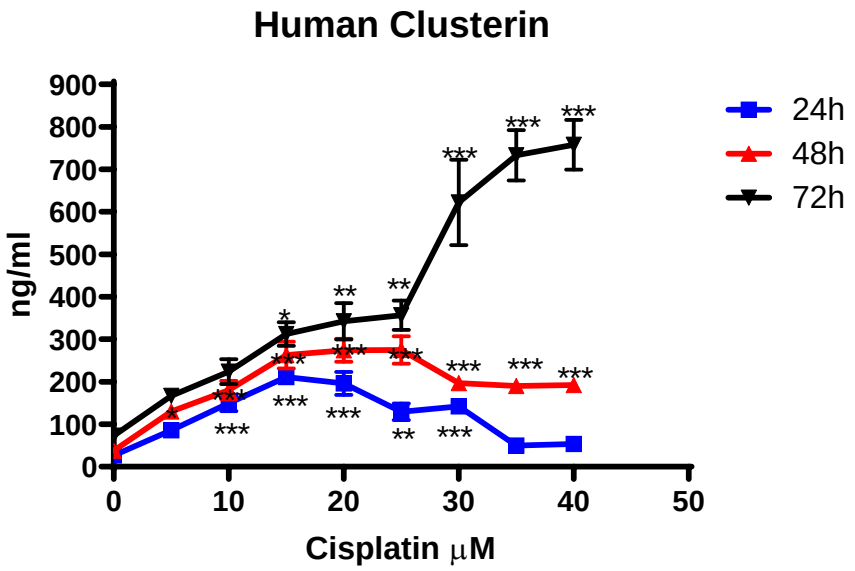

Figure 4.22: Measurement of clusterin production from human PTCs treated with range concentrations of cisplatin for 24, 48 and 72 hours.

*Levels were normalised to MTS absorbance value to account for cell numbers after nephrotoxin treatments. Human PTCs were treated with a range of cisplatin concentration (5 to 40 µM). For example, clusterin production after 25 µM cisplatin treatment for 24h was 129.4±33.9 ng/ml and after 40 µM the level of clusterin decreased to 53.3±9.6 ng/ml. The level of clusterin after 30 µM cisplatin treatment for 48h was 196.9±6.1 ng/ml and after 72h the level increased to 621.9±174.1 ng/ml. Statistical analysis was conducted using repeated-measures-paired-one-way ANOVA the data are representative of three independent experiments (n=3). Each point mean ± S.E.M values of each group. (*p < 0.05, **p < 0.01, ***p < 0.001).*

4.4.5 MTS and ATP cells viability assays

The cell viability was measured after treatment of human PTCs for 24 and 48 hours with 25 µM cisplatin. In the presence of cimetidine co-treatment, cell viability was also measured. Both MTS and ATP assays were used to assess cell viability from the same plate. No major difference was discovered between the two methods of assessment. The results are shown in Figure 4.23**.**

After 24h, the results showed that cell viability was considerably reduced to 71.25±2.98% as a result of exposure to cisplatin. The co-treatment with cimetidine hasn't altered cell viability (93.79±3.1% live cells). The treatment of cisplatin with cimetidine increased the live cells compared to only cisplatin (83.11±1.83%).

The cell viability was reduced significantly by cisplatin (61.18±3.76%) after 48h treatment. However, the cell viability did not change with cimetidine (93.44±1.36%). Cisplatin with cimetidine cell viability was higher than cisplatin alone (74.43±2.82% viable cells)

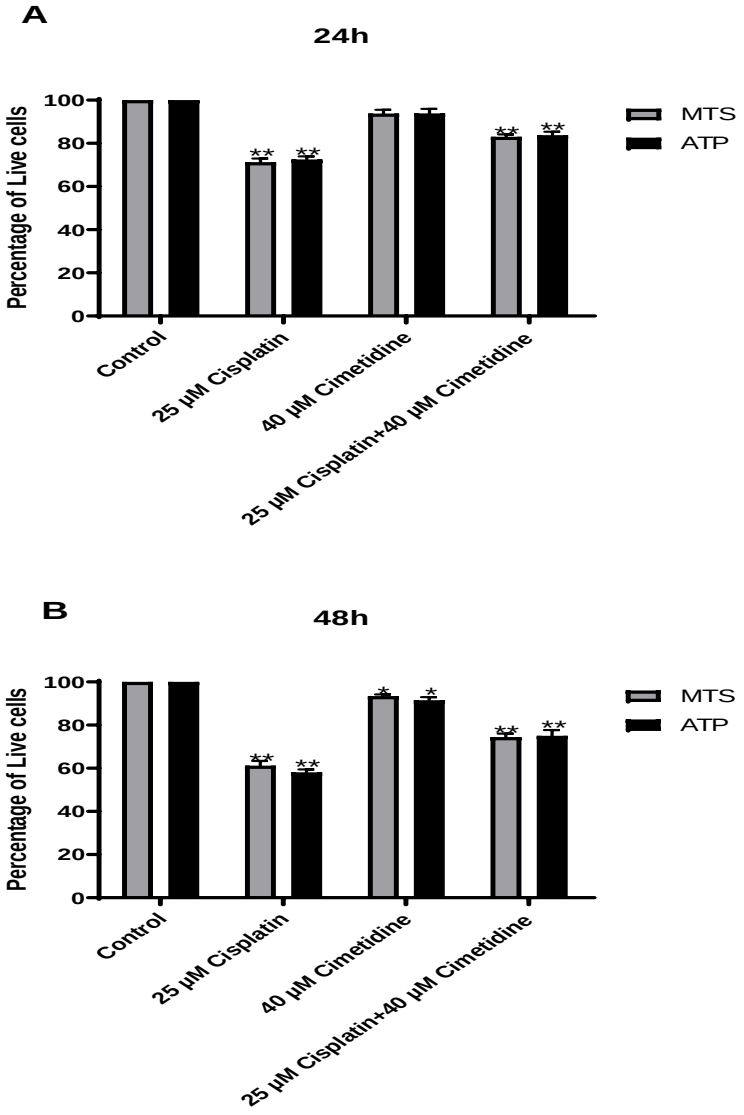

Figure 4.23: Cells Viability of human PTCs after treatment of cisplatin for 24 and 48 hours.

*MTS and ATP assays were used to measure the cell viability. Viability is measured as a percentage of the control. For example, MTS percentage after cisplatin treatment for 24h was 71.2% and ATP percentage was 72.5%. In addition, the co-treatment of cimetidine with cisplatin for 48h showed, the percentage of MTS was 74.4% and ATP percentage was 75.1%. Statistical analysis was conducted using repeated-measures-paired-one-way ANOVA the data are representative of three independent experiments (n=3). Bars represent mean ± S.E.M values of each group. (*p < 0.05, **p < 0.01, ***p < 0.001).*

4.4.6 Lactate dehydrogenase (LDH) cytotixicy assay

A common method for determining cytotoxicity is the measurement of cytoplasmic enzymes released by damaged cells. Treatment of human PTCs for 24 and 48 hours with 25 µM cisplatin and then LDH was measured. In addition, we measured the LDH after cimetidine co treatment. The results is consistent with cell viability data. Result shown in Figure 4.24.

After 24h, the results revealed that LDH increased significantly in response to cisplatin exposure to 34.38±2.72%. The cimetidine co treatment did not change the LDH (14.88±1.58%). The treatment of cisplatin with cimetidine decreased the LDH compared to only cisplatin (24.49±2.01%).

The LDH was increased significantly by cisplatin (47.1±1.67%) after 48h.However, the LDH did not change with cimetidine (18.89±1.39%). The LDH after cisplatin with cimetidine was lower than only cisplatin (32.59±2.33%).

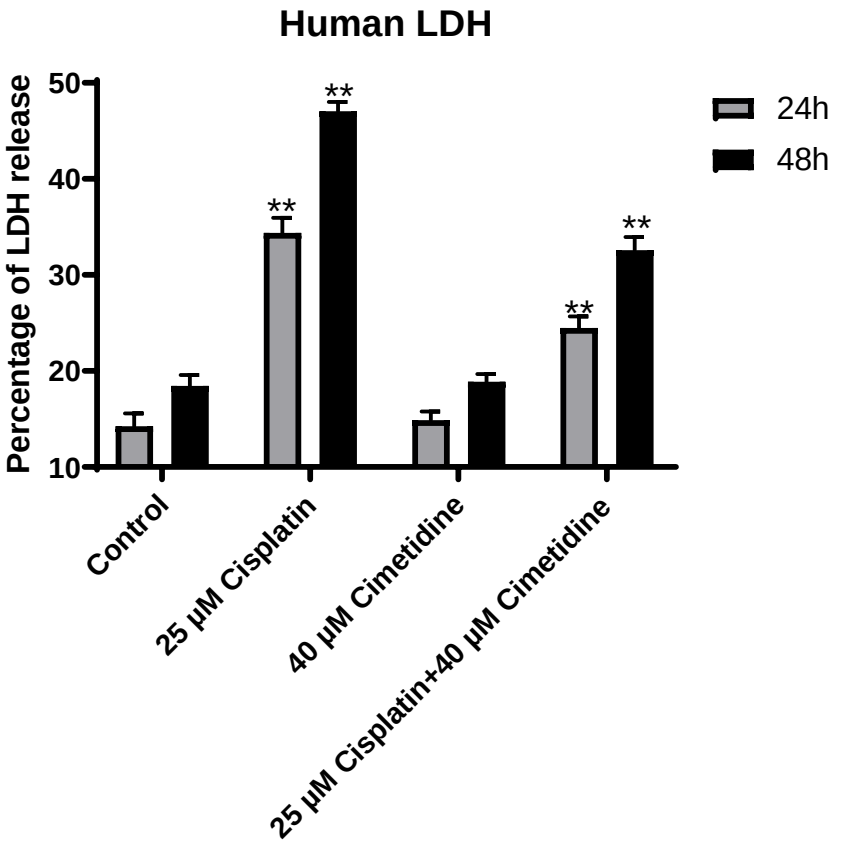

Figure 4.24: LDH of human PTCs after treatment of cisplatin for 24 and 48 hours.

*LDH is measured as a percentage of the control. LDH percentage after cisplatin treatment for 24h was 34.3% and after 48h the percentage increased to 47.1%. In addition, LDH percentage decreased after cimetidine co-treatment with cisplatin for 48h to 32.5% Statistical analysis was conducted using repeated-measures-paired-one-way ANOVA the data are representative of three independent experiments (n=3). Bars represent mean ± S.E.M values of each group. (*p < 0.05, **p < 0.01, ***p < 0.001).*

4.4.7 KIM-1 production after treatment of human PTCs in presence of cisplatin +/- cimetidine

The quantity KIM-1 generated after 24 and 48 hours of human PTC treatment in the presence of 25 μM cisplatin were investigated. In presence of cimetidine co-treatments, the levels of KIM-1 were also measured. The concentrations of KIM-1 was normalised to the cell viability as determined from their MTS absorbance's, expressed as ng/ml. The results are shown in Figure 4.25.

After 24h treatment of cisplatin, the amount of KIM-1 in the apical membrane did change significantly from the control (3.55±1.07 ng/ml, $P < 0.01$). However, the presence of cimetidine did not change KIM-1 level 0.074±0.22 ng/ml compared to control 0.077±0.21 ng/ml. The co-treatment of cisplatin with cimetidine caused a significant decrease in KIM-1 in the apical membrane (2.10±0.66 ng/ml, $P < 0.0001$) compared to only cisplatin. KIM-1 levels in the basolateral membrane were undetectable compared to apical membrane.

After 48h treatment of cisplatin, the amount of KIM-1 in the apical membrane did increase significantly from the control (14.61±3.49 ng/ml, $P < 0.01$). However, when we added cimetidine did not change KIM-1 level 4.49±0.61 ng/ml compared to control 4.96±1.48 ng/ml. The co-treatment of cisplatin with cimetidine caused a significant decrease in KIM-1 in the apical membrane (8.99±1.95 ng/ml, $P < 0.0001$) compare to only cisplatin. Compared to apical membrane, KIM-1 concentrations in the basolateral membrane were low.

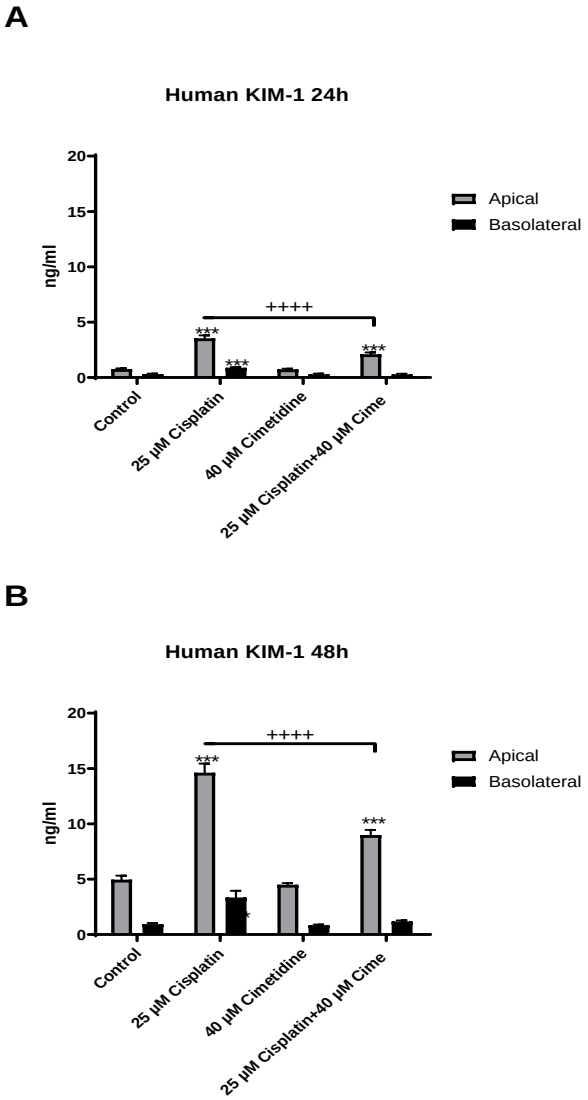

Figure 4.25: The amount of KIM-1 produced after treatment of human PTCs for 24 and 48 hours in presence of cisplatin +/- cimetidine.

*ELISA was used to measure KIM-1 production. For example, KIM-1 production in the apical membrane is significantly higher than basolateral membrane. The amount of KIM-1 in the apical membrane change significantly from the control (3.55±1.07 ng/ml, P < 0.01) after 24h cisplatin treatment. After co-treatment with cimetidine, KIM-1 level decreased to (2.10±0.66 ng/ml, P < 0.0001) compared to only cisplatin. The level of KIM-1 after 48h treatment was almost 4 fold compared to 24h. Statistical analysis was conducted using repeated-measures-paired-one-way ANOVA the data are representative of three independent experiments (n=3). Bars represent mean ± S.E.M values of each group. (*p < 0.05, **p < 0.01, ***p < 0.001, ++++p < 0.0001).*

4.4.8 NGAL production after treatment of human PTCs in presence of cisplatin +/- cimetidine

NGAL production for 24 and 48 hours in the presence of cisplatin following treatment of human PTCs. In the presence of cimetidine co-treatment, levels of NGAL were also measured. NGAL concentrations had been normalized to cell viability based on the MTS absorption of the PTCs, resulting in ng / ml. The results are shown in Figure 4.26**.**

In 24h treatment of cisplatin, the amount of NGAL in the apical membrane did increase significantly from the control (489.77±120.25 ng/ml, $P < 0.01$). In contrast, the presence of cimetidine did not change NGAL level 172.32±59.59 ng/ml compared to control 170.14±5.32 ng/ml. The co-treatment of cisplatin with cimetidine caused a significant decrease in NGAL in the apical membrane (254.28±82.1 ng/ml, $P < 0.0001$) compared to only cisplatin. Compared to apical membrane, NGAL levels in the basolateral membrane were low.

After 48h treatment of cisplatin, the amount of NGAL in the apical membrane did rise significantly from the control (3936.2±1828.69 ng/ml, $P < 0.01$). However, the presence of cimetidine did not change NGAL level 702.46±133.38 ng/ml compared to control 735.12±180.97 ng/ml. The co-treatment of cisplatin with cimetidine caused a significant decline in NGAL in the apical membrane (1207.11±442.01 ng/ml, $P < 0.0001$) compared to only cisplatin NGAL concentrations were low in the basolateral membrane compared to apical membrane.

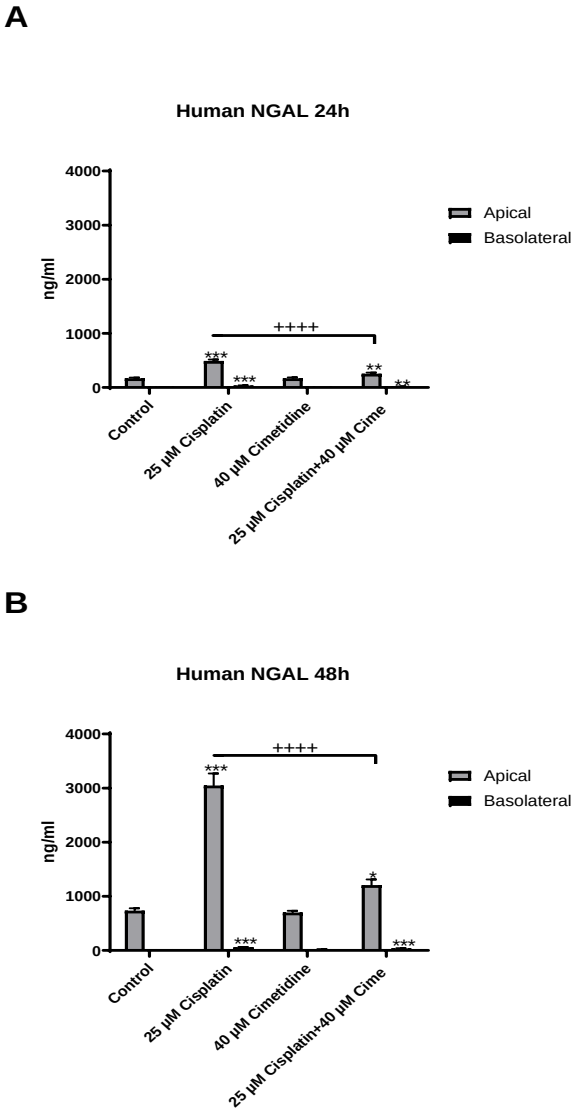

Figure 4.26: The amount of NGAL produced after treatment of human PTCs for 24 and 48 hours in presence of cisplatin +/- cimetidine.

*ELISA was used to measure NGAL production. For example, NGAL production in the apical membrane is significantly higher than basolateral membrane. The amount of NGAL in the apical membrane change significantly from the control (489.77±120.25 ng/ml, P < 0.01) after 24h cisplatin treatment. After co-treatment with cimetidine, NGAL level decreased to (254.28±82.1 ng/ml, P < 0.0001) compared to only cisplatin. The level of NGAL after 48h treatment was more than 8 fold compared to 24h. Statistical analysis was conducted using repeated-measures-paired-one-way ANOVA the data are representative of three independent experiments (n=3). Bars represent mean ± S.E.M values of each group. (*p < 0.05, **p < 0.01, ***p < 0.001, ++++p < 0.0001).*

4.4.9 Clusterin production after treatment of human PTCs in presence of cisplatin +/- cimetidine

Human PTCs were treated for 24 and 48 hours with 25 µM cisplatin and clusterin production was measured. In the presence of cimetidine co-treatment, levels of clusterin were also measured. Clusterin concentrations had been normalized to cell viability based on the MTS absorption of the PTCs, resulting in ng / ml. The result is shown in Figure 4.27.

After 24h treatment of cisplatin, the amount of clusterin in the apical membrane did elevate significantly compared the untreated cells (200.05±67.43 ng/ml, $P < 0.01$). In contrast, the presence of cimetidine did not change clusterin level 40.23±15.71 ng/ml compared to control 39.62±14.27 ng/ml. The co-treatment of cisplatin with cimetidine caused a significant decline in clusterin in the apical membrane (119.34±23.60 ng/ml, $P < 0.0001$) compared to only cisplatin. Compared to apical membrane, clusterin levels in the basolateral membrane were low.

After 48h treatment of cisplatin, the amount of clusterin in the apical membrane did increase significantly compared the untreated cells (613.90±286.48 ng/ml, $P < 0.01$). However, the presence of cimetidine did not change clusterin level 80.38±18.57 ng/ml compared to control 79.57±18.16 ng/ml. The co-treatment of cisplatin with cimetidine caused a significant decrease in clusterin in the apical membrane (274.60±160.79 ng/ml, $P < 0.0001$) compared to only cisplatin. Compared to apical membrane, clusterin levels in the basolateral membrane were low.

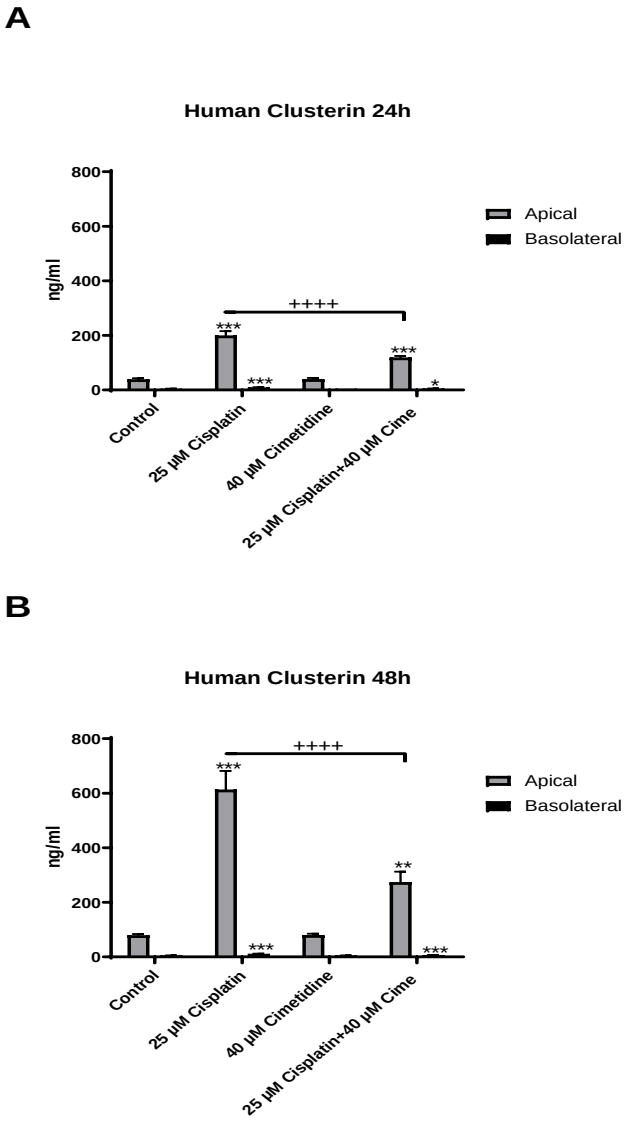

Figure 4.27: The amount of clusterin produced after treatment of human PTCs for 24 and 48 hours in presence of cisplatin +/- cimetidine.

*ELISA was used to measure clusterin production. For example, clusterin production in the apical membrane is significantly higher than basolateral membrane. The amount of clusterin in the apical membrane change significantly from the control (200.05±67.43 ng/ml, P < 0.01) after 24h cisplatin treatment. After co-treatment with cimetidine, clusterin level decreased to (119.34±23.60 ng/ml, P < 0.0001) compared to only cisplatin. The level of clusterin after 48h treatment was more than 3 fold compared to 24h. Statistical analysis was conducted using repeated-measures-paired-one-way ANOVA the data are representative of three independent experiments (n=3). Bars represent mean ± S.E.M values of each group. (*p < 0.05, **p < 0.01, ***p < 0.001, ++++p < 0.0001).*

4.5 Discussion

This chapter aims to explore how primary human PTCs might serve as in-vitro models for nephrotoxicity. Monolayers were subjected to established nephrotoxins - cisplatin, gentamicin and polymyxin B, and the expression of KIM-1, NGAL and clusterin was also determined. The effects of the co-administration of rosuvastatin, cilastatin and cimetidine with polymyxin B, gentamicin and cisplatin were invest aged in this chapter. Using primary cultured cells carries several benefits. Compared to some established cell lines, The primary cells kept their full array of expression of drug transporters, much more than many established cell lines [116]. In exploring the effect of toxic xenobiotics on the kidneys, primary cells are thus thought to be more stable.

4.5.1 Cell viability of human PTCs

The MTS and ATP assays were used to assess the number of live cells. The mechanism of MTS assay by metabolically active mitochondria to reduce a tetrazolium salt to formazan, which is spectrophotometrically distinguishable from the former. On the other hand, the ATP Cell Viability Assay is a homogeneous method for determining the number of viable cells in culture based on the quantity of the present ATP, which indicates the presence of metabolically active cells. The first step was to evaluate the viability of cells after being treated by nephrotoxins. Three types of nephrotoxins were employed: cisplatin, gentamicin and polymyxin B. Those are known nephrotoxins and they use different transporters to cause nephrotoxicity to human PTCs. The result was as predicted.

Our results observed a time and concentrations dependent after treatment human PTCs with gentamicin, polymyxin B and cisplatin, indicating that our in vitro model is an ideal tool to study renal toxicity caused by different nephrotoxins. For example, after exposure of human PTCs with a range concentration of cisplatin, the cell viability after 15 µM cisplatin treatment for 24h was 82.1% and after 48h the percentage of live cells dropped to 71%. At the same time for example, the percentage of live cells after 72h treatment with 25 and 30 µM cisplatin were 39% and 16% respectively.

Another goal was to compare MTS and ATP assays results for cells that came into contact with nephrotoxins in similar conditions. Human PTCs following exposure to nephrotoxins,

similarities in the viability data from both assays were found. The effect of treating human PTC monolayers with cisplatin, a commonly used nephrotoxin, was then observed, with regard to the monolayer production of KIM-1, NGAL and clusterin. Given the identical conditions of the controlled experiment, similar results were expected as mitochondrial enzymes reduce the reagents from both MTS and ATP. These results show the reproducible of the model we are using to predict nephrotoxicity. We can use any assay to measure the cell viability and the results will be the same.

4.5.2 LDH

In this study, LDH assay was used to measure the cytotoxicity of human PTCs after nephrotoxins exposure. The results were consistent with cell viability data. The data showed as the human PTCs exposed to different nephrotoxins the release of LDH is increased. A study used LLC-PK1 cells to measure the LDH release after treatment with 375 μM polymyxin B for 24 and 72 hours. They found a significant increase in LDH release after exposure, indicating the time dependent of polymyxin B by using LDH release in LLc-PK1 cells [117].

4.5.3 Human Biomarkers

The monolayer production of KIM-1, NGAL and clusterin was significantly higher when treated with polymyxin B over 24, 48 and 72 hours, than when not subjected to this treatment in the control samples. The release of KIM-1 was dependent on the concentration of the polymyxin B, and the same was found to be true with cisplatin and gentamicin.

NGAL concentrations after a range concentrations treatment of polymyxin B is increasing in very high amount compared to 24 and 48 hours treatment. This might due to polymyxin B needing more time to invoke the release NGAL from the apical membrane of the PTCs.

Our data showed non-saturatable effect of cisplatin treatment to human PTCs on biomarkers production. This might due to physiological response to cisplatin. In this study, biomarkers levels were measured after 3 days of nephrotoxins treatment. It might need more time to reach the saturatable point. This has been shown in another study there the authors measured urinary KIM-1 from rat with obstructive AKI. The data showed that KIM-1 was increasing even at day 7 of obstruction [118].

Our results also showed differences in response in biomarkers concentrations after treatment with cisplatin. In contrast to KIM-1, the levels of NGAL and clusterin started to decrease at high levels of cisplatin treatment on day 2 and at day 3. This might due to delayed response of the biomarkers to the nephrotoxin. For instance, overloading the monolayers the proximal tubular cells with cisplatin has been shown to alter cell signaling pathways and gene transcription, and as a result the renal transporter expression and function – they are modulated to compensate for the loss of nutrients [119]. These changes could explain the stalling of NGAL and clusterin production during 24 and 48 hours, but increased significantly at the 72 hour treatment.

Urinary KIM-1 has been reported to be specific to proximal tubular damage. In preclinical biomarker qualification studies, it has proven that it was a sensitive and early diagnostic indicator for renal injury, with superior precision and susceptibility to traditional biomarkers [120]. Changes of the expression of NGAL were one of the most recent effects seen in kidneys of animals treated with 50 or 100 mg / kg body weight gentamicin at times when epithelial tubular cells were affected by little histopathological changes[121]. Compared to NGAL, after 7 days of gentamicin treatment, mRNA level of KIM-1 became more prominent. Both genes were considered to be related to proliferation / regeneration and repair, according to the histopathological changes observed after gentamicin in response to toxicity and disease[121].

A study showed that the excretion of urinary clusterin peaks 2 days after an ischemia insult. This is well connected to its production peak of 24h in the damaged of the proximal tubule as determined by confocal laser quantitative microscopy. It is believed that most of the excreted clusterin is derived from cell debris floating in the lumen so that it can be explained by the time it takes to clear the scarcity out of the kidney between the clusterin and the urinary excretion of clusterin[122].

Cisplatin nephrotoxicity has been studied for many years and however, the cisplatin-induced kidney injury molecular mechanism has yet to be clarified. Nephrotoxicity results directly from the loss of kidney function, including serious decreases in the level of glomerular filtration, clearance of Creatinine (CRE) and associated rises in serum creatinine and BUN[123]. The effects of cisplatin are seen to be a disruption of DNA replication, and a crosslinking of DNA. It induces apoptosis as a result of its accumulation in the mitochondria [124, 125]. The

nephrotoxic action of cisplatin is therefore likely to be a result of apoptosis via the intrinsic pathway and the mitochondrial release of cytochrome C. This would also account for the PTCs being a target site of toxicity that has been induced by cisplatin, as they contain high densities of mitochondria [124].

Cimetidine has been reported to inhibit cisplatin transport via OCT2 on a competitive basis and affect cell toxicity [126]. A study showed that, cimetidine inhibited the cytotoxicity of cisplatin in renal cells. Cimetidine obviously inhibits cisplatin-induced nephrotoxicity and damage to the kidneys without influence over cisplatin in vitro and in vivo antitumor activity. While the cimetidine's in vitro activities are mainly due to the injections of ROS production, both inhibitory reactive oxygen species(ROS) and OCT2 measures, which are intrinsically expressed in the kidney, appear to have an in vivo protection effect on the nephrotoxicity of cisplatin[127].

One of the aims of this study was therefore to determine whether similar protective effects were seen when cilastatin was administered in conjunction with gentamicin. There was seen to be a significant difference after 24h in the release of KIM-1 when cells were treated with gentamicin on its own. There was a one fold change in KIM-1 release after 48h in cells treated with gentamycin, compared to the untreated cells. This suggests that, when administered with gentamicin with cilastatin may have a protective effect. This needs to be confirmed by further studies, which should also explore whether this effect is also present when cilastatin is given alongside other nephrotoxins.

This is another study done by using different co-treatment studied the impact of atorvastatin on the nephrotoxicity of gentamicin induced rats. Gentamicin infusion significantly reduced the function of the kidney, enhanced oxidative stress, and tubular necrosis in the renal cortex was associated. The tissue and renal function have normalized the stress parameters, and tube necrosis in atorvastatin-treated animals has been attenuated. Atorvastatin reduced expressions of kinase, kappa B nuclear factor and synthase of inducible nitric oxide, which confirmed an anti-inflammatory and anti-oxidant action caused by statin[128]. Simvastatin has been found to improve gentamicin-induced changes in renal histopathology and dose dependent function in a similar rodent model[128].

Polymyxin B is nephrotoxic and may cause renal injury. Polymyxin B antimicrobial have a small therapeutic window due to the necessary balance between their antibacterial activity and nephrotoxicity [129]. The data showed that, the treatment of human PTCs with 250 μg/ml polymyxin B for 24 and 48 hours increase the production of KIM-1, NGAL and clusterin. For instance, the level of KIM-1 produced after 24h treatment with polymyxin B was 5.2 ng/ml and there was a 4 fold increase after 48h treatment. In addition, rosuvastatin was used as a co treatment to reduce the nephrotoxicity of polymyxin B. For example, NGAL production after 48h treatment with polymyxin B was 77.1 ng/ml and co treatment with rosuvastatin the level of NGAL reduced to 43.7 ng/ml, suggesting the rosuvastatin of decreasing the nephrotoxicity of polymyxin B.

The protective effects of rosuvastatin have been previously shown. Studies carried out on the effects of statins suggest that they decrease albuminuria and oxidative stress and lessen epithelial dysfunction; however, it is believed that they do not directly cause the decreased GFR associated with nephrotoxicity [130]. In HIV patients, when they are treated with combined antiretroviral therapy, there is an increased incidence of nephrotoxicity, thought to be caused by the drugs used in the therapy [131]. The results of a study by Longenecker et al. (2014) revealed that if HIV patients were also administered rosuvastatin, their circulating cystatin C reduced and their GFR was preserved [132]. Furthermore, compared to the controls, serum NGAL, cystatin c and creatinine were reduced in patients who were administered a contrast media for coronary angiography, when rosuvastatin was given two days before and three days after the contrast media was administered [133].

The biomarkers concentration were more in the apical membrane than the basolateral membrane. This results were expecting and reflecting what really happen in vivo. Those renal biomarkers are detectible in urine. NGAL is upregulated and can be detected in mice's kidney and urine three hours after cisplatin treatment and has been suggested a good biomarker for nephrotoxicity[134]. The significant in the basolateral membrane was expecting due to the cells leakage and lose their integrity after drugs treatment.

Our results showed the increase production of the all 3 biomarkers used in this study after treatment with 3 known nephrotoxins. In addition, the use of 3 co-treatment showed a decline

in biomarkers levels when treated 24h before the nephrotoxins treatment. Our human PTCs model could be a good model for early prediction of nephrotoxicity. It is assumed that early detection of nephrotoxicity biomarkers would be available for use in laboratory research and clinical studies relatively soon. The development of rapid, dipstick assays for KIM-1, NGAL and clusterin could enable a better nephrotoxins associated AKI diagnosis, also improving patients' care. Urinary biomarkers levels are elevated in nephrotoxins induced AKI and may help in the differential diagnosis of PTCs injuries. Although further studies are needed to explore the mechanisms behind nephrotoxic drugs and the role of KIM-1, NGAL and clusterin in this setting, those biomarkers are showing promise in early diagnosis and prognosis of AKI.

5 Rat biomarkers

5.1 Introduction

Experimental models are required for essential understanding and the underlying drug action mechanisms to define new therapeutic goals and create new therapeutic strategies. In the first few stages of drug development, animal models, including both in vivo and in vitro methods, are frequently used before human testing in clinical trials. In this chapter, rat PTCs were used as in vitro model as an early way to detect nephrotoxicity. These studies will provide an indication as to the suitability of human and rat PTC monolayers as in vitro models of nephrotoxicity and also possible mechanisms of toxicity. Rats have been selected as a source of PTCs because they are often used in drug development preclinical studies[135]. In parallel, an animal model, specifically a rat, would provide translation data to what really happen in vivo.

Rat kidney have been revealed to upregulate KIM-1 gene expression and the existence of the KIM-1 ectodomain in the urine [136]. Moreover, the KIM-1 protein ectodomain is separated and released into the urine in rats and humans, after exposure to chemicals, ischemia, and protein overload, in a number of nephrotoxic models [137].

Preclinical studies found that NGAL in animal models was one of the most upregulated genes and proteins in the kidney immediately after AKI[138]. In animal models of AKI, NGAL protein was identified in urine and plasma, preceding the rise in plasma creatinine levels [139].

In animal models and cultured cells, the majority of gentamicin enter tubular cells quantitatively through endocytosis mediated by the (megalin / cubilin) [140]. Gentamicin moves to the endosomal compartment through pinocytosis. The drug mainly builds up in the lysosomes, retrogrades through the secretory path to the Golgi and endoplasmic reticula (ER)[141]. Gentamicin generates membrane destabilization, lysosomal aggregation, lipid metabolism modification, and phospholipidosis connected with cell death in the lysosomes[140].

Cisplatin movement through the renal tubular cells is from basolateral to apical[142]. It is now known that two main transporters are engaged in the transport of cisplatin to the tubular cells,

the human copper transport protein 1 (Ctr1) and the organic cation transporter 2 (OCT2)[143]. Once cisplatin has entered the cell, many impacts have been observed, leading to apoptosis and necrosis of the cell. The frequently recognized objective is to harm nuclear DNA, but about 1% of cytosolic cisplatin is found in the nucleus [144].

The purpose of this study is to identify and substantiate the use of rat primary proximal tubular cells (PTCs) as appropriate models for nephrotoxicity study. By using polymyxin B, gentamicin and cisplatin as a known nephrotoxins to treat our rat PTCs, measuring the expression of different nephrotoxicity biomarkers, such as KIM-1 and NGAL were done in this chapter.

5.2 Large molecule nephrotoxin – Gentamicin

Rat PTCs were treated with gentamicin, a known nephrotoxin, before the biomarker expression was quantified using ELISA. The use of gentamicin is important because of the well-characterized and known toxicity caused by gentamicin in vivo.

5.2.1 MTS Cell viability of rat in gentamicin concentration range

The results of the MTS assay showed the time and concentration dependent effect of gentamicin on cell viability in rat PTCs. With a rise in gentamicin concentration, cell viability reduced significantly. For example, after 24h treatment with 100 µg/ml gentamicin the cell viability was 23% less than the non-treated cells. The percentage of live cells was less than 50% after 250 µg/ml gentamicin treatment. The results are shown in Figure 5.1**.**

The percentage of live cells decreased with the rise of the gentamicin dose after 48h incubations. For instance, after 300 µg/ml gentamicin the percentage of live cells was 44%. The live cells were less than 40% after 400 µg/ml gentamicin treatment.

After 72h treatment with a range of gentamicin concentrations, cell viability decreased significantly. After 100 µg/ml gentamicin treatment, live cells was 71%. In addition, after 500 µg/ml gentamicin incubation the cell viability was only 29%.

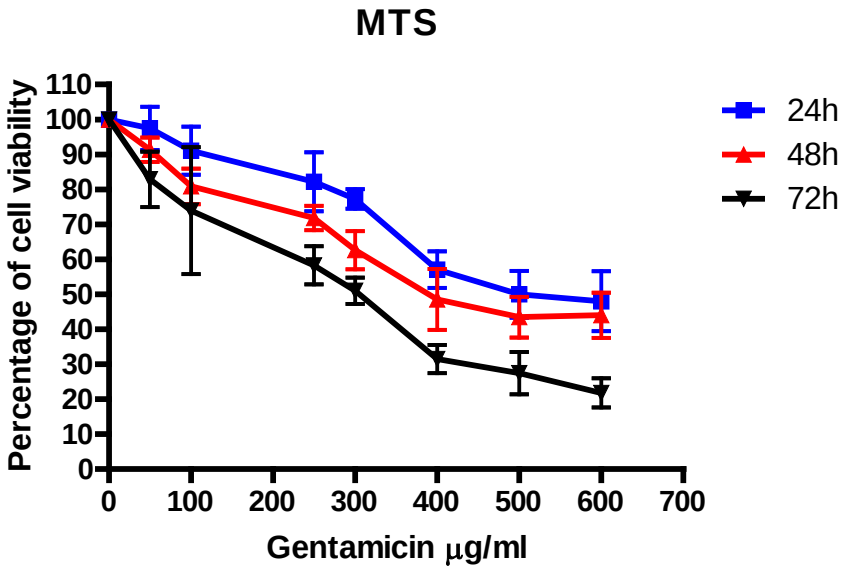

Figure 5.1: Cell viability in rat PTCs treated with range concentrations of gentamicin for 24, 48 and 72 hours.

MTS assay was used to measure the cell viability. For example, the cell viability after 250 µg/ml gentamicin for 24h was 82.2% and the percentage dropped to 71.8% after 48h. In addition, cell viability after 300 µg/ml gentamicin treatment for 72h was 49.9% and after 500 µg/ml gentamicin the cell viability decreased to 20%. Each point represent mean ± S.E.M values of each gentamicin concentration.

5.2.2 KIM-1 production after treatment of rat PTCs in presence of a range concentration of gentamicin:

The level of KIM-1 produced after rat PTCs were treated with a range of gentamicin concentrations were investigated. The concentrations of the biomarker were normalised to the cell viability. The results are shown in Figure 5.2.

The KIM-1 levels after 24h treatment of gentamicin increased significantly compared to non-treated cells. For instance, the level of KIM-1 production after 300 µg/ml gentamicin was 7.75±2.85 ng/ml compared with the control 1.11±0.23 ng/ml and then the level of KIM-1 started to increase slightly as the concentration of gentamicin increases up to 600 µg/ml.

The levels of KIM-1 increased significantly in comparison with non-treated cells after 48h of gentamicin treatment. The KIM-1 levels increased by 50 to 600 µg/ ml gentamicin treatment. The highest level of KIM-1, compared to control 2.90±0.30 ng/ ml, was after 600 µg / ml gentamicin treatment at 31.87±936 ng/ ml.

The KIM-1 concentrations risen considerably compared to non-treated cells after 72h of gentamicin treatment. For instance, the level of KIM-1 production after 250 µg/ml gentamicin treatment was 34.80±6.49 ng/ml compared with the control 7.74±1.51 ng/ml and then the level of KIM-1 increased as the concentration of gentamicin increases up to 600 µg/ml.

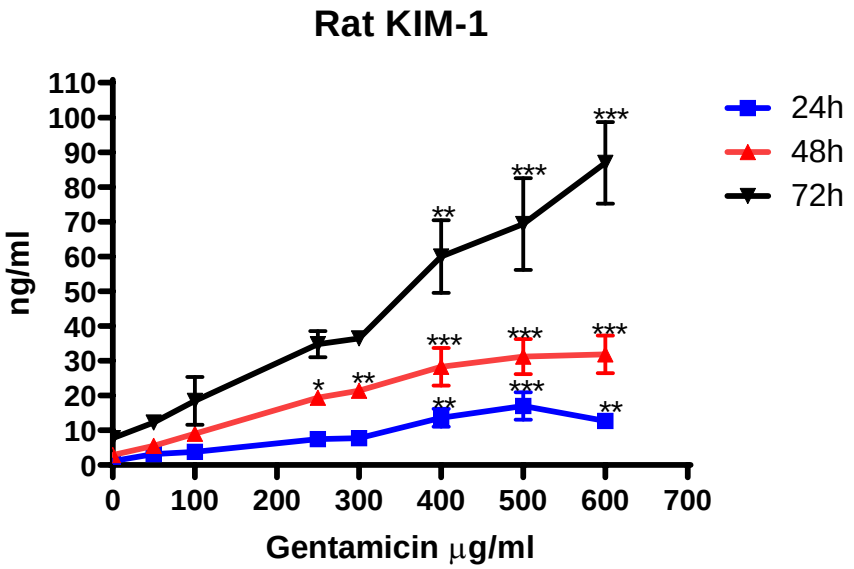

Figure 5.2: Measurement of KIM-1 production from rat PTCs treated with range concentrations of gentamicin for 24, 48 and 72 hours.

*Levels were normalised to MTS absorbance value to account for cell numbers after nephrotoxin treatments. Rat PTCs were treated with a range of gentamicin concentration (50 to 600 µg/ml). For example, NGAL production after 300 µg/ml gentamicin treatment for 24h was 65.8±4.7 ng/ml and after 500 µg/ml the level of KIM-1 increased to 131.4±19.5 ng/ml. The level of KIM-1 after 250 µg/ml gentamicin treatment for 48h was 180.4±43.5 ng/ml and after 72h the level increased to 307.8±35.7 ng/ml. Statistical analysis was conducted using repeated-measures-paired-one-way ANOVA the data are representative of three independent experiments (n=3). Each point mean ± S.E.M values of each group. (*p < 0.05, **p < 0.01, ***p < 0.001).*

5.2.3 NGAL production after treatment of rat PTCs in presence of a range concentration of gentamicin:

After a rat PTC had been incubated with a range of gentamicin levels, NGAL production was examined. NGAL levels have been normalized to cell viability. The results showed the time and concentration dependent effect of gentamicin on rat PTCs. The results are shown in Figure 5.3.

There were a significant increase in NGAL levels after 24h treatment of gentamicin compared to non-treated cells. NGAL levels were elevated significantly by (50 to 600) µg/ml gentamicin concentrations. The level of KIM-1 production after 400 µg/ml gentamicin was 114.62±37.32 ng/ml compared with the control 7.66±2.18 ng/ml and then the level of NGAL remained almost the same as the concentration of gentamicin increases up to 600 µg/ml.

The levels of NGAL increased significantly in comparison with non-treated cells after 48h of gentamicin treatment. The maximum level of NGAL was after 500 µg / ml gentamicin treatment 193.83±42.23 ng / ml compared to the control 20.30±3.10 ng / ml.

The NGAL levels after 72h treatment of gentamicin increased significantly compared to non-treated cells. For example, the level of NGAL production after 250 µg/ml gentamicin treatment was 273.17±47.36 ng/ml compared with the control 47.36±1.95 ng/ml and then the level of NGAL increased as the concentration of gentamicin increases up to 600 µg/ml.

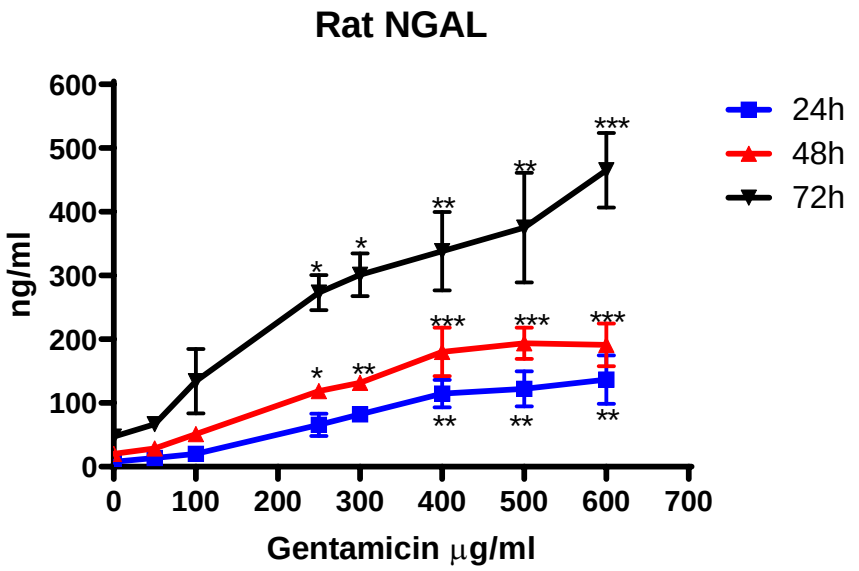

Figure 5.3: Measurement of NGAL production from rat PTCs treated with range concentrations of gentamicin for 24, 48 and 72 hours.

*Levels of NGAL were normalised to MTS absorbance value to account for cell numbers after nephrotoxin treatments. Rat PTCs were treated with a range of gentamicin concentration (50 to 600 µg/ml). For example, NGAL production after 300 µg/ml gentamicin treatment for 24h was 82.3±17.4 ng/ml and after 500 µg/ml the level of NGAL increased to 122.1±47.9 ng/ml. The level of NGAL after 250 µg/ml gentamicin treatment for 48h was 118.5±14.9 ng/ml and after 72h the level increased to 273.1±47.3 ng/ml. Statistical analysis was conducted using repeated-measures-paired-one-way ANOVA the data are representative of three independent experiments (n=3). Each point mean ± S.E.M values of each group. (*p < 0.05, **p < 0.01, ***p < 0.001).*

5.2.4 MTS and ATP Cells viability assays:

The cell viability was measured after treatment of rat PTCs for 24 and 48 hours with 250 µg/ml gentamicin. The cell viability was also measured in the presence of cilastatin co-treatments. Both MTS and ATP assays were used to assess cell viability from the same plate. The results revealed no significant difference between the two assessment methods. The results are shown in Figure 5.4**.**

After 24h, the results revealed that cell viability reduced significantly in response to exposure to gentamicin to (65.74±3.29%, $P < 0.01$) of control. The cilastatin co treatment did not change the cell viability (97.98±3.28% live cells). The treatment of gentamicin with cilastatin increased the live cells compared to only gentamicin (74.38±4.12%, $P < 0.01$).

After 48h, the cell viability was reduced significantly by gentamicin (58.95±3.1%, $P < 0.01$). However, the cell viability did not change with cilastatin (98.66±1.86%). The cell viability after gentamicin with cilastatin was higher than only gentamicin (70.37±4.21%, $P < 0.01$ live cells).

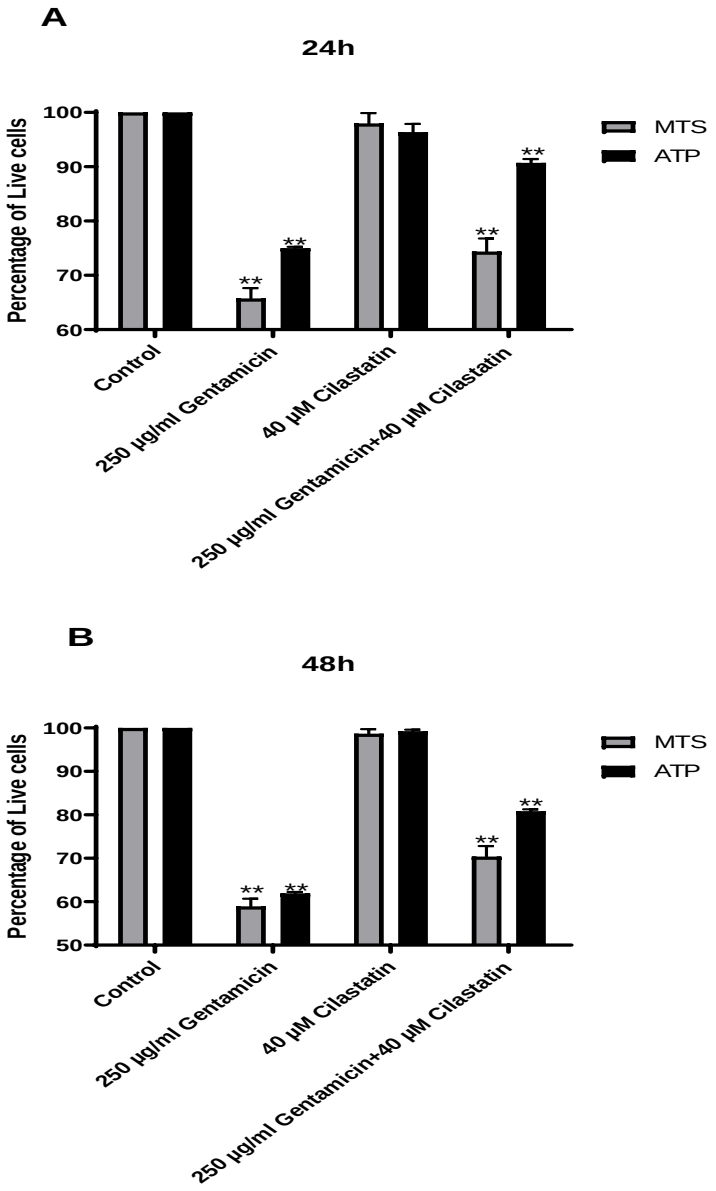

Figure 5.4: Cells Viability of rat PTCs after treatment of gentamicin for 24 and 48 hours.

*MTS and ATP assays were used to measure the cell viability. Viability is measured as a percentage of the control. For example, MTS percentage after gentamicin treatment for 24h was 65.7% and ATP percentage was 75.1%. In addition, the co-treatment of cilastatin with gentamicin for 48h showed, the percentage of MTS was 70.3% and ATP percentage was 80.8%. Statistical analysis was conducted using repeated-measures-paired-one-way ANOVA the data are representative of three independent experiments (n=3). Bars represent mean ± S.E.M values of each group. (*p < 0.05, **p < 0.01, ***p < 0.001).*

5.2.5 Lactate dehydrogenase (LDH) cytotixicy assay:

The measurement of cytoplasmic enzymes released by damaged cells is a common method for determining cytotoxicity. In this experiment, we treated rat PTCs for 24 and 48 hours with 250 µg/ml gentamicin and LDH was measured. In addition, we measured the LDH after cilastatin co treatment. The results are consistent with cell viability data. Result shown in Figure 5.5**.**

After 24h, the results revealed that LDH increased significantly in response to exposure to gentamicin to (29.26±1.14%, $P < 0.01$). The cilastatin co treatment did not change the LDH (17.1±1.26%). The treatment of gentamicin with cilastatin increased the decreased the LDH compared to only gentamicin (26.72±1.23%, $P < 0.01$).

After 48h, the LDH was increased significantly by gentamicin (37.91±1.90%, $P < 0.01$). However, the LDH did not change with cilastatin (19.97±0.86%). The LDH after gentamicin with cilastatin was lower than only gentamicin (27.60±0.74%, $P < 0.01$).

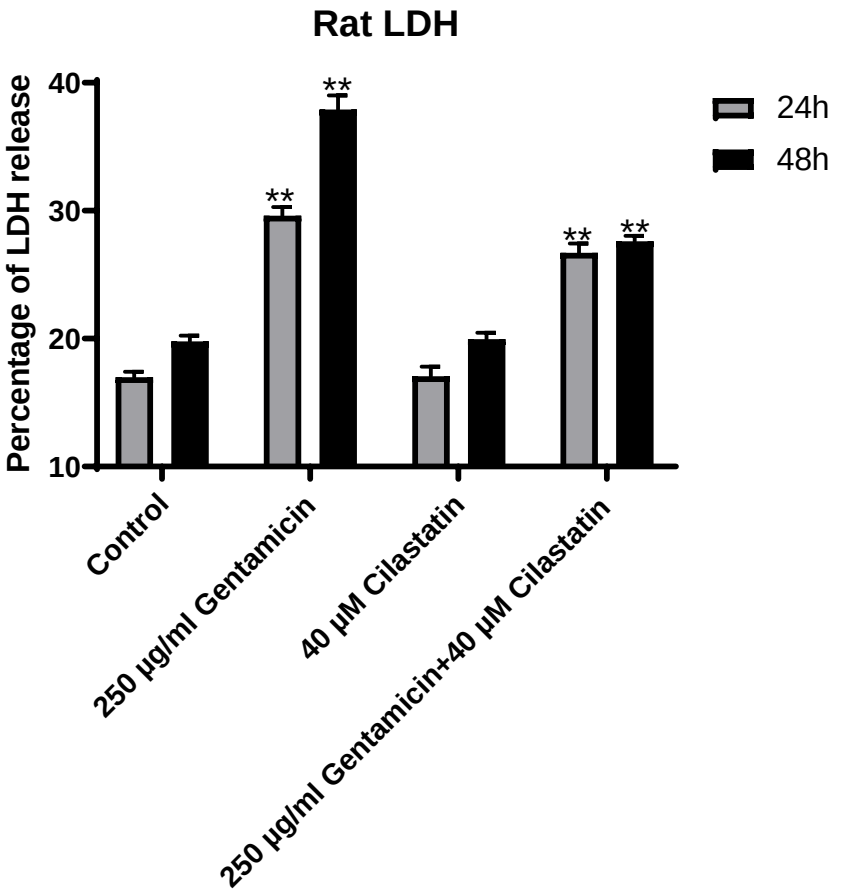

Figure 5.5: LDH released from rat PTCs after treatment of gentamicin for 24 and 48 hours.

*LDH is measured as a percentage of the control. LDH percentage after gentamicin treatment for 24h was 29.6% and after 48h the percentage increased to 37.9%. In addition, LDH percentage decreased after cilastatin co-treatment with gentamicin for 48h to 27.6%. Statistical analysis was conducted using repeated-measures-paired-one-way ANOVA the data are representative of three independent experiments (n=3). Bars represent mean ± S.E.M values of each group. (*p < 0.05, **p < 0.01, ***p < 0.001).*

5.2.6 KIM-1 expression after treatment of rat PTCs in presence of gentamicin +/- cilastatin

The amount of KIM-1 produced after treatment of rat PTCs for 24 and 48 hours in presence of 250 µm/ml gentamicin were investigated. The levels of KIM-1 was also measured in the presence 40 µM cilastatin co-treatments. The concentrations of KIM-1 was normalised to the cell viability as determined from their MTS absorbance, results of which were therefore expressed as ng/ml. The results are shown in Figure 5.6.

After 24h treatment of gentamicin, the amount of KIM-1 in the apical membrane did change significantly from the control (3.86±0.28 to 10.31±0.72 ng/ml, $P < 0.01$). However, the presence of cilastatin did not change KIM-1 level 4.31±0.36 ng/ml compared to control 3.86±0.28 ng/ml. The co-treatment of gentamicin with cilastatin caused a significant decrease in KIM-1 in the apical membrane (7.35±0.48 ng/ml, $P < 0.0001$) compared to only gentamicin.

After 48h treatment of gentamicin, the amount of KIM-1 in the apical membrane did change significantly from the control (28.70±0.48 ng/ml, $P < 0.01$). However, when we added cilastatin did not change KIM-1 level 12.83±0.37 ng/ml compared to control 10.48±0.35 ng/ml. A significant reduction in KIM-1 was monitored in apical membrane (20.82±1.11 ng / ml, $P<0.0001$) compared to only gentamicin by co-treatment of cilastatin with gentamicin. Basolateral membrane KIM-1 production were undetectable in comparison with apical membrane.

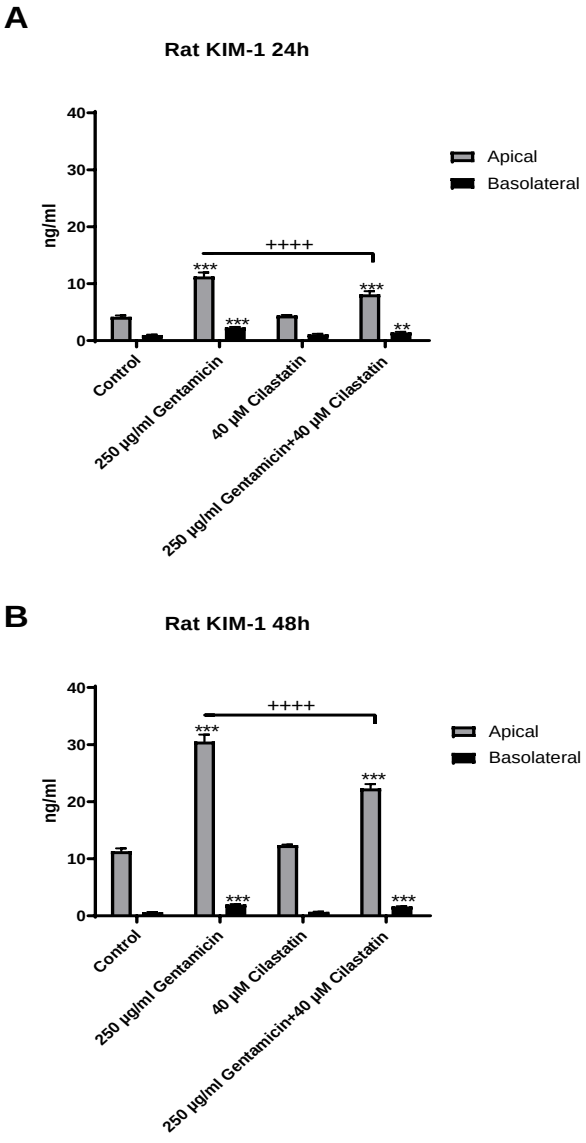

Figure 5.6: The amount of KIM-1 produced after treatment of rat PTCs for 24 and 48 hours in presence of gentamicin +/- cilastatin.

*ELISA was used to measure KIM-1 production. The amount of KIM-1 in the apical membrane change significantly from the control (*3.86±0.28 to *10.31±0.72 ng/ml, P < 0.01) after 24h gentamicin treatment. After co-treatment with cilastatin, KIM-1 level decreased to (7.35±0.48 ng/ml, P < 0.0001) compared to only gentamicin. The level of KIM-1 after 48h treatment was more than 3 fold compared to 24h. Statistical analysis was conducted using repeated-measures-paired-one-way ANOVA the data are representative of three independent experiments (n=3). Bars represent mean ± S.E.M values of each group. (*p < 0.05, **p < 0.01, ***p < 0.001, ++++p < 0.0001).*

5.2.7 NGAL production after treatment of rat PTCs in presence of gentamicin +/- cilastatin

NGAL production for 24 and 48 hours in the presence of gentamicin following treatment of rat PTCs. In the presence of cilastatin co-treatment, levels of NGAL were also measured. NGAL concentrations had been normalized to cell viability based on the MTS absorption of the PTCs, resulting in ng / ml. Figure 5.7 shows the results.

The quantity of NGAL in the apical membrane increased significantly after 24h incubation with gentamicin (146.38±21.49 ng / ml, $P<0.01$).However, the presence of cilastatin did not change NGAL level 28.42±6.16 ng/ml compared to control 28.52±5.28 ng/ml. The co-treatment of gentamicin with cilastatin caused a significant decrease in NGAL in the apical membrane (113.09±14.21 ng/ml, $P < 0.0001$) compared to only gentamicin. Compared to apical membrane, NGAL levels in the basolateral membrane were low.

After 48h treatment of gentamicin, the amount of NGAL in the apical membrane did increase significantly from the control (400.65±130.9 ng/ml, $P < 0.01$). However, the presence of cilastatin did not change NGAL level 67.10±3.86 ng/ml compared to control 67.14±13.92 ng/ml. The co-treatment of gentamicin with cilastatin caused a significant decrease in NGAL in the apical membrane (251.34±5.46 ng/ml, $P < 0.0001$) compared to only gentamicin.

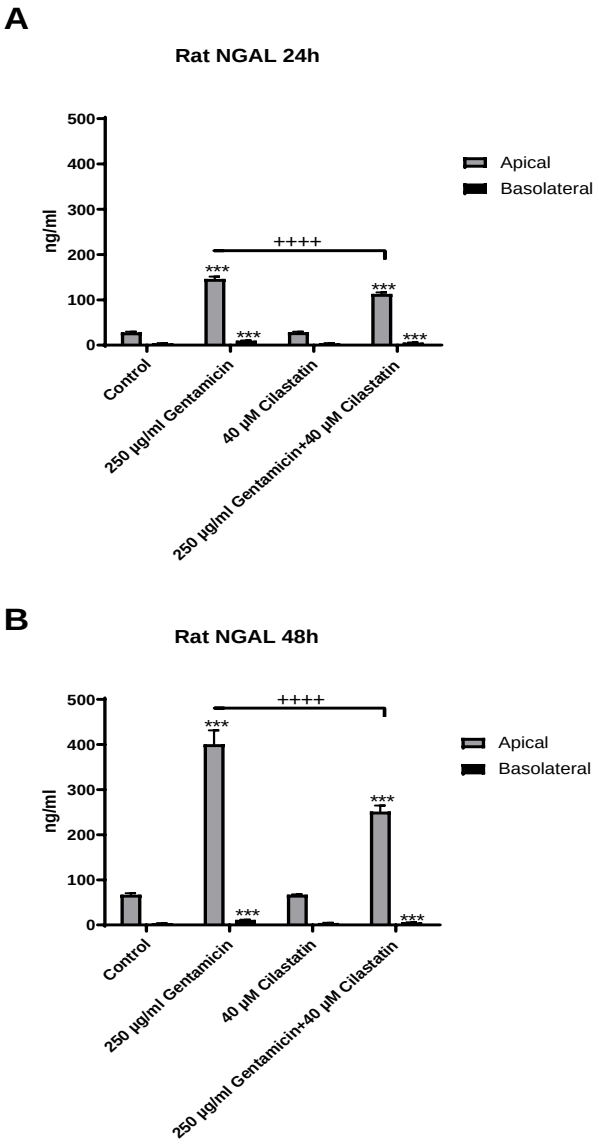

Figure 5.7: The amount of NGAL produced after treatment of rat PTCs for 24 and 48 hours in presence of gentamicin +/- cilastatin.

*ELISA was used to measure NGAL production. The amount of NGAL in the apical membrane change significantly from the control (146.38±21.49 ng / ml, P<0.01) after 24h gentamicin treatment. After co-treatment with cilastatin, NGAL level decreased to (113.09±14.21 ng/ml, P < 0.0001) compared to only gentamicin. The level of NGAL after 48h treatment was almost 3 fold higher than 24h. Statistical analysis was conducted using repeated-measures-paired-one-way ANOVA the data are representative of three independent experiments (n=3). Bars represent mean ± S.E.M values of each group. (*p < 0.05, **p < 0.01, ***p < 0.001, ++++p < 0.0001).*

5.3 Large molecule nephrotoxin – Polymyxin B

Before expression of biomarkers was quantified with ELISA, Rat PTCs were treated with polymyxin B. Polymyxin B impacts on PTCs were important because polymyxin B toxicity was already well known in vivo.

5.3.1 MTS Cell viability of rat with polymyxin B concentration range

The cell viability was measured after treatment of rat PTCs with a range of concentration of polymyxin B (50 to 600 μg/ml) for 24, 48 and 72 hours. MTS assay was used to assess cell viability. The MTS absorbance show as a percentage normalised to control cells. The results are shown in Figure 5.8**.**

The impact of polymyxin B on cell viability in rat PTCs was found in the quantity of the MTS. The cell viability decreased steadily with an increase in polymyxin B concentration. For example, after 24h treatment with 300 μg/ml polymyxin B the cell viability was 63%. The percentage of live cells was less than 48% after 500 μg/ml polymyxin B treatment.

After 48h incubation with polymyxin B the percentage of live cells decrease as the dose of polymyxin B increase. For instance, at 250 μg/ml polymyxin B the percentage of live cells was 61%. The live was less more than 65% after 400 μg/ml polymyxin B.

There were a major decrease in cell viability after 72h treatment with a range of concentration of polymyxin B. after 100 μg/ml polymyxin B treatment, live cells reduced more than 40%. In addition, after 500 μg/ml polymyxin B incubation the cell viability was only 28%.

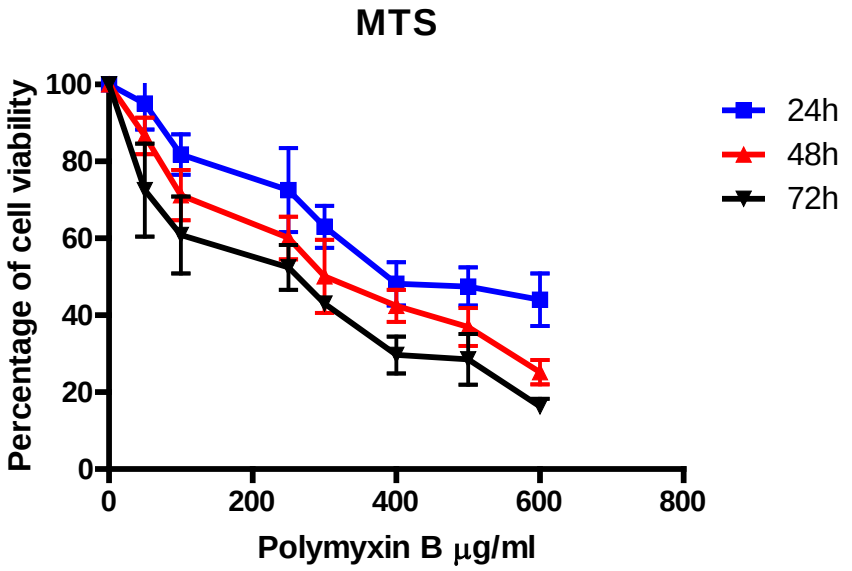

Figure 5.8: Cell viability in rat PTCs treated with range concentrations of polymyxin B for 24, 48 and 72 hours.

MTS assay was used to measure the cell viability. Polymyxin B showed a time and concentrations dependent. For example, the cell viability after 250 μg/ml polymyxin B treatment for 24h was 72.5% and the percentage dropped to 60.1% after 48h. In addition, cell viability after 300 μg/ml polymyxin B treatment for 72h was 43.1% and after 500 μg/ml polymyxin B the cell viability decreased to 28.5%. Each point represent mean ± S.E.M values of each polymyxin B concentration.

5.3.2 KIM-1 production after treatment of rat PTCs in presence of a range concentration of polymyxin B

The KIM-1 level was investigated after rat PTCs were treated with a range of polymyxin B concentrations. The results were normalised to the cell viability. The results are shown in Figure 5.9.

The KIM-1 levels after 24h treatment of polymyxin B increased significantly compared to non-treated cells. KIM-1 levels were elevated significantly and gradually by 50 to 250 μg/ml polymyxin B concentrations. The level of KIM-1 production at 250 μg/ml polymyxin B treatment was 9.79±1.25 ng/ml compared with the control 1.34±0.45 ng/ml and then the level of KIM-1 remained almost the same as the concentration of polymyxin B increases up to 600 μg/ml.

The levels of KIM-1 increased significantly in comparison with non-treated cells after 48h of polymyxin B treatment. The level of KIM-1, compared to control 3.89±0.93 ng / ml, was after 300 μg / ml polymyxin B treatment at 32.14±10.59 ng / ml, and then the KIM-1 level, with the polymyxin B treatment rising up to 600 μg / ml, started to slightly decrease.

The KIM-1 levels after 72h treatment of polymyxin B increased significantly compared to untreated cells. For instance, KIM-1 levels were elevated significantly by 50 to 400 μg/ml gentamicin concentrations. The level of KIM-1 production reached the highest at 400 μg/ml polymyxin B treatment to 81.78±36.52 ng/ml compared with the control 10.63±1.02 ng/ml and then the level of KIM-1 decreased as the concentration of polymyxin B increases up to 600 μg/ml.

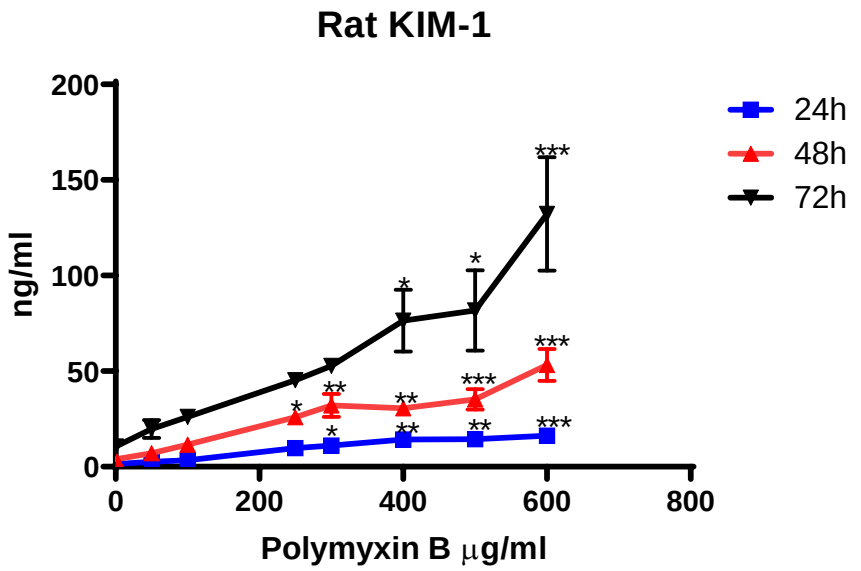

Figure 5.9: Measurement of KIM-1 production from rat PTCs treated with range concentration of polymyxin B for 24, 48 and 72 hours.

*Levels of KIM-1 were normalised to MTS absorbance value to account for cell numbers after nephrotoxin treatments. Rat PTCs were treated with a range of polymyxin B concentration (50 to 600 µg/ml). For example, KIM-1 production after 100 µg/ml polymyxin B treatment for 24h was 3.3±0.4 ng/ml and after 250 µg/ml the level of KIM-1 increased to 9.7±1.2 ng/ml. The level of KIM-1 after 400 µg/ml polymyxin B treatment for 48h was 30.6±2.7 ng/ml and after 72h the level increased to 81.7±36.5 ng/ml. Statistical analysis was conducted using repeated-measures-paired-one-way ANOVA the data are representative of three independent experiments (n=3). Each point mean ± S.E.M values of each group. (*p < 0.05, **p < 0.01, ***p < 0.001).*

5.3.3 NGAL production after treatment of rat PTCs in presence of a range concentration of polymyxin B

The production of NGAL after treated rat PTCs with a range concentration of polymyxin B were investigated. The NGAL levels were normalized to cell viability. The results are shown in Figure 5.10.

There was a significant increase in NGAL levels after 24h treatment of polymyxin B compared to non-treated cells. NGAL levels were elevated significantly by (50 to 600) µg/ml polymyxin B concentrations. For example, the level of NGAL production was at 400 µg/ml polymyxin B to 79.1±56.1 ng/ml compared with the control 8.53±3.60 ng/ml and then the level of NGAL remained stable as the concentration of polymyxin B increases up to 600 µg/ml.

The levels of NGAL increased in comparison with non-treated cells after 48h of gentamicin treatment. The maximum level of NGAL was after 600 µg / ml polymyxin B treatment 332.18±76.95ng / ml compared to the control 20.79±2.58 ng / ml.

The NGAL levels after 72h treatment of polymyxin B increased significantly compared to non-treated cells. For example, the level of NGAL production reached the first peak at 250 µg/ml polymyxin B treatment to 203.04±45.67 ng/ml compared with the control 37.98±3.26 ng/ml and then the level of NGAL increased as the concentration of polymyxin B increases up to 600 µg/ml.

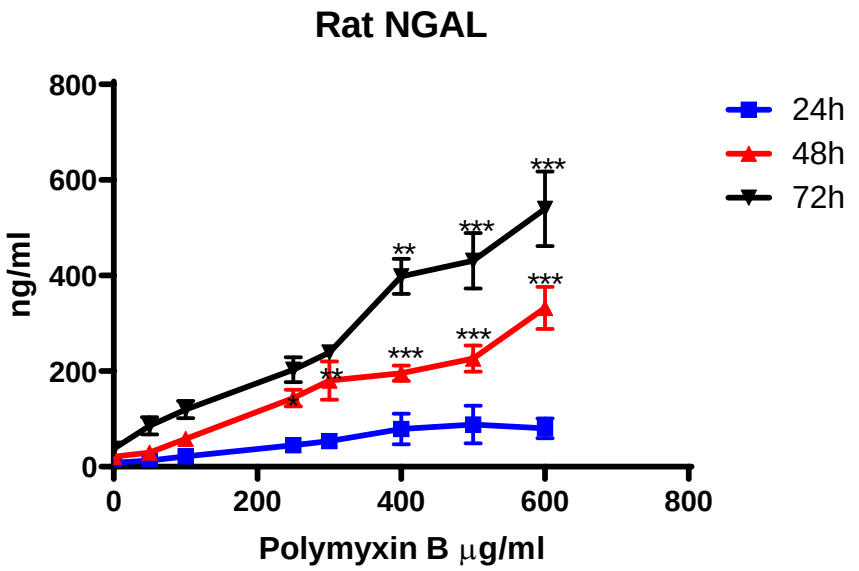

Figure 5.10: Measurement of NGAL production from rat PTCs treated with rang concentrations of polymyxin B for 24, 48 and 72 hours.

*Levels of NGAL were normalised to MTS absorbance value to account for cell numbers after nephrotoxin treatments. Rat PTCs were treated with a range of polymyxin B concentration (50 to 600 µg/ml). For example, NGAL production after 300 µg/ml polymyxin B treatment for 24h was 53.4±27.2 ng/ml and after 400 µg/ml the level of NGAL increased to 79.1±56 ng/ml. The level of NGAL after 250 µg/ml polymyxin B treatment for 48h was 143.9±30.1 ng/ml and after 72h the level increased to 203.1±45.6 ng/ml. Statistical analysis was conducted using repeated-measures-paired-one-way ANOVA the data are representative of three independent experiments (n=3). Each point mean ± S.E.M values of each group. (*p < 0.05, **p < 0.01, ***p < 0.001).*

5.3.4 MTS and ATP Cells viability assays

After 24 and 48 hours treatment with 250 µg / ml polymyxin B, the cell viability was measured. Cell viability was also evaluated with 50 µM of rosuvastatin co-treatment. The cell viability from the same plate was measured using MTS and ATP assays. The outcomes of the two cell viability techniques had no difference. The results are shown in Figure 5.11**.**

After 24h of treatment, the results revealed that cell viability reduced significantly in response to exposure to polymyxin B to (74.7±4.9%, $P < 0.01$) of control. The rosuvastatin co treatment did not change the cell viability (96.2±1.9%, $P < 0.01$ live cells). The treatment of polymyxin B with rosuvastatin increased the live cells compared to only gentamicin (87.3±4.5%).

The cell viability was reduced significantly by polymyxin B (68.3±5.8%, $P < 0.01$) after 48h of treatment. However, the cell viability did not change with rosuvastatin (94.1±2.6 %). The cell viability after polymyxin B with rosuvastatin was higher than only polymyxin B (76.9±4%, $P < 0.01$ viable cells).

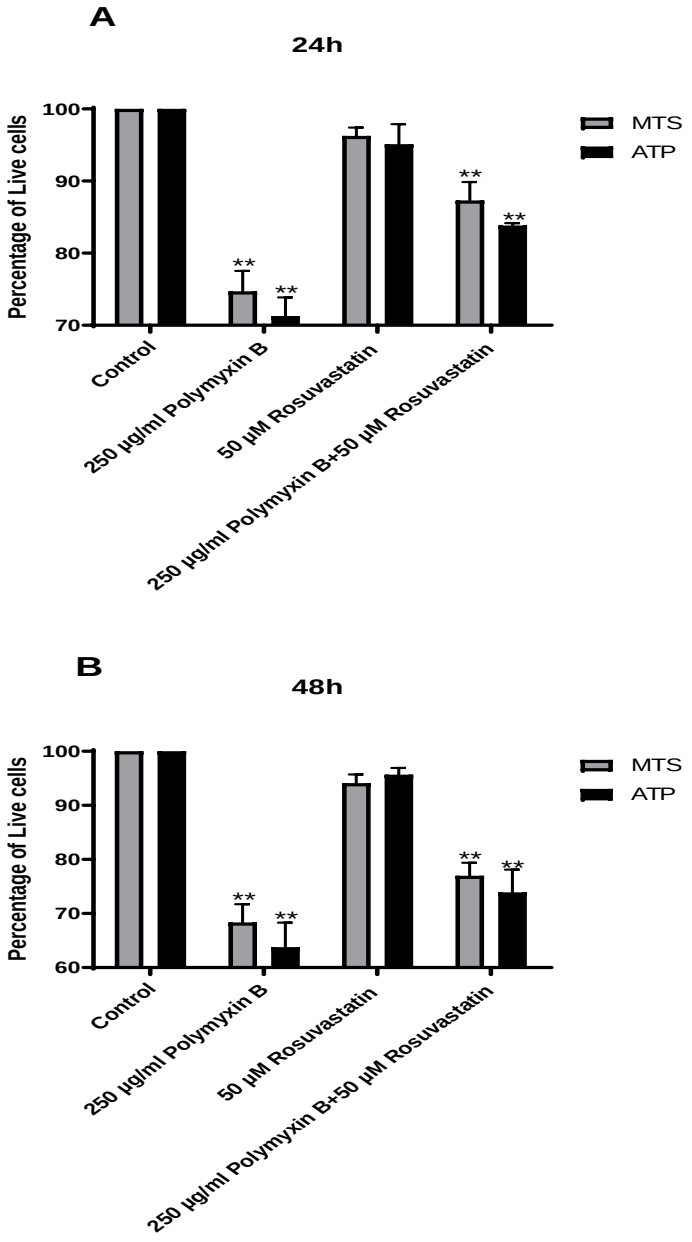

Figure 5.11: Cells Viability of rat PTCs after treatment of polymyxin B for 24 and 48 hours.

MTS and ATP assays were used to measure the cell viability. Viability is measured as a percentage of the control. For example, MTS percentage after polymyxin B treatment for 24h was 74.7% and ATP percentage was 71.2%. In addition, the co-treatment of rosuvastatin *with polymyxin B for 48h showed, the percentage of MTS was 76.9% and ATP percentage was 73.8%. Statistical analysis was conducted using repeated-measures-paired-one-way ANOVA the data are representative of three independent experiments (n=3). Bars represent mean ± S.E.M values of each group. (*p < 0.05, **p < 0.01, ***p < 0.001).*

5.3.5 Lactate dehydrogenase (LDH) cytotoxic assay

In this experiment, rat PTCs treated for 24 and 48 hours with 250 µg/ml polymyxin B and LDH was measured. In addition, LDH was measured after rosuvastatin co treatment. The results is typically with cell viability data. Result shown in Figure 5.12**.**

After 24h, the results revealed that LDH increased significantly in response to exposure to polymyxin B to 41.6±3.3%. The rosuvastatin co treatment did not change the LDH (10.7±1.2%). The treatment of polymyxin B with cilastatin increased the decreased the LDH compared to only polymyxin B (28.3±3.7%).

The LDH was increased significantly by polymyxin B (49.1±4.6%) after 48h treatment. However, the LDH did not change with rosuvastatin (12.2±0.84%). The LDH after polymyxin B with cilastatin was lower than only polymyxin B (33.8±3.6%).

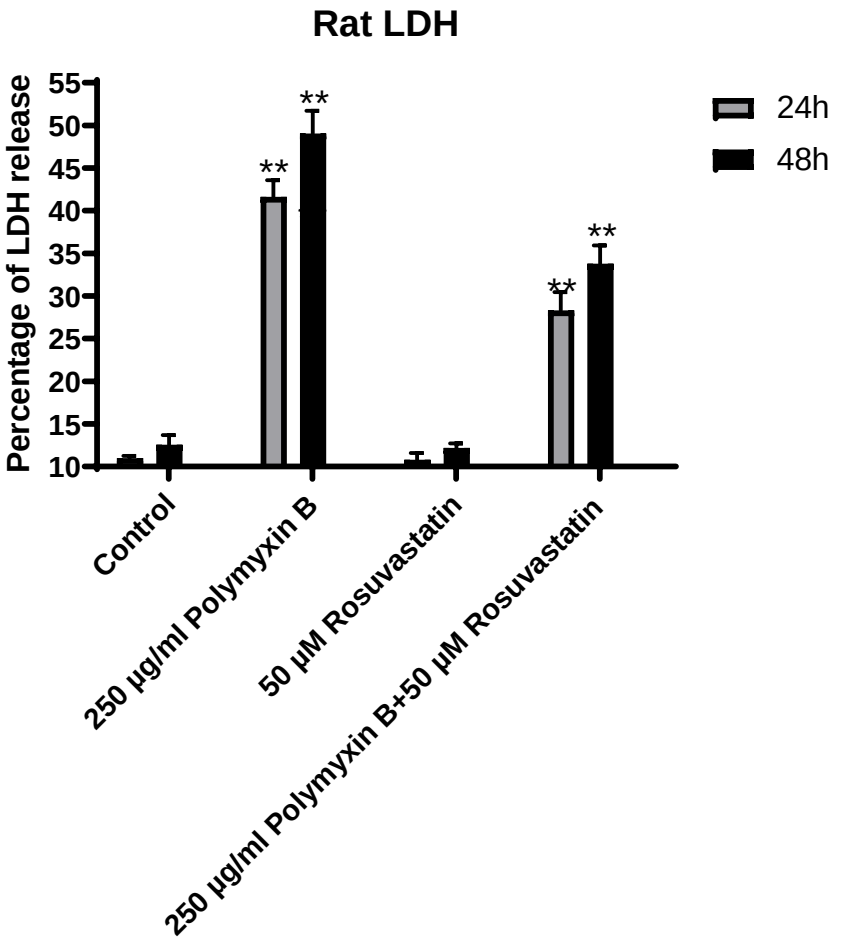

Figure 5.12: LDH released from rat PTCs after treatment of polymyxin B for 24 and 48 hours.

LDH is measured as a percentage of the control. LDH percentage after polymyxin B treatment for 24h was 41.6% and after 48h the percentage increased to 49.1%. In addition, LDH percentage decreased after rosuvastatin *co-treatment with polymyxin B for 48h to 33.8% Statistical analysis was conducted using repeated-measures-paired-one-way ANOVA the data are representative of three independent experiments (n=3). Bars represent mean ± S.E.M values of each group. (*p < 0.05, **p < 0.01, ***p < 0.001).*

5.3.6 KIM-1production after treatment of rat PTCs in presence of polymyxin B +/- rosuvastatin

The level of KIM-1 produced after rat PTCs have been treated with 250 μg/ml polymyxin B for 24 and 48 hours. KIM-1 production was also measured in the presence rosuvastatin co-treatments. The concentrations of KIM-1 was normalised to the cell viability as determined from their MTS absorbance's, expressed as ng/ml. The results are shown in Figure 5.13**.**

After 24h treatment of polymyxin B, the amount of KIM-1 in the apical membrane did change significantly from the control (5.42±1.19 ng/ml, $P < 0.01$). However, the presence of rosuvastatin did not change KIM-1 level to 1.53±0.44 ng/ml compared to control 1.58±0.56 ng/ml. The co-treatment of polymyxin B with rosuvastatin caused a significant decrease in KIM-1 in the apical membrane (2.76±0.73 ng/ml, $P < 0.0001$) compared to only polymyxin B. In comparison with apical membrane, basolateral membrane levels of KIM-1 were low.

The amount of KIM-1 on the apical membrane changed significantly from the control after 48h of treatment with polymyxin B (24.84±8.65 ng/ml, $P < 0.01$). However, when we added rosuvastatin did not change KIM-1 level 6.46±1.14 ng/ml compared to control 6.15±1.18 ng/ml. The co-treatment of polymyxin B with rosuvastatin caused a significant decline in KIM-1 in the apical membrane (13.69±3.03 ng/ml, $P < 0.0001$) compare to only polymyxin B.

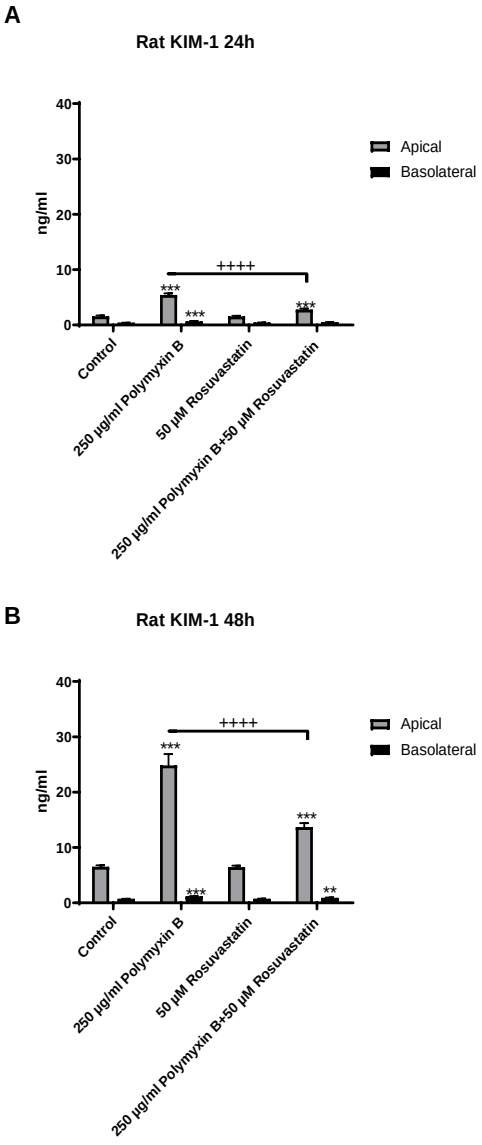

Figure 5.13: The amount of KIM-1 produced after treatment of rat PTCs for 24 and 48 hours in presence of polymyxin B +/- rosuvastatin.

*ELISA was used to measure KIM-1 production. The amount of KIM-1 in the apical membrane change significantly from the control (5.42±1.19 ng/ml, P < 0.01) after 24h polymyxin B treatment. After co-treatment with rosuvastatin, KIM-1 level decreased to (2.76±0.73 ng/ml, P < 0.0001) compared to only polymyxin B. The level of KIM-1 after 48h treatment was more than 4 fold compared to 24h. Statistical analysis was conducted using repeated-measures-paired-one-way ANOVA the data are representative of three independent experiments (n=3). Bars represent mean ± S.E.M values of each group. (*p < 0.05, **p < 0.01, ***p < 0.001, ++++p < 0.0001).*

5.3.7 NGAL production after treatment of rat PTCs in presence of polymyxin B +/- rosuvastatin

The NGAL production in 24 and 48 hours treatment of rat PTCs with 250 μg/ml polymyxin B. In the presence of rosuvastatin co-treatment, levels of NGAL were also measured. NGAL level had been normalized to cell viability based on the MTS absorption of the rat PTCs, resulting in ng / ml. The results are shown in Figure 5.14.

After 24h treatment of 250 μg/ml polymyxin B, the amount of NGAL in the apical membrane did elevated significantly from the control (76.62±14.25 ng/ml, $P < 0.01$). However, the presence of rosuvastatin did not change NGAL level 19.18±6.28 ng/ml compared to control 19.10±5.74 ng/ml. The co-treatment of polymyxin B with rosuvastatin caused a significant decrease in NGAL in the apical membrane (42.42±11.94 ng/ml, $P < 0.0001$) compared to only polymyxin B. NGAL levels were low in the basolateral membrane compared to apical membrane.

After 48h treatment of polymyxin B, the amount of NGAL in the apical membrane did increase significantly from the control (324.28±65.52 ng/ml, $P < 0.01$). However, the presence of rosuvastatin did not change NGAL level 94.26±13.76 ng/ml compared to control 94.85±11.36 ng/ml. The co-treatment of polymyxin B with rosuvastatin caused a significant decrease in NGAL in the apical membrane (220.95±47.97 ng/ml, $P < 0.0001$) compared to only polymyxin B.

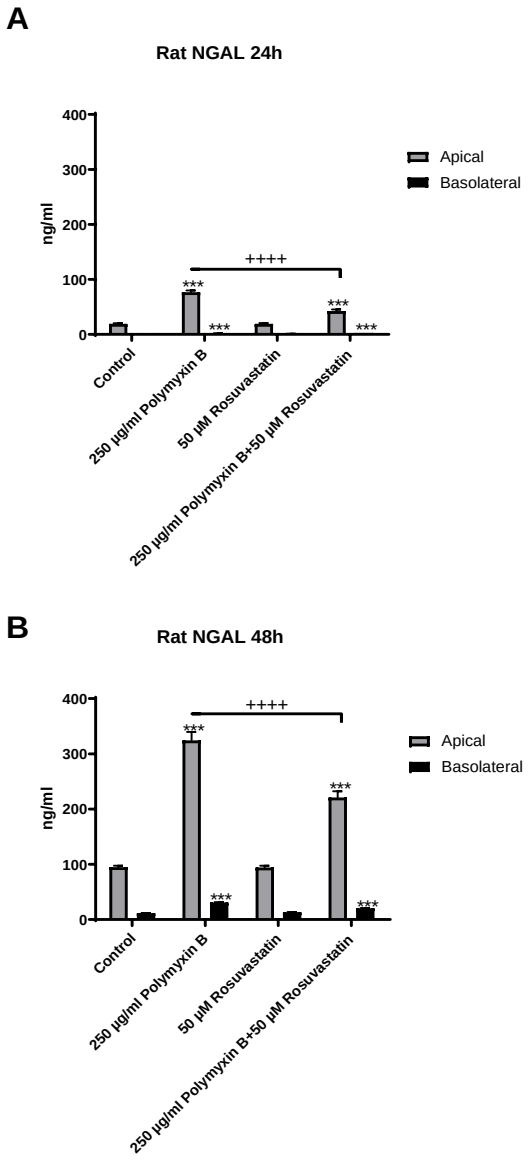

Figure 5.14: The amount of NGAL produced after treatment of rat PTCs for 24 and 48 hours in presence of polymyxin B +/- rosuvastatin.

*ELISA was used to measure NGAL production. The amount of NGAL in the apical membrane change significantly from the control (76.62±14.25 ng/ml, P < 0.01) after 24h polymyxin B treatment. After co-treatment with rosuvastatin, NGAL level decreased to (42.42±11.94 ng/ml, P < 0.0001) compared to only polymyxin B. The level of NGAL after 48h treatment was more than 4 fold compared to 24h. Statistical analysis was conducted using repeated-measures-paired-one-way ANOVA the data are representative of three independent experiments (n=3). Bars represent mean ± S.E.M values of each group. (*p < 0.05, **p < 0.01, ***p < 0.001, $^{++++}$p < 0.0001).*

5.4 Small molecule nephrotoxin – Cisplatin

Rat PTCs were treated with cisplatin, a known nephrotoxin before the expression of KIM-1 and NGAL biomarkers were quantified using ELISA. Cisplatin's effects on rat PTC monolayers have been significant since cisplatin-induced toxicity is already well characterized and can be compared in vivo.

5.4.1 MTS cell viability after treatment in presence of range of concentrations of cisplatin

After cisplatin concentration ranges (5 to 40 µM) were used for 24, 48 and 72 hours with rat PTCs, the cell viability was measured. CellTiter 96® AQueous Non-Radioactive Cell Proliferation Assay (MTS) was used to assess cell viability. The MTS absorbance show as a percentage normalised to control cells. The results are shown in Figure 5.15.

The MTS assay results showed the effect of cisplatin treatment on the cell viability of rat PTCs. With the rise in cisplatin concentration, cell viability decreased significantly. For example, after 24h treatment with 15 µM cisplatin the cell viability was 80.92% compared to non-treated cells. The percentage of live cells was less than 64% after 30 µM cisplatin treatment.

After 48h, the quantity of live cells reduces after cisplatin treatment. For example, the percentage of live cells in 20 µM cisplatin was 60%. After 35 µM cisplatin, the live was less than 45%.

There was a major decrease in cell viability after 72h treatment with a range of concentration of cisplatin. After 20 µM cisplatin treatment, live cells was 44%. In addition, after 35 µM cisplatin incubation the cell viability was only 15%.

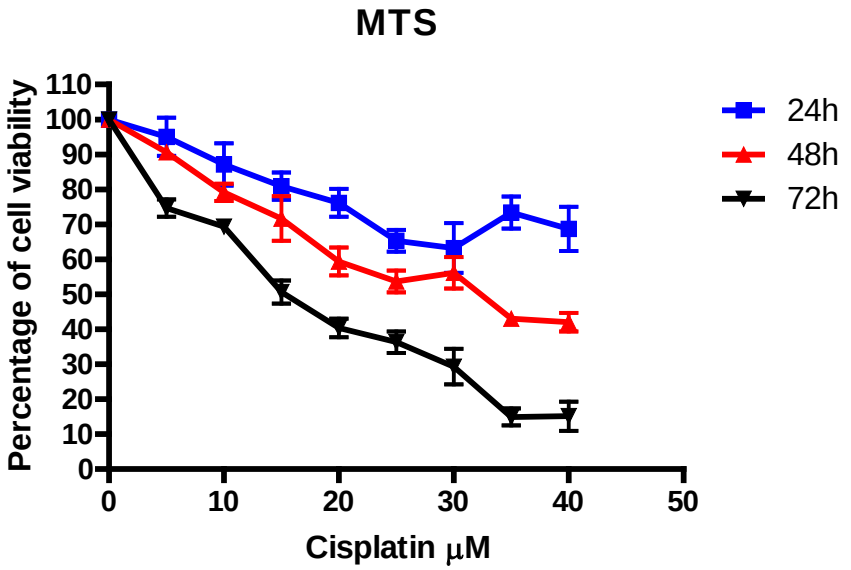

Figure 5.15: Cell viability in rat PTCs treated with range concentrations of cisplatin for 24, 48 and 72 hours.

MTS assay was used to measure the cell viability. For example, the cell viability after 25 μM cisplatin for 24h was 65.3% and the percentage dropped to 53.6% after 48h. In addition, cell viability after 10 μM cisplatin treatment for 72h was 69.3% and after 20 μg/ml cisplatin the cell viability decreased to 41%. Each point represent mean ± S.E.M values of each cisplatin concentration.

5.4.2 KIM-1 production after treatment of rat PTCs in presence of a range concentration of cisplatin:

The production of KIM-1 from rat PTCs after treatment with a range of concentrations of cisplatin were examined. The concentrations of the biomarker was normalised to the cell viability. The results are shown in Figure 5.16**.**

The KIM-1 levels after 24h treatment of cisplatin increased significantly compared to control. For instance, KIM-1 levels were elevated gradually and significantly by 5 to 20 µM cisplatin concentrations. The level of KIM-1 after 25 µM cisplatin treatment was 42.28±5.88 ng/ml compared with the control 2.57±0.41 ng/ml and then the level of KIM-1 increased slightly as the concentration of cisplatin increases up to 40 µM.

The levels of KIM-1 increased significantly in comparison with the control after 48h of cisplatin treatment. Compared to control 7.22±2.53 ng / ml, the level of KIM-1 after 20 µM cisplatin treatment was 62.84±0.99 ng / ml, and then the KIM-1 level remained the same, with cisplatin levels rising to 40 µM.

The KIM-1 levels after 72h treatment of cisplatin increased significantly compared to control. For instance, the level of KIM-1 production reached the first peak at 20 µM cisplatin treatment to 51.13±5.82 ng/ml compared with the control 7.29±1.53 ng/ml and then the level of KIM-1 was stable as the concentration of cisplatin increases up to 40 µM.

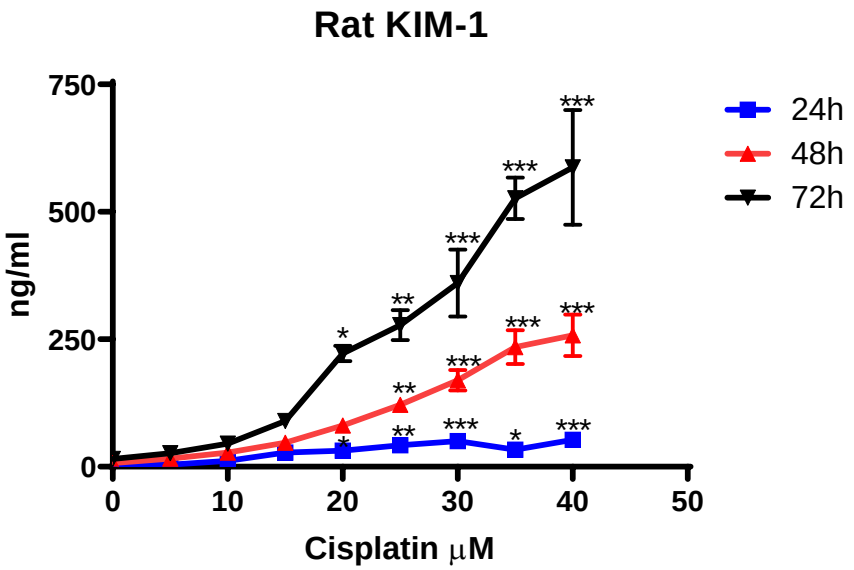

Figure 5.16: Measurement of KIM-1 production from rat PTCs treated with range concentrations of cisplatin for 24, 48 and 72 hours.

*Levels of KIM-1 were normalised to MTS absorbance value to account for cell numbers after nephrotoxin treatments. Rat PTCs were treated with a range of cisplatin concentration (5 to 40 µM). The levels of KIM-1 showed, cisplatin is time and concertation dependent. For example, KIM-1 production after 10 µM cisplatin treatment for 24h was 11.8±3.6 ng/ml and after 25 µM the level of KIM-1 increased to 42.2±5.8 ng/ml. The level of KIM-1 after 30 µM cisplatin treatment for 48h was 127.7±28.2 ng/ml and after 72h the level increased to 360.1±113.9 ng/ml. Statistical analysis was conducted using repeated-measures-paired-one-way ANOVA the data are representative of three independent experiments (n=3). Each point mean ± S.E.M values of each group. (*p < 0.05, **p < 0.01, ***p < 0.001).*

5.4.3 NGAL production after treatment of rat PTCs in presence of a range concentration of cisplatin:

The production of NGAL was investigated after treating the rat PTCs with a concentration range of cisplatin. NGAL concentrations were normalized to the viability of the cell. The results are shown in Figure 5.17**.**

There was a significant increase in NGAL levels after 24h treatment of cisplatin compared to control. NGAL levels were elevated significantly by (20 to 40) µM cisplatin concentrations. The level of NGAL production after 30 µM cisplatin was 144.76±33.1 ng/ml compared with the control 9.64±2.1 ng/ml and then the level of NGAL increased as the concentration of cisplatin increases up to 40 µM.

NGAL levels increased significantly after 48h of cisplatin treatment compared to control. The level of NGAL reached the peak after 25 µM cisplatin treatment 292.42±53.31 ng / ml compared to the control 33.55±4.77 ng / ml, and then the NGAL level remained the same, with the level of cisplatin rising to 40 µM.

The NGAL levels increased in comparison with control after 72h of cisplatin treatment. For example, the level of NGAL production after 30 µM cisplatin treatment was 336.73±112.34 ng/ml compared with the control 82.63±12.82 ng/ml and then the level of NGAL increased as the concentration of cisplatin increases up to 40 µM.

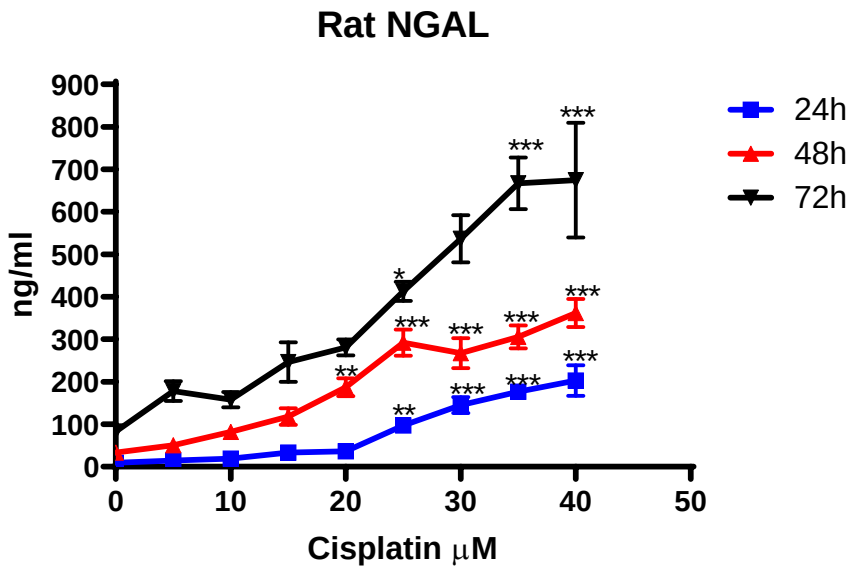

Figure 5.17: Measurement of NGAL production from rat PTCs treated with range concentrations of cisplatin for 24, 48 and 72 hours.

*Levels of NGAL were normalised to MTS absorbance value to account for cell numbers after nephrotoxin treatments. Rat PTCs were treated with a range of cisplatin concentration (5 to 40 µM). The levels of NGAL showed, cisplatin is time and concertation dependent. For example, NGAL production after 20 µM cisplatin treatment for 24h was 36.1±4.1 ng/ml and after 30 µM the level of NGAL increased to 144.7±33.1. The level of NGAL after 25 µM cisplatin treatment for 48h was 292.4±53.3 ng/ml and after 72h the level increased to 413.2±39.1 ng/ml. Statistical analysis was conducted using repeated-measures-paired-one-way ANOVA the data are representative of three independent experiments (n=3). Each point mean ± S.E.M values of each group. (*p < 0.05, **p < 0.01, ***p < 0.001).*

5.4.4 MTS and ATP cell viability assays:

After 24 and 48 hours treatment of rat PTCs with 25 µM cisplatin, cell viability was measured. The cell viability was also measured in the presence of cimetidine co-treatments. Both MTS and ATP assays were used to assess cell viability from the same plate. No major difference was discovered between the two methods. The results are shown in Figure 5.18**.**

After 24h, the results showed that cell viability was considerably reduced to 73.29±1.43% as a result of exposure to cisplatin. The co-treatment with cimetidine hasn't altered cell viability (94.82±1.27% live cells). The treatment of cisplatin with cimetidine increased the live cells compared to only cisplatin (82.41±1.46%).

The cell viability was reduced significantly by cisplatin (65.17±4.47%) after 48h treatment. However, the cell viability did not change with cimetidine (94.11±4.16%). Cisplatin with cimetidine cell viability was higher than cisplatin alone (73.77±3.26% viable cells).

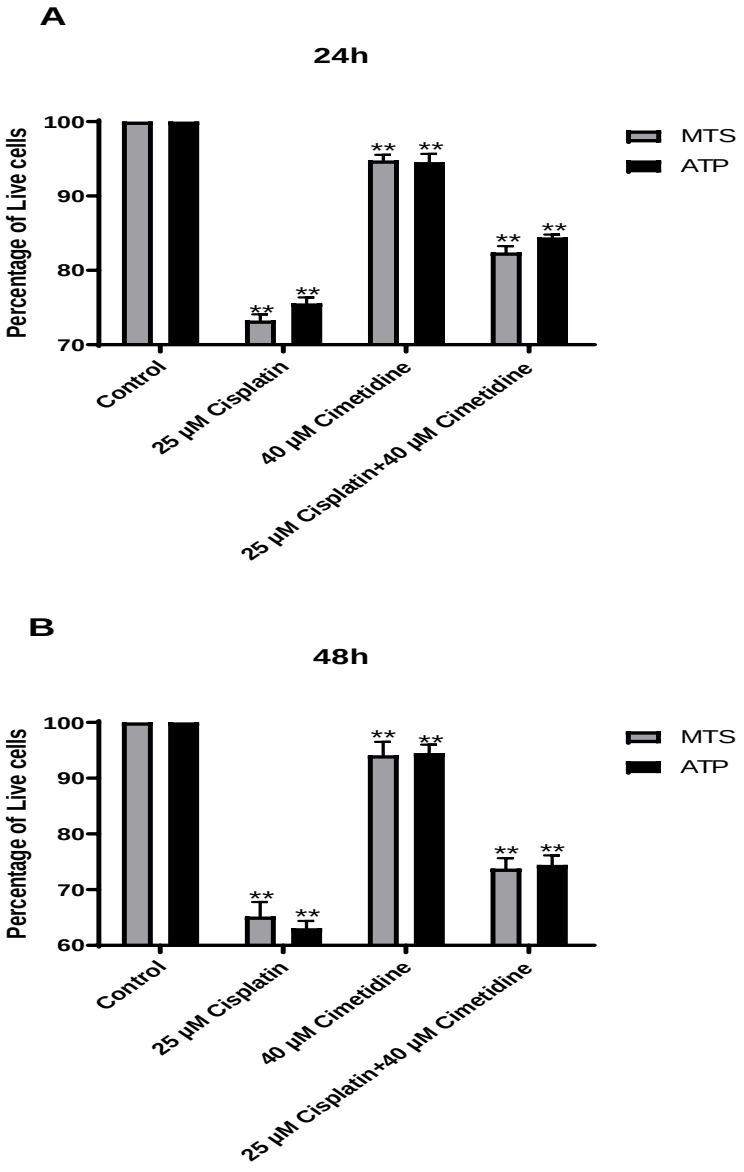

Figure 5.18: Cells Viability of rat PTCs after treatment of cisplatin for 24 and 48 hours.

*MTS and ATP assays were used to measure the cell viability. Viability is measured as a percentage of the control. For example, MTS percentage after cisplatin treatment for 24h was 73.2% and ATP percentage was 75.6%. In addition, the co-treatment of cimetidine with cisplatin for 48h showed, the percentage of MTS was 73.7% and ATP percentage was 74.4%. Statistical analysis was conducted using repeated-measures-paired-one-way ANOVA the data are representative of three independent experiments (n=3). Bars represent mean ± S.E.M values of each group. (*p < 0.05, **p < 0.01, ***p < 0.001).*

5.4.5 Lactate dehydrogenase (LDH) cytotixicy assay:

Measuring cytoplasmic enzymes released by damaged cells is a common method for determining cytotoxicity. In this experiment, we treated rat PTCs for 24 and 48 hours with 25 µM cisplatin and LDH was measured. In addition, we measured the LDH after cimetidine co treatment. The results are consistent with cell viability data. Result shown in Figure 5.19.

After 24hour, the results revealed that LDH increased significantly in response to cisplatin exposure to 34.72±3.51%. The cimetidine co treatment did not change the LDH (14.74±2.98%) compared to control. The treatment of cisplatin with cimetidine increased the LDH compared to only cisplatin (27.15±1.15%).

The LDH was increased significantly by cisplatin (50.72±0.40%) after treatment for 48h .However, the LDH did not change with cimetidine (16.85±1.58%). The LDH after cisplatin with cimetidine was lower than only cisplatin (32.92±2.50%).

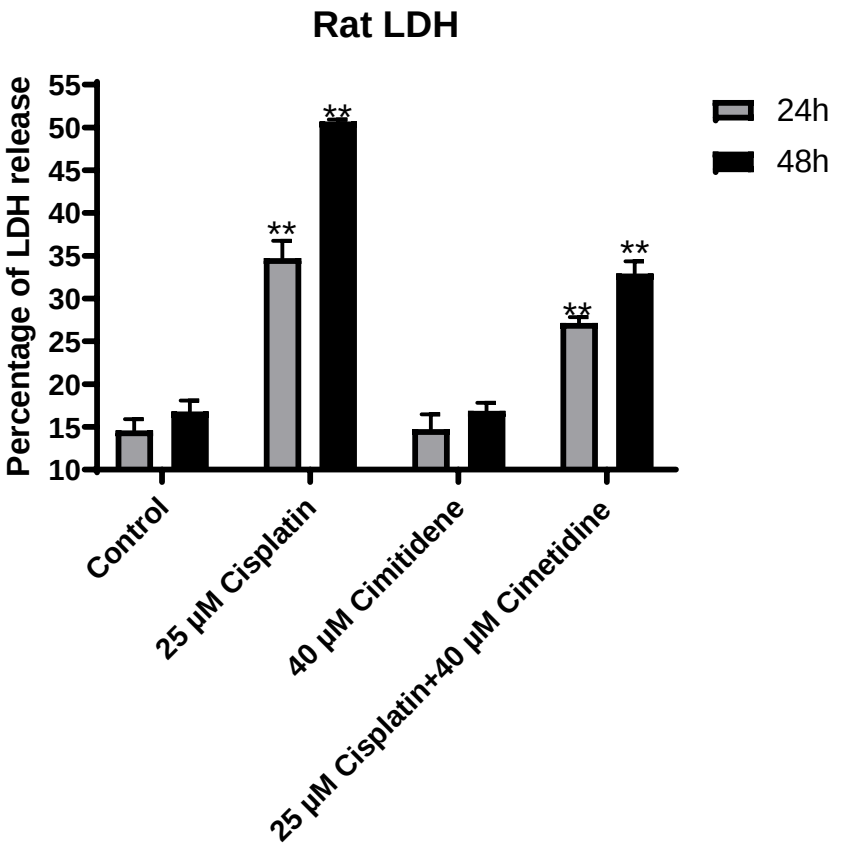

Figure 5.19: LDH of rat PTCs after treatment of cisplatin for 24 and 48 hours.

*LDH is measured as a percentage of the control. LDH percentage after cisplatin treatment for 24h was 34.7% and after 48h the percentage increased to 50.7%. In addition, LDH percentage decreased after cimetidine co-treatment with cisplatin for 48h to 33.1% Statistical analysis was conducted using repeated-measures-paired-one-way ANOVA the data are representative of three independent experiments (n=3). Bars represent mean ± S.E.M values of each group. (*p < 0.05, **p < 0.01, ***p < 0.001).*

5.4.6 KIM-1 production after treatment of rat PTCs in presence of cisplatin +/- cimetidine

The amount of KIM-1 produced after 24 and 48 hours treatment of rat PTCs in the presence of 25 μM cisplatin. The KIM-1 levels were also measured in the presence of cimetidine co-treatments. The concentrations of KIM-1 was normalised to the cell viability as determined from their MTS absorbance's, expressed as ng/ml. The results are shown in Figure 5.20.

After 24h treatment of cisplatin, the amount of KIM-1 in the apical membrane did change significantly from the control (2.51±0.18 ng/ml, $P < 0.01$). However, the presence of cimetidine did not change KIM-1 level 0.59±0.12 ng/ml compared to control 0.58±0.11 ng/ml. The co-treatment of cisplatin with cimetidine caused a significant decrease in KIM-1 in the apical membrane (1.34±0.24 ng/ml, $P < 0.0001$) compared to only cisplatin. KIM-1 levels in the basolateral membrane were low compared to apical membrane.

After 48h treatment of cisplatin, the amount of KIM-1 in the apical membrane did increase significantly from the control (14.25±0.46 ng/ml, $P < 0.01$). However, when we added cimetidine did not change KIM-1 level 4.03±1.03 ng/ml compared to control 4.18±0.36 ng/ml. The co-treatment of cisplatin with cimetidine caused a significant decrease in KIM-1 in the apical membrane (7.53±1.99 ng/ml, $P < 0.0001$) compare to only cisplatin. KIM-1 levels in the basolateral membrane were low compared to apical membrane.

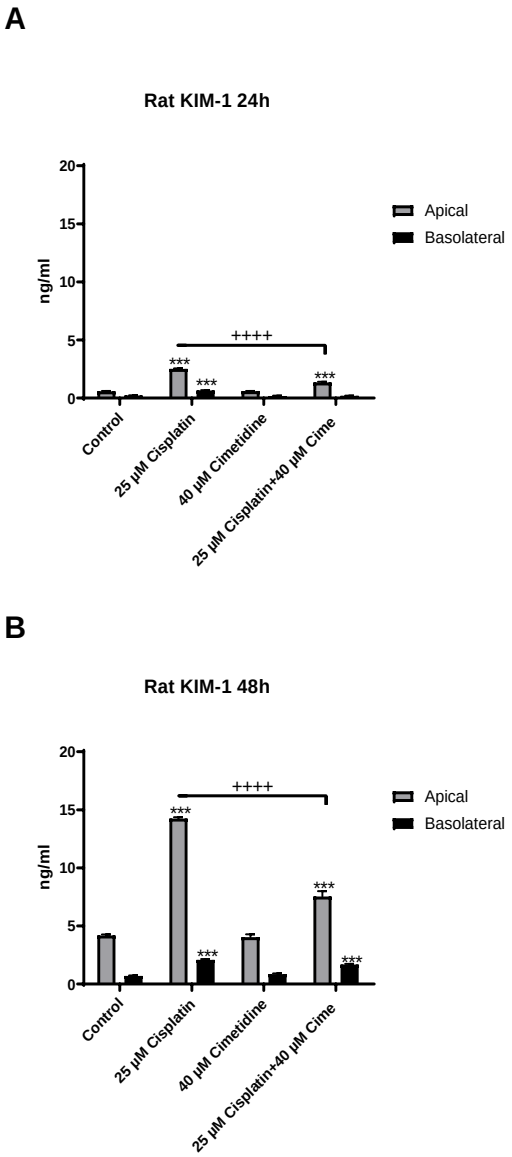

Figure 5.20: The amount of KIM-1 produced after treatment of rat PTCs for 24 and 48 hours in presence of cisplatin +/- cimetidine.

ELISA was used to measure KIM-1 production. The amount of KIM-1 in the apical membrane change significantly from the control (0.58±0.11 to 2.51±0.18 ng/ml, P < 0.01) *after 24h cisplatin treatment. After co-treatment with cimetidine, KIM-1 level decreased to* (1.34±0.24 ng/ml, P < 0.0001*) compared to only cisplatin. The level of KIM-1 after 48h treatment was almost 5 fold higher than 24h. Statistical analysis was conducted using repeated-measures-paired-one-way ANOVA the data are representative of three independent experiments (n=3). Bars represent mean ± S.E.M values of each group. (*p < 0.05, **p < 0.01, ***p < 0.001, ++++p < 0.0001).*

5.4.7 NGAL production after treatment of rat PTCs in presence of cisplatin +/- cimetidine

NGAL production for 24 and 48 hours after treatment of rat PTCs in the presence of 25 µM of cisplatin. In the presence of cimetidine co-treatment, levels of NGAL were also measured. NGAL concentrations had been normalized to cell viability based on the MTS absorption of the rat PTCs, resulting in ng / ml. The results are shown in Figure 5.21.

After 24h treatment of cisplatin, the amount of NGAL in the apical membrane did increase significantly from the control (330.61±22.37 ng/ml, $P < 0.01$). However, the presence of cimetidine did not change NGAL level 117.41±5.35 ng/ml compared to control 114.12±5.83 ng/ml. The co-treatment of cisplatin with cimetidine caused a significant decrease in NGAL in the apical membrane (178.31±9.58 ng/ml, $P < 0.001$) compared to only cisplatin. Compared to apical membrane, NGAL levels in the basolateral membrane were low.

After 48h treatment of cisplatin, the amount of NGAL in the apical membrane did rise significantly from the control (1910.42±205.1 ng/ml, $P < 0.01$). However, the presence of cimetidine did not change NGAL level 407.16±33.67 ng/ml compared to control 406.88±91.31 ng/ml. The co-treatment of cisplatin with cimetidine caused a significant decline in NGAL in the apical membrane (890.28±126.72 ng/ml, $P < 0.001$) compared to only cisplatin NGAL concentrations were low in the basolateral membrane compared to apical membrane.

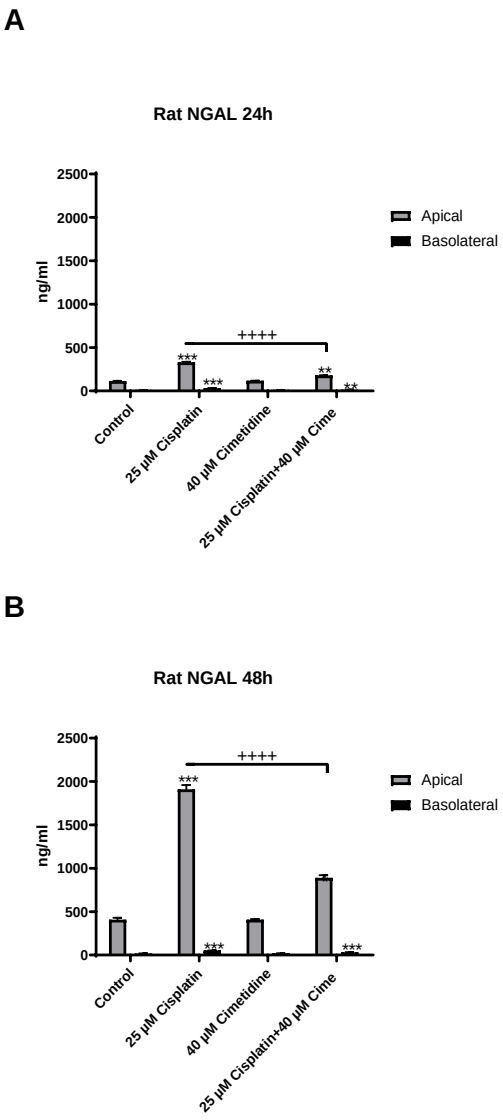

Figure 5.21: The amount of NGAL produced after treatment of rat PTCs for 24 and 48 hours in presence of cisplatin +/- cimetidine.

*ELISA was used to measure NGAL production. For example, NGAL production in the apical membrane is significantly higher than basolateral membrane. The amount of NGAL in the apical membrane change significantly from the control (114.12±5.83 to 330.61±22.37 ng/ml, P < 0.01) after 24h cisplatin treatment. After co-treatment with cimetidine, NGAL level decreased to (178.31±9.58 ng/ml, P < 0.001) compared to only cisplatin. The level of NGAL after 48h treatment was more than 6 fold compared to 24h. Statistical analysis was conducted using repeated-measures-paired-one-way ANOVA the data are representative of three independent experiments (n=3). Bars represent mean ± S.E.M values of each group. (*p < 0.05, **p < 0.01, ***p < 0.001, $^{++++}$p < 0.0001).*

5.5 Discussion

Nephrotoxicity is a major adverse effect of many drugs on the market. Multiple toxic compound tests are used in vivo, cost-effective, practical and expedient in vitro tests that support the predictive early toxicity of the big amounts of compounds ahead of in vivo tests.[145] while many nephrotoxicity biomarkers have been assessed and implemented in preclinical and clinical studies, at an early screening point, they are rarely examined in vitro. We explored the potential of nephrotoxicity biomarkers in rat PTCs an in vitro screening model in this chapter and compared the predictive results of nephrotoxicity biomarkers. KIM-1 and NGAL were further investigated in PTCs, which were freshly isolated from rat kidney. High doses of gentamicin, polymyxin B and cisplatin-induced significant upregulation of KIM-1 and NGAL levels within 24h and 48h.

5.5.1 MTS and ATP

In this study, one further goal was to compare MTS and ATP assay results from rat PTCS treated with different nephrotoxins. Similarities in the viability data from both assays were found, similar results were expected as mitochondrial enzymes reduce the reagents from both MTS and ATP. For example, percentage of live cells using MTS assay after 250 µg/ml polymyxin B treatment for 24h was 74.52% and after using APT assay was 69.7%. There were only 5% difference between the two assays, suggesting the reproducible of our in vitro rat PTCs model by using different types of cell viability assays.

5.5.2 LDH

On the other hand, percentage of dead cells were quantified by measuring the LDH release from rat PTCs after nephrotoxins treatment for 24 and 48 hours. A study done showed, LDH release from mice primary PTCs after 50 µM cisplatin treatment was 40% compared to only 8% of control cells and the co treatment with caspase inhibitor reduce the LHD percentage to 13.5%[146].

In this chapter, the viability of rat PTCS was analysed during exposure to different nephrotoxins for 24, 48 and 72 hours. Using our rat PTCs model, our data shows that nephrotoxins used are cytotoxic in vitro in a dose-and time-dependent manner and this was directly proportional to drug accumulation. In the dose-response study, KIM-1 and NGAL produced from rat PTCs are

very sensitive to the renal injury produced by different nephrotoxins (gentamicin, polymyxin and cisplatin). Gentamicin accumulates in rat PTCs, resulting in structural modifications and functional impairment of the plasma membrane, mitochondria and lysosome [147]. Compared with a recent study observing increases of KIM-1/urinary creatinine levels in patients after 72h of Polymyxin B exposure, they observed significant accumulation of KIM-1 and NGAL at both 24 and 48 hours of exposure, demonstrating the sensitivity of the rat PTCs model to detect early injury [148]. Our results demonstrate the potential of KIM-1 as well as NGAL to be significantly induced for detection of nephrotoxicity in a sensitive and timely manner.

5.5.3 Rat Biomarkers

The cellular toxicity of gentamicin was monitor after treated rat PTCs for 24 and 48 hours. For example, after treatment with 250 μg/ml gentamicin for 24h, the level of KIM-1 significantly increased (10.31±0.72 ng/ml, $P < 0.001$) compared to control (3.86±0.28 ng/ml). In addition, after 48h the level of KIM-1 increased to 28.70±0.50 ng/ml.

Around 80% of the gentamicin dose is excreted by glomerular filtration into the urine within 24h. However, accumulation within the kidney cortex continues high relative to other bodies, particularly in the proximal tubule epithelial cells (5–10% dose)[149]. In the pathogenesis of nephrotoxicity, this is considered significant[150]. It has been shown that receptor-mediated endocytosis binding of gentamicin to the multi-ligand receptor, megalin, and cellular uptake is the main pathway for accumulation. The abundant adverse charges on the extracellular receptor domain facilitate interactions among polybasic substances like gentamicin[151].

After therapy with gentamicin, a study noted upregulation of mRNA expression of KIM-1 and NGAL in rats in the lack of impacts of nephrotoxicity on traditional clinical chemistry markers. These rise were apparent 1 day after gentamicin was handled and lasted 3 to 7 days. The timing and degree of reaction were well associated with the severity of tissue injury. Immunohistochemistry subsequently verified changes in protein expression. They found that KIM-1 and NGAL expressions occur within 1 day of gentaimcin's treatment acknowledge that these two biomarkers reflected renal injury quicker and more precisely than SCr and BUN[121].

In this chapter demonstrating that cilastatin, a particular tubular brush-border DHP-I inhibitor, attenuates in vitro nephrotoxicity caused by gentamicin. The pre-treatment of 40 μM cilastatin

before treated the rat PTCs with gentamicin decrease the production of nephrotoxins biomarkers (KIM-1 and NGAL). For instance, NGAL production after gentamicin treatment for 48h was 400.6 ng/ml and after co-treatment with cilastatin NGAL level decrease to 251.3 ng/ml suggesting the role of cilastatin of preventing the nephrotoxicity of gentamicin. The results are consistent with another study suggest cilastatin inhibit the binding of megalin with polymyxin B and gentamicin. The same study showed that cilastatin suppresses colistin-induced nephrotoxicity through competition for binding to megalin [73].

Polymyxin B used as a nephrotoxic drug and the levels of KIM-1 and NGAL were measured after the exposure rat PTCs. Our results showed a significant increase in biomarkers levels after polymyxin B treatment compared to non-treated cells. In addition, rosuvastatin used as co treatment against polymyxin B nephrotoxicity and the data showed the reduction in the levels of biomarkers production in comparison to only polymyxin B incubation. KIM-1 level after 250 µg/ml polymyxin B treatment for 24h was 5.42 ng/ml compare to 1.58 ng/ml for control cells. However, after the co-treatment with rosuvastatin the production of KIM-1 reduce to 2.76 ng/ml showing a possible protective process against polymyxin B nephrotoxicity.

Our hypothesis that statins, are inhibiting megalin-mediated endocytosis, would inhibit uptake of polymyxin B, and therefore decrease nephrotoxicity in PTCs. This hypothesis was tested in vitro study using an OK cell model but with gentamicin not polymyxin B[152]. The synthesis of cholesterol in OK cell was shown to be inhibited by statins (simvastatin, pravastatin, and rosuvastatin).They also led to dose dependent inhibition of gentamicin accumulation and cytotoxicity, which were related to the degree of GTP-binding protein unprenylation[152].

One of the nephrotoxic drugs used in this study is cisplatin. Rat PTCs treated with 25 µM cisplatin for 24 and 48 hours and KIM-1 and NGAL biomarkers were measured. The production of KIM-1 after 24h treatment with cisplatin was 2.51±0.18 ng/ml and the NGAL production was 330.6±22.3 ng/ml. Furthermore, co treatment with cimetidine was measured. The results showed a reduction of biomarkers production after cisplatin treated with cimetidine compared to only cisplatin. For example, NGAL level after cisplatin treatment for 48h was 1910.4±205.1

ng/ml and the level dropped significantly to 890.2±126.7 ng/ml after the co treatment with cimetidine.

In the original clinical trials of cisplatin chemotherapy, nephrotoxicity was reported. The intracellular transport mechanism of cisplatin is not evident and vary between cells. A research showed that removal of Ctr1, a highly affinity copper transporter, reduces cisplatin intracellular accumulation in yeasts, which is linked to enhanced cisplatin toxicity resistance[65]. The same findings show that copper transporters are allowed for cisplatin in mouse cell lines, lacking either one or two Ctr1 alleles. In the renal system, however, cisplatin is taken by organic cation transporters (OCTs)[153]. OCTs mediate the transport of several cationic compounds into renal tubular cells from basolateral to apical compounds. A research showed that cisplatin caused greater toxicity in MDCK cells in apical side implementation when applied on the basolateral side[67]. These findings show that tubular cell injury caused by cisplatin may be linked with OCT2. In particular, cimetidine, an OCT inhibitor, could partly stop cytotoxicity caused by cisplatin by decreasing transepithelial electrical resistance[110]. Another study showed, cimetidine obviously inhibits cisplatin-induced nephrotoxicity or kidney cell damage with no impact on cisplatin in vitro or in vivo antitumor activities [154]. Although cimetidine's in vitro actions were mainly due to inhibition the production of ROS, the in vivo protective impact of cimetidine on cisplatin's nephrotoxicity seems to be due to both inhibitory actions in ROS manufacturing and OCT2 expressed intrinsically in the kidney[127].

The concentration of the biomarkers was more in the apical membrane than in the basolateral membrane. Such findings predicted and represented what's really happening in vivo. Those biomarkers are detectable in urine. NGAL is upregulated and can be detected in the kidney and urine of mice three hours after treatment with cisplatin, and a good nephrotoxicity biomarker has been suggested [133]. Due to the leakage of the cells, the significant in the basolateral membrane was expected and lost their integrity after treatment with drugs.

These findings may reflect what is really happen in vivo. The findings suggest new possibilities for early prediction of nephrotoxicity by measuring the production of KIM-1 and NGAL when the kidney exposed to different drugs. The rat data is almost consistent with human data, this may show the possibility of using rat PTCs model in to investigate nephrotoxic drugs. However,

more drugs are still need to examine and more biomarker need to screen to confirm this finding. Our data showed cilastatin, rosuvastatin and cimetidine could be a good co-treatment for kidney from damaging because of using different drugs by using our rat PTCs model.

6 Measurement of cisplatin apoptosis activity

6.1 Introduction

Nephrotoxicity of cisplatin may occur in a variety of forms, for example, distal renal tubular acidosis, renal concentrating defect and chronic renal failure. However, the most severe and frequent occurrence in 20–30 % of patients is acute renal injury (AKI) [63]. Evidence of basolateral to apical transportation of cisplatin has been provided in previous studies using kidney slices, cultures of renal epithelial cells and isolated perfuse proximal tubule segments[155]. The nephrotoxicity mechanisms of cisplatin are complicated and require many pathways and molecules. Using newly isolated or cultured renal tubular epithelial cells, cellular pathways of cisplatin injury to kidney cells were mainly examined in vitro [156]. In vitro, low cisplatin levels preferably lead to apoptotic death, whereas necrosis occurs at greater concentrations [111]. In vivo administration of nephrotoxic cisplatin doses results in a significant rise in necrosis and apoptosis in the kidney [63].

Apoptosis is programmed cell death, includes the regulated dismantling of the intracellular elements while the adjacent cells are prevented from inflammation and harm[157]. Cisplatin has been found to cause cancer cell death by apoptosis as well as many chemical agents and it is interesting to determine if apoptosis is also the mechanism of cell death in a nephrotoxic injury[158]. Strategies can be created to minimize or stop nephrotoxicity by increasing a knowledge of the particular mechanisms responsible for nephrotoxic cell injury.

P53 can be one of the pathways for cell killing triggered by cisplatin [159]. P53 can induce apoptosis by transcription of proapoptotic genes or by direct interaction and activation of existing proapoptotic molecules, as a tumour suppressing protein[160]. P53 is activated by cisplatin in cultured renal tubular cells[161]. P53 can upregulate proapoptotic genes including apoptosis-α modulator p53-upregulator, resulting in the permeability of mitochondrial outer membrane and release of apoptogenic factors, including cytochrome c and inducing apoptosis factor[162]. However, it is not clear yet how is p53 cause nephrotoxicity in vivo.

Caspase activation is considered important in apoptosis, and a large number of stimuli activate caspases, including plasma membrane death receptors (caspase8) and mitochondrial dysfunction (caspase9)[161]. Initiator caspases include caspases 8 and 9, and activation of

those caspases results in activation of downstream and executioner caspases such as caspases 3 and 7[163].

The goal of this chapter is the quantification of a variety of proteins that influence apoptosis (p53, caspase 3, caspase 8 and caspase 9) after treatment of human and rat PTCs with cisplatin. The expressions will be quantified at the protein and mRNA levels, using caspase-Glo® 3/7 Assay and qPCR respectively. The results will provide an indication of the molecular mechanism of apoptosis in PTCs after cisplatin treatment. The purpose of this chapter is to use human and rat primary proximal tubule cells (PTCs) as suitable models for cisplatin apoptosis mechanisms.

6.2 Caspase-Glo® 3/7 Assay

Caspase-3/7 activity was detected using a Caspase-Glo 3/7 assay system after treated human PTCs with different nephrotoxins (cisplatin, polymyxin B and gentamicin) for 48h. The results are shown in Figure 6.1**.**

The results revealed that caspase 3/7 activity increased significantly in response to exposure to cisplatin to 5.64±0.63% of control. The polymyxin B treatment did increase but not significantly the 3/7 activity (1.55±0.29%). The treatment of gentamicin increased the 3/7 activity cells compared control (3.35±0.77%).

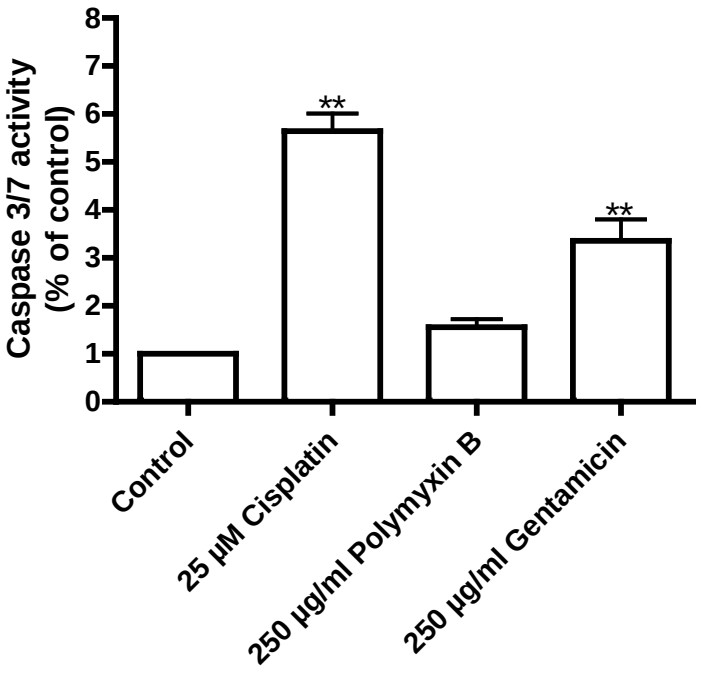

Figure 6.1: Caspase 3/7 activity after treated human PTCs with cisplatin, polymyxin B and gentamicin for 48h.

*Caspase-Glo 3/7 assay system was used to measure the caspase activity. Activity is measured as a percentage of the control. Caspase 3/7 activity increased significantly in response to exposure to cisplatin to 5.64±0.63% of control. The treatment of gentamicin increased the 3/7 activity cells compared control (3.35±0.77%). Statistical analysis was conducted using repeated-measures-paired-one-way ANOVA the data are representative of three independent experiments (n=3). Bars represent mean ± S.E.M values of each group. (*p < 0.05, **p < 0.01, ***p < 0.001).*

6.3 The mRNA level of caspase 3, 8, 9 and p53 after treatment of human PTCs with cisplatin +/- cimetidine

To investigate the mRNA levels of caspase 3 in the presence of cisplatin, the cell total RNA of human PTCs were isolated and screened. The results are shown in Figure 6.2, which are normalised to the reference gene GAPDH.

mRNA level of caspase 3 appeared to be increased significantly ($P< 0.01$) with the treatment of cisplatin (3.51±0.34%) compared to control. In addition, cimetidine did not change caspase 3 mRNA levels significantly, its co-treatment with cisplatin did decrease caspase 3 mRNA levels significantly to (2.45±0.32, $P< 0.05$) when compared only cisplatin treatment.

mRNA level of caspase 8 increased significantly with the treatment of cisplatin compared to control (3.06±1%, $P< 0.01$). In addition, cimetidine did not change caspase 8 mRNA levels significantly, its co-treatment with cisplatin did decrease caspase 8 mRNA levels significantly to (1.76±0.48, $P< 0.05$) when compared to cisplatin alone.

mRNA level of caspase 9 increased significantly with the treatment of cisplatin compared to control (2.47±0.30%, $P< 0.01$). Furthermore, cimetidine has not changed caspase 9 mRNA level, its co-treatment with cisplatin has considerably reduced caspase 9 mRNA level to (1.90±0.36, $P<0.05$) compared to cisplatin alone.

After cisplatin treatment, the mRNA level of p53 increased significantly compared to control (7.30±1.25%, $P< 0.01$). Furthermore, cimetidine has not changed p53 mRNA level, its co-treatment with cisplatin has considerably reduced p53 mRNA level to (3.99±1.75, $P<0.05$) compared to only cisplatin treatment.

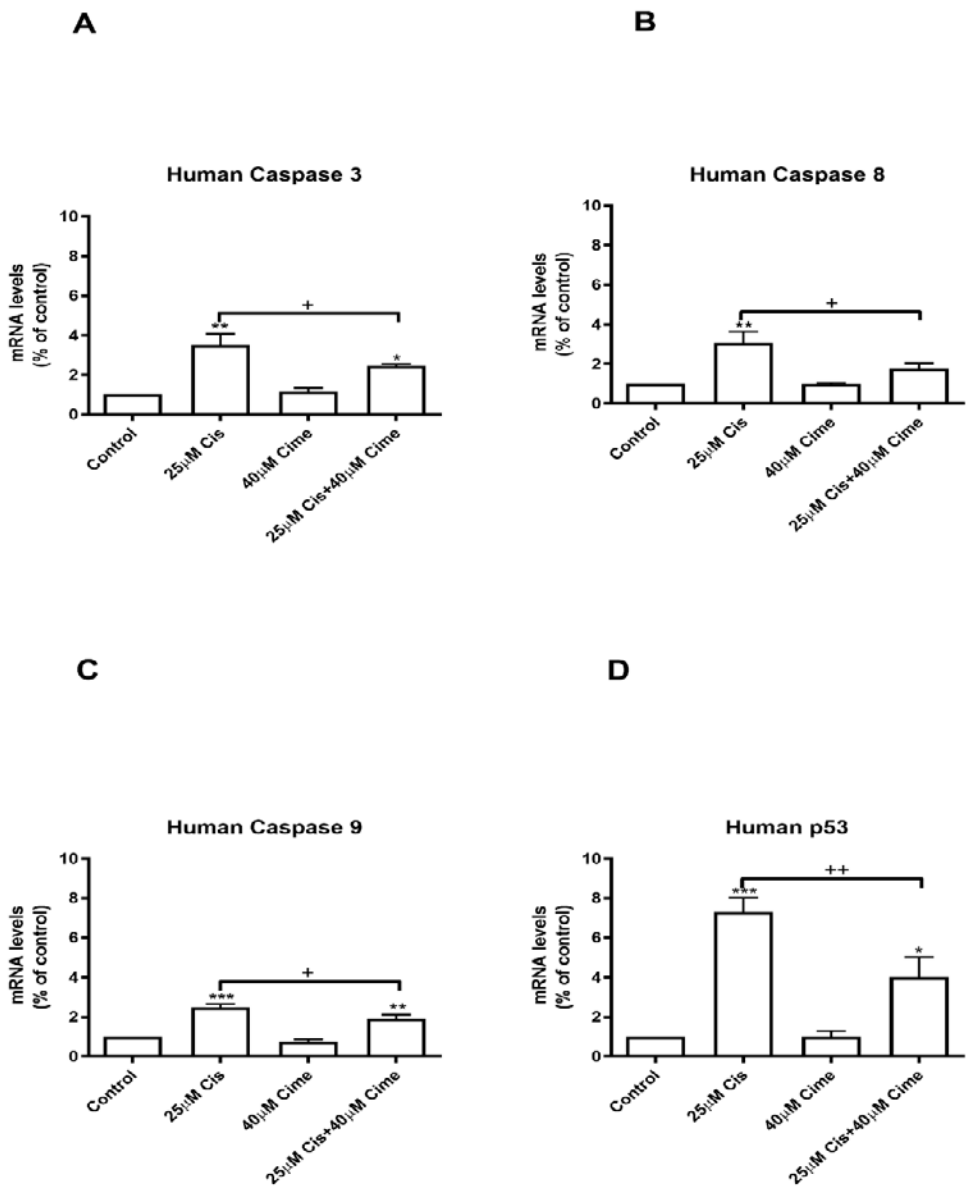

Figure 6.2: The mRNA level after treatment of human PTCs in presence of cisplatin +/- cimetidine.

*(A) (B) Caspase 8 (C) Caspase 9 (D) p53.mRNA is measured as a percentage of the control. For example, after cisplatin treatment, the mRNA level of p53 increased significantly compared to control (7.30±1.25%, P< 0.01). Furthermore, cimetidine has not changed p53 mRNA level, its co-treatment with cisplatin has considerably reduced p53 mRNA level to (3.99±1.75, P<0.05) compared to only cisplatin treatment. Statistical analysis was conducted using repeated-measures-paired-one-way ANOVA the data are representative of three independent experiments (n=3). Bars represent mean ± S.E.M values of each group. (*p < 0.05, **p < 0.01, $^{+++}$p < 0.001).*

6.4 The mRNA level of caspase 3, 8, 9 and p53 after treatment of rat PTCs with cisplatin +/- cimetidine

The total RNA from rat PTCs was separated and screened in order to explore the mRNA expression of caspase 3 after cisplatin treatment. The results are shown in Figure 6.3, which are normalised to the reference gene GAPDH.

mRNA level of caspase 3 appeared to be increased significantly ($P< 0.001$) with the treatment of cisplatin (3.35±0.12%) compared to control. In addition, cimetidine did not change caspase 3 mRNA levels significantly, its co-treatment with cisplatin did decrease caspase 3 mRNA levels significantly to (2.19±0.51, $P< 0.001$) when compared to only cisplatin treatment.

mRNA level of caspase 8 increased significantly with the treatment of cisplatin compared to control (4.40±1.03%, $P< 0.001$). In addition, cimetidine did not change caspase 8 mRNA levels significantly, its co-treatment with cisplatin did decrease caspase 8 mRNA levels significantly to (2.67±0.65, $P< 0.001$) when compared to cisplatin alone.

mRNA level of caspase 9 increased significantly with the treatment of cisplatin compared to control (3.35±0.58%, $P< 0.001$). Furthermore, cimetidine has not changed caspase 9 mRNA level, its co-treatment with cisplatin has considerably reduced caspase 9 mRNA level to (1.92±0.48, $P<0.01$) compared to only cisplatin.

After cisplatin treatment, the mRNA level of p53 increased significantly compared to control (3.19±0.44%, $P< 0.001$). Furthermore, cimetidine has not changed p53 mRNA level, its co-treatment with cisplatin has considerably reduced p53 mRNA level to (2.25±0.61, $P<0.05$) compared to cisplatin alone.

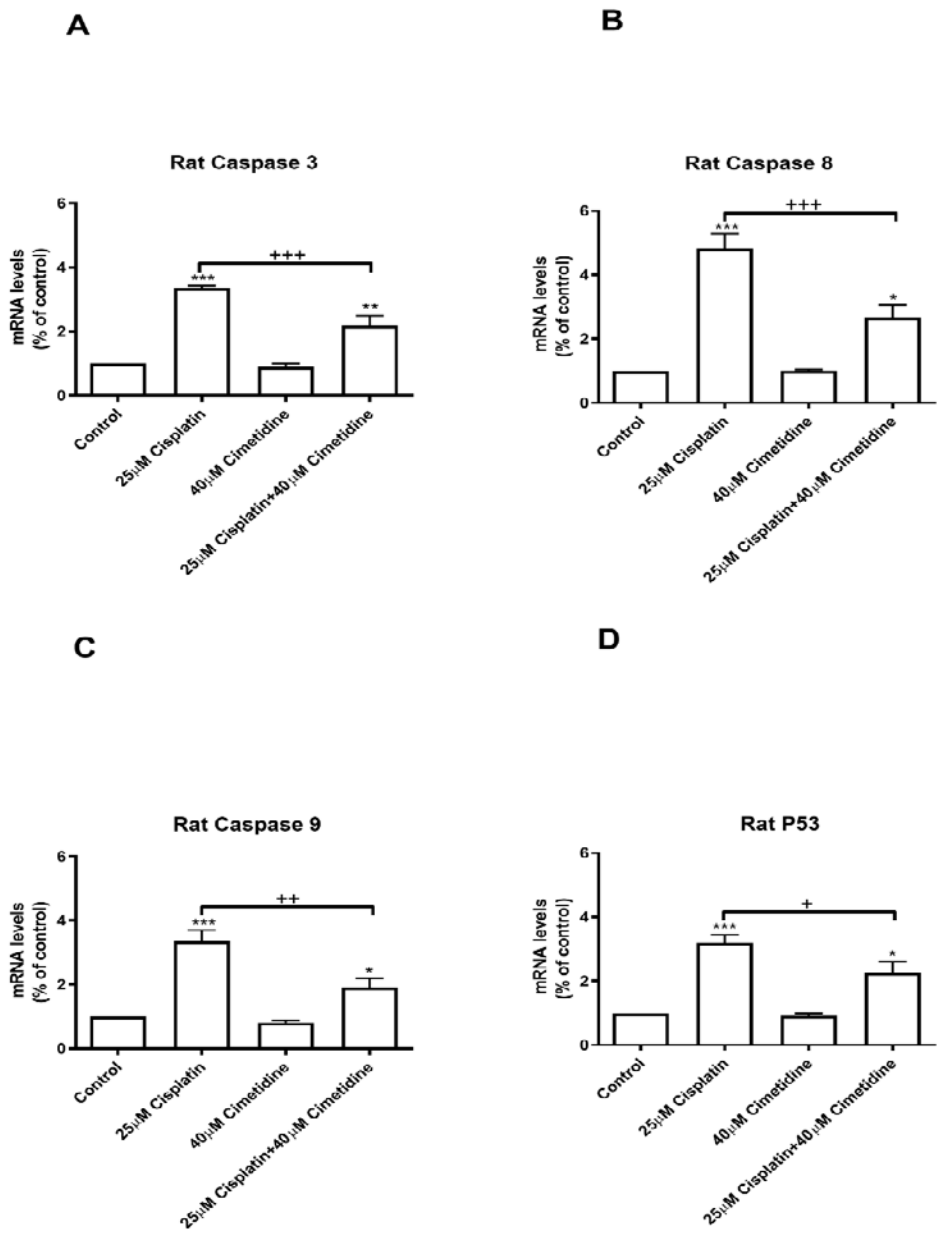

Figure 6.3: The mRNA level after treatment of rat PTCs in presence of cisplatin +/- cimetidine.

(*A) Caspase 3 (B) Caspase 8 (C) Caspase 9 (D) p53. mRNA is measured as a percentage of the control. For example, mRNA level of caspase 3 appeared to be increased significantly (P< 0.001) with the treatment of cisplatin (3.35±0.12%) compared to control. In addition, cimetidine did not change caspase 3 mRNA levels significantly, its co-treatment with cisplatin did decrease caspase 3 mRNA levels significantly to (2.19±0.51, P< 0.001) when compared to only cisplatin treatment. Statistical analysis was conducted using repeated-measures-paired-one-way ANOVA the data are representative of three independent experiments (n=3). Bars represent mean ± S.E.M values of each group. (*p < 0.05, **p < 0.01, $^{+++}$p < 0.001).*

6.5 Discussion

Cisplatin is one of the most common chemotherapeutic agents to treat testes and bladder, head and neck, ovarian, breast, pulmonary cancers, and refractory lymphoma non-Hodgkin[164]. Nephrotoxicity is the significant adverse effect of cisplatin use in which proximal cells in the kidney are particularly susceptible. Its anticancer activity is likely to depend on the formation of intrinsic DNA links [63]. A number of different mechanisms for kidney tubule cisplatin cytotoxicity were suggested, including direct DNA damage, caspase activation, mitochondrial dysfunction, reactive oxygen formation species, effects on the endoplasmic reticulum, and TNF-α apoptotic pathway activating[165]. The purpose of this chapter was to determine the cisplatin apoptosis mechanism by using our human and rat proximal tubule models.

In this chapter, caspase 3/7 was measured after human PTCs treated with different nephrotoxins. Our results significant increase in caspase 3/7 activity compared to control cells after cisplatin and gentamicin treatments. However, there was increase after polymyxin B treatment. It might suggest gentamicin has the same apoptosis mechanism like cisplatin. A study used NRK-52E cells (rat renal proximal tubular cell line) showed after, a significant increase in caspase 3 and caspase 8 after gentamicin treatment, indicting gentamicin trigger the apoptosis mechanism in PTCs[166].

In order to evaluate the cisplatin apoptosis mechanism in PTCs, this chapter results detected the expression of caspase-3, 8, 9 and p53 at the mRNA levels after treated human and rat PTCs with cisplatin and we used cimetidine as a co treatment. After cisplatin exposure, the mRNA levels of caspase 3, 8, 9 and p53 were increased compared to no treated cells. For instance, mRNA expression of caspase 3 after rat PTCs treated with cisplatin was 3.35% and after the co treatment with cimetidine the level reduced to 2.19%. Furthermore, human PTCs cells treated with cisplatin and mRNA level p53 was 7.30% and with cimetidine co-treatment the mRNA level dropped to 3.99%.

A study showed p53 activation by cisplatin in cultured renal tubular cells[161]. DNA damage is induced by cisplatin and then enzymes like telangiectasis-mutated ataxia (ATM) are activated to cause p53 phosphorylation[167]. Cisplatin has been discovered to reduce taurine

transporter gene (TauT) expression in proximal tubular kidney cells by activating p53[162]. TauT's overexpression also has been shown to prevent transgenic TauT's cisplatin-related apoptosis and renal dysfunction. By attenuating the p53-dependent pathway, functional TauT can stop cisplatin-induced nephrotoxicity[168]. Activated p53 is present for cisplatin-induced AKI and cisplatin-induced AKI for p53 inhibition may decrease. The inhibition of p53, however, may also boost cancer cell survival and thereby reduce cisplatin therapeutic effectiveness[165].

Inhibition of caspase prevents the cultured cells from apoptosis caused by cisplatin. In vitro cisplatin-induced AKI, the function of caspase-3 and apoptosis is more complicated. In vivo, besides tubular apoptosis, cisplatin causes comprehensive acute tubular necrosis (ATN). The absence of a direct role of caspase- 3 mediated apoptosis as a cause of functioning disruptions of AKI has not been noted to protect against cisplatin-induced AKI[169].

Recently, cisplatin therapy in kidney proximal tubular cells has shown that caspase-3 is activated. However, no data is provided regarding the particular functions and the underlying signalling pathway processes responsible for regulating downstream caspase-3 and other upstream caspases that may be activated in renal tubular epithelial cells during cisplatin-induced injury. A research showed that cisplatin leads to selective and differential activation of caspase, not proinflammatory caspase-1, but including the executioner caspase-3 and the initiator caspase-8 and -9[170]. The selective activation of these caspases was significantly affected by their corresponding peptide inhibiting agents and suggests that these caspases play a significant role in a renal tubular epithelial cell injury caused by cisplatin [171].

Therefore, the amount of cell injury induced by the toxic agent depends on how well the toxic agent activates caspases and on the induction of signals of survival that block the caspase activation. The data presented in this chapter demonstrate that cisplatin treatment triggers caspase activation, but also causes increase of p53 mRNA levels in both human and rat PTCs. In addition, the co-treatment with cimetidine showed a reduction in mRNA levels of caspases and p53 in both species, suggesting the role of cimetidine for decreasing the nephrotoxicity of cisplatin.

7 Final discussion and Conclusion

The kidney is an essential organ which the body needs to perform many important functions, including homeostasis sustaining, extracellular environment control, such as detoxification, and toxic metabolism and drugs excretion [165, 172]. The kidney can therefore be treated as a major target site for exogenous toxicants. Drug transporters expressed in the PTCs are identified as one of the key factors in the organ's ability to perform its function successfully[173]. There are numerous renal drug transport models in vitro, but mostly do not express the width of transporters to establish good correlations with in vivo [174]. In recognition of this issue, regulatory authorities demanded that alternative in-vitro-cell-based testing be established to minimize or replace existing animal testing. Nephrotoxicity is estimated to be 8% of pre-clinical safety failures and 9% of safety failures in the drugs clinical trials [175]. The aim of my PhD project is the development of rat and human primary proximal tubule cell models as predictive *in-vitro* models of proximal tubule drug handling.

The results from chapter 3 showed, human and rat PTCs were successfully isolated and cultured. The mRNA and functional expressions of drug transporters, such as OCT2, Mrp2, Oat1 and mdr1a/b, found in the native tissue were retained in the cells. In addition, the expression of megalin and cubilin receptors were also detected in both human and rat PTCs. This is important as these transporters influence renal drug disposition [176], and their expression would enhance the utility of the human and rat PTC as an *in vitro* model of renal drug transport. Furthermore, in chapter 3 albumin uptake was measured in human and rat PTCs to show the functional expression of megalin and cubilin receptors by using albumin-FITC as a tracer substrate. In addition FITC-albumin was measured after polymyxin B incubated for the time as albumin. The data showed, polymyxin B is may enter the PTCs by megalin/cubilin endocytosis process. The amount of FITC- albumin is significantly less after polymyxin B treatment compared to control cells. This results were shown in both human and rat PTCs. This may be due to the competitive between albumin and polymyxin B to enter the PTCs by using megalin and cubilin receptors. The proximal tubular re absorption of gentamicin is linked to megalin, a study with megalin deficient mice[177]. Another study also showed that colistin (structural similar to polymyxin B) is a megalin ligand and that megalin plays a major role in the uptake of colistin [178]. Further characterisation of the human and rat PTCs model was also performed.

Results of the handling of creatinine by rat PTCs monolayer. The uptake was more in the basolateral membrane than apical membrane, and the same was human PTCs monolayer. This indicated the suitability of both species as models for renal creatinine transport. However, after adding dolutegravir (OCT2 inhibitor), creatinine was significant in rat PTCs but not in human PTCs.

Chapter 4 showed the results of exposure of human PTCs to nephrotoxins. There were two types of drugs used in this chapter. Large molecules include, gentamicin and polymyxin B and cisplatin as a small molecule. The purpose of using different sizes is to show the ability of our in vitro model to detect the nephrotoxicity of any drug. Furthermore, 3 biomarkers (KIM-1, NGAL and clusterin) were measured successfully after nephrotoxins treatment. Those biomarkers gives us an early prediction of nephrotoxicity. The results showed the time and concentrations dependant of the all 3 drugs used in this chapter. For example, after 100 µg/ml gentamicin for 24h the KIM-1 level was 7.7±1.7 ng/ml and after 48h incubation the level rose to 14.8±2.5 ng/ml. In addition, KIM-1 production after 300 µg/ml gentamicin for 72h was 63.6±15.4 ng/ml and after 500 µg/ml gentamicin treatment increased to 235.66±12.8 ng/ml. To show the reproducibility of the human PTCs model, two cell viability assay (MTS and ATP) were used to measure the percentage of live cells after nephrotoxins treatment. When comparing between the results, we can see how similar the data is. For example, MTS percentage after 25 µM cisplatin treatment for 48h was 61.1% and ATP was 58.1%. The similarity between the two assays indicate that we could use any cell viability assay to measure number of live cells after nephrotoxins treatment. In chapter4, results showed after the use of co-treatment (cilastatin, rosuvastatin and cimetidine) our in vitro model could be a good model for finding ways to reduce the nephrotoxicity of some drugs. The results showed the reduction of all 3 biomarkers production after the co-treatment compared to only nephrotoxins. This suggest the role of these co-treatment for protecting the human PTCs from damaging by drugs. However, even the actual mechanism of preventing the nephrotoxicity is not clear and more investigation is needed.

In chapter 5, rat PTCs were isolated and grown successfully. Gentamicin, polymyxin B and cisplatin used to treat our rat PTCs. After exposure to those nephrotoxins, measuring the expression of different nephrotoxicity biomarkers, such as KIM-1 and NGAL were done. All

nephrotoxins were treated in a range of concentrations to monitor the time and concentration of those drugs by using our in vitro model. An example, confluent monolayers of rat PTCs were treated with a range concentrations of polymyxin B (50 to 600 μg/ml). After 24h of treatment with 250 μg/ml polymyxin B the percentage of live cells was 72.5% and after 400 μg/ml polymyxin B exposure the percentage dropped to 48.1%. In addition, after 100 μg/ml polymyxin B treatment for 48 and 72 hours the cell viability were 71.2% and 60.8% respectively. In addition, the measurement of KIM-1 and NGAL were quantified after nephrotoxins were treated for 24, 48 and 72 hours with a range of concentrations. MTS and ATP were measured after nephrotoxins treatment and normalised to control cells. The results showed the similarity between the 2 assays. This determine the reproducibility of our rat PTCs by using any cell viability assay. In addition, LHD were measured after nephrotoxins incubation to quantify the damage PTCs. The data was consistent with cell viability data. This is a good indication of our in vitro model, the ability of grow the rat PTCs and treat the PTC monolayers with different nephrotoxins and measure the live cells and the damage cells as well. In rat PTCs, KIM-1 and NGAL were measured but not clusterin like human PTCs. This is due to the high cost of rat clusterin kit and it is hard to afford it.

The study of cisplatin nephrotoxicity mechanism has been studied in chapter 6. The cisplatin concentration decides if the cells die from necrosis and apoptosis [111]. High concentrations of cisplatin in cell culture experiments induce necrotic cell death while lower doses result in apoptosis[165]. Cisplatin triggered p53 in cultured renal tubular cells[161]. mRNA were isolated from human and rat PTCs and expression of p53 were done after cisplatin treatment. Our results showed the increase expression of p53 after cisplatin treatment compared to control cells. In addition, co-treatment with cimetidine showed a reduction in p53 expression, may suggesting the role of p53 in cisplatin apoptosis in both human and rat PTCs. Activation of caspases is considered a key phase in apoptosis mechanism. A research in renal cell lines undergoing cisplatin induced apoptosis has shown that the release of cytochromes from mitochondria activate the caspase 3 by caspase 9 [179]. Our data showed caspases 3, 8 and 9 mRNA levels were significantly high compared to control cells. P53 and caspases may have a role in cisplatin apoptosis in human and rat PTCs and further investigation is needed.

Rat and human PTC are not limited only to work on the transport of drugs and drugs interactions. Different studies have confirmed the suitability of rat and humans as in-vitro models of nephrotoxicity proximal tubular cell cultures [180, 181]. Nevertheless, the limited life cycle of human and rat PTCs is a drawback of their use in nephrotoxicity studies. In our project human and rat PTCs were grown successfully. Nephrotoxicity biomarkers were measured in both species. The biomarkers data is almost identical in both human and rat PTCs. However, this is does not mean both human and have the interaction to nephrotoxins drugs. In this study, only 3 drugs were used and only 3 biomarkers were measured. Further work on the use of human and rat PTCs in other areas of drug development is also needed.

There are some challenges in our in vitro model in order to quantify the production of nephrotoxicity biomarkers. The short time life of PTCs were grown does not give us enough time to test out nephrotoxins drugs for longer time. The levels of biomarkers were normalised to the amount percentage change of live cells in compared to control cells. This is was done to show the production of biomarkers is based on numbers of live cells. Cell viability data were measure to determine the compatible with biomarkers data. The level of biomarkers produced after nephrotoxins exposure is different based on the physiological condition of the kidney used and biomarkers are produce as an immune response to a harmful. So, there is a need to use an internal control in each kidney used to quantify the biomarkers levels. Equally important, reference values of biomarkers has to be identified for routine use in clinical practice, especially in the early stage of kidney damage.

Culture cells in a 3D setting are becoming more and more involved and have been found in rat and human PTC culture. This includes using the flow medium to replicate what happen in vivo, the motion of basolateral and apical fluid. This provides an interesting expansion of the model for more drug transporters and drug interaction studies. Research group designed human 3D PTCs. There data showed that, 3D PTCs tissues could have a positive impact on the pre-clinical drug discovery process and help prevent costly failures in late-stage clinical trials. Treatment of 3D proximal tubular tissue with cisplatin resulted in dose-dependent loss of live cells and epithelial cells, and cimetidine rescued these results, confirming the role of the OCT2 transporter in the nephrotoxicity caused by cisplatin. The tissue also displayed a fibrotic

response to TGFβ as determined by increased gene expression associated with human fibrosis and histological analysis of excess matrix deposition in extracellular cells [182].

Developing in vitro models to reliably predict the nephrotoxicity of potential pharmacological agents requires a solid understanding of the basic cellular targets and consequences of nephrotoxicants, as well as robust and reliable nephrotoxicity mechanistic biomarkers[183].

A golden in vitro model for nephrotoxicant evaluation has historically been represented by two-dimensional cultures of primary or conditionally immortalised renal epithelial cells.

Pharmaceutical researchers have for many years concentrated on pharmaceutical metabolism pathways research for new molecular entities (NMEs) as a framework for studying pharmacokinetic processes and causes of inter-individual variation in pharmacokinetics and pharmacodynamics. It has recently become apparent that transporters play a major role in pharmacokinetics and are, together with drug-metabolizing enzymes, the main determinants of both the degradation of hepatic and renal drugs[184]. In our PTCs model we are be able to detect drugs transporters and we did some functional experiments to those transporters. Our model may be useful for drugs companies to test for nephrotoxicity of drugs and their molecular cause of cell deaths to renal epithelial cells. Nephrotoxicants cause injuries by choosing specific cell types or, depending on the mechanism of their action, by intentionally injuring several cell types within the kidney[185].

Human and rat PTCs are validated as physiologically relevant proximal tubular models in the kidney and demonstrated as predictive methods for the handling of renal drugs. KIM-1, NGAL and clusterin were increased to response to nephrotoxins drugs treatment and they can used as a predictive biomarkers for nephrotoxicity. The implications of these findings should be explored further in a longer follow-up.

8 Reference

1. Mazer, M. and J. Perrone, *Acetaminophen-induced nephrotoxicity: Pathophysiology, clinical manifestations, and management.* Journal of Medical Toxicology, 2008. **4**(1): p. 2-6.
2. Homan, K.A., et al., *Bioprinting of 3D Convoluted Renal Proximal Tubules on Perfusable Chips.* Scientific Reports, 2016. **6**: p. 34845.
3. Dinesh, K.D., et al., *Drug-induced nephrotoxicity.* Int J Basic Clin Pharmacol, 2014. **3**(4): p. 591-597.
4. Bo Feng, J.L.L., George Chang & Manthena VS Varma, *Renal clearance in drug discovery and development: molecular descriptors, drug transporters and disease state.* Expert Opinion on Drug Metabolism & Toxicology, 2010. **6**(8): p. 939-952.
5. Tiong, H.Y., et al., *Drug-Induced Nephrotoxicity: Clinical Impact and Preclinical in Vitro Models.* Molecular Pharmaceutics, 2014. **11**(7): p. 1933-1948.
6. Choudhury, D. and Z. Ahmed, *Drug-associated renal dysfunction and injury.* Nat Clin Pract Neph, 2006. **2**(2): p. 80-91.
7. Chung, G.W., et al., *Chapter 4 Drug Transporters in the Kidney*, in *Drug Transporters: Volume 1: Role and Importance in ADME and Drug Development*. 2016, The Royal Society of Chemistry. p. 109-150.
8. Brown, C.D., et al., *Characterisation of human tubular cell monolayers as a model of proximal tubular xenobiotic handling.* Toxicol Appl Pharmacol, 2008. **233**(3): p. 428-38.
9. HF, G., *Can acute renal failure be prevented?* J R Coll Surg Edinb., 2000. **45**(1).
10. Finn, W.F. and G.A. Porter, *Urinary biomarkers and nephrotoxicity*, in *Clinical Nephrotoxins: Renal Injury from Drugs and Chemicals*, M.E. de Broe, et al., Editors. 2003, Springer Netherlands: Dordrecht. p. 621-655.
11. Nagai, J. and M. Takano, *Molecular-targeted approaches to reduce renal accumulation of nephrotoxic drugs.* Expert Opinion on Drug Metabolism & Toxicology, 2010. **6**(9): p. 1125-1138.
12. Kim, S.Y. and A. Moon, *Drug-Induced Nephrotoxicity and Its Biomarkers.* Biomolecules & Therapeutics, 2012. **20**(3): p. 268-272.
13. Brown, C.D.A., et al., *Characterisation of human tubular cell monolayers as a model of proximal tubular xenobiotic handling.* Toxicology and Applied Pharmacology, 2008. **233**(3): p. 428-438.
14. Otsuka, M., et al., *A human transporter protein that mediates the final excretion step for toxic organic cations.* Proceedings of the National Academy of Sciences of the United States of America, 2005. **102**(50): p. 17923-17928.
15. Omote, H., et al., *The MATE proteins as fundamental transporters of metabolic and xenobiotic organic cations.* Trends Pharmacol Sci, 2006. **27**(11): p. 587-93.
16. Masuda, S., et al., *Identification and Functional Characterization of a New Human Kidney–Specific H⁺/Organic Cation Antiporter, Kidney-Specific Multidrug and Toxin Extrusion 2.* Journal of the American Society of Nephrology, 2006. **17**(8): p. 2127-2135.
17. Terada, T., et al., *Molecular cloning, functional characterization and tissue distribution of rat H+/organic cation antiporter MATE1.* Pharm Res, 2006. **23**(8): p. 1696-701.
18. Ohta, K.Y., et al., *Molecular identification and functional characterization of rat multidrug and toxin extrusion type transporter 1 as an organic cation/H+ antiporter in the kidney.* Drug Metab Dispos, 2006. **34**(11): p. 1868-74.
19. Lickteig, A.J., et al., *Tissue distribution, ontogeny and induction of the transporters Multidrug and toxin extrusion (MATE) 1 and MATE2 mRNA expression levels in mice.* Life sciences, 2008. **83**(1-2): p. 59-64.

20. Masuda, S., et al., *Identification and functional characterization of a new human kidney-specific H+/organic cation antiporter, kidney-specific multidrug and toxin extrusion 2.* J Am Soc Nephrol, 2006. **17**(8): p. 2127-35.
21. Komatsu, T., et al., *Characterization of the human MATE2 proton-coupled polyspecific organic cation exporter.* The international journal of biochemistry & cell biology, 2011. **43**: p. 913-8.
22. Tanihara, Y., et al., *Substrate specificity of MATE1 and MATE2-K, human multidrug and toxin extrusions/H(+)-organic cation antiporters.* Biochem Pharmacol, 2007. **74**(2): p. 359-71.
23. Konig, J., et al., *Double-transfected MDCK cells expressing human OCT1/MATE1 or OCT2/MATE1: determinants of uptake and transcellular translocation of organic cations.* Br J Pharmacol, 2011. **163**(3): p. 546-55.
24. Ito, S., et al., *Competitive inhibition of the luminal efflux by multidrug and toxin extrusions, but not basolateral uptake by organic cation transporter 2, is the likely mechanism underlying the pharmacokinetic drug-drug interactions caused by cimetidine in the kidney.* J Pharmacol Exp Ther, 2012. **340**(2): p. 393-403.
25. Keppler, D., *Multidrug Resistance Proteins (MRPs, ABCCs): Importance for Pathophysiology and Drug Therapy*, in *Drug Transporters*, M.F. Fromm and R.B. Kim, Editors. 2011, Springer Berlin Heidelberg: Berlin, Heidelberg. p. 299-323.
26. Belinsky, M.G. and G.D. Kruh, *MOAT-E (ARA) is a full-length MRP/cMOAT subfamily transporter expressed in kidney and liver.* Br J Cancer, 1999. **80**(9): p. 1342-9.
27. Cole, S.P., et al., *Overexpression of a transporter gene in a multidrug-resistant human lung cancer cell line.* Science, 1992. **258**(5088): p. 1650-4.
28. Kool, M., et al., *Analysis of expression of cMOAT (MRP2), MRP3, MRP4, and MRP5, homologues of the multidrug resistance-associated protein gene (MRP1), in human cancer cell lines.* Cancer Res, 1997. **57**(16): p. 3537-47.
29. Gros, P., et al., *Isolation and expression of a complementary DNA that confers multidrug resistance.* Nature, 1986. **323**(6090): p. 728-31.
30. Ueda, K., et al., *The mdr1 gene, responsible for multidrug-resistance, codes for P-glycoprotein.* Biochem Biophys Res Commun, 1986. **141**(3): p. 956-62.
31. Chen, C.J., et al., *Internal duplication and homology with bacterial transport proteins in the mdr1 (P-glycoprotein) gene from multidrug-resistant human cells.* Cell, 1986. **47**(3): p. 381-9.
32. Croop, J.M., et al., *The three mouse multidrug resistance (mdr) genes are expressed in a tissue-specific manner in normal mouse tissues.* Mol Cell Biol, 1989. **9**(3): p. 1346-50.
33. Thiebaut, F., et al., *Cellular localization of the multidrug-resistance gene product P-glycoprotein in normal human tissues.* Proc Natl Acad Sci U S A, 1987. **84**(21): p. 7735-8.
34. Fujita, T., et al., *Transport of drugs in the kidney by the human organic cation transporter, OCT2 and its genetic variants*. Vol. 95. 2006. 25-36.
35. George, B., et al., *Xenobiotic transporters and kidney injury.* Advanced drug delivery reviews, 2017. **116**: p. 73-91.
36. Otani, N., et al., *Roles of organic anion transporters (OATs) in renal proximal tubules and their localization.* Anatomical Science International, 2017. **92**(2): p. 200-206.
37. Moller, J.V. and M.I. Sheikh, *Renal organic anion transport system: pharmacological, physiological, and biochemical aspects.* Pharmacol Rev, 1982. **34**(4): p. 315-58.
38. Wright, S.H. and W.H. Dantzler, *Molecular and cellular physiology of renal organic cation and anion transport.* Physiol Rev, 2004. **84**(3): p. 987-1049.
39. Nielsen, R., E.I. Christensen, and H. Birn, *Megalin and cubilin in proximal tubule protein reabsorption: from experimental models to human disease.* Kidney Int, 2016. **89**(1): p. 58-67.
40. Mahadevappa, R., et al., *Megalin in acute kidney injury: foe and friend.* Am J Physiol Renal Physiol, 2014. **306**(2): p. F147-54.

41. Cez, A., et al., *Decreased expression of megalin and cubilin and altered mitochondrial activity in tenofovir nephrotoxicity.* Human Pathology, 2018. **73**: p. 89-101.
42. Leheste, J., et al., *Megalin Knockout Mice as an Animal Model of Low Molecular Weight Proteinuria*. Vol. 155. 1999.
43. Shrestha, S., et al., *Circulating FABP4 is eliminated by the kidney via glomerular filtration followed by megalin-mediated reabsorption.* Scientific reports, 2018. **8**(1): p. 16451-16451.
44. Nagai, J., et al., *Megalin/Cubilin-mediated Uptake of FITC-labeled IgG by OK Kidney Epithelial Cells.* Drug Metabolism and Pharmacokinetics, 2011. **26**(5): p. 474-485.
45. Ferguson, M.A., V. Vaidya, and J.V. Bonventre, *Biomarkers of Nephrotoxic Acute Kidney Injury.* Toxicology, 2008. **245**(3): p. 182-193.
46. Perazella, M.A., *Drug-induced nephropathy: an update.* Expert Opin Drug Saf, 2005. **4**(4): p. 689-706.
47. Dantas, R.T., et al., *Evaluation of KIM-1 as an early biomarker of snakebite-induced AKI in mice.* Toxicon, 2018. **151**: p. 24-28.
48. Nogare, A.L., et al., *Kidney injury molecule-1 expression in human kidney transplants with interstitial fibrosis and tubular atrophy.* BMC nephrology, 2015. **16**: p. 19-19.
49. Moresco, R.N., et al., *Urinary kidney injury molecule-1 in renal disease.* Clinica Chimica Acta, 2018. **487**: p. 15-21.
50. George, B., M.S. Joy, and L.M. Aleksunes, *Urinary protein biomarkers of kidney injury in patients receiving cisplatin chemotherapy.* Experimental biology and medicine (Maywood, N.J.), 2018. **243**(3): p. 272-282.
51. Bonventre, J.V., *Kidney injury molecule-1: a translational journey.* Transactions of the American Clinical and Climatological Association, 2014. **125**: p. 293-299.
52. Sweetman, D.U., *Neonatal acute kidney injury – Severity and recovery prediction and the role of serum and urinary biomarkers.* Early Human Development, 2017. **105**: p. 57-61.
53. Phillips, J.A., et al., *Rat Urinary Osteopontin and Neutrophil Gelatinase-Associated Lipocalin Improve Certainty of Detecting Drug-Induced Kidney Injury.* Toxicological Sciences, 2016. **151**(2): p. 214-223.
54. Andreucci, M., et al., *The ischemic/nephrotoxic acute kidney injury and the use of renal biomarkers in clinical practice.* European Journal of Internal Medicine, 2017. **39**: p. 1-8.
55. Palm, C.A., et al., *Urinary Neutrophil Gelatinase-associated Lipocalin as a Marker for Identification of Acute Kidney Injury and Recovery in Dogs with Gentamicin-induced Nephrotoxicity.* Journal of veterinary internal medicine, 2016. **30**(1): p. 200-205.
56. Mishra, J., et al., *Identification of Neutrophil Gelatinase-Associated Lipocalin as a Novel Early Urinary Biomarker for Ischemic Renal Injury.* Journal of the American Society of Nephrology, 2003. **14**(10): p. 2534-2543.
57. Bolignano, D., et al., *Neutrophil gelatinase-associated lipocalin (NGAL) and progression of chronic kidney disease.* Clinical journal of the American Society of Nephrology : CJASN, 2009. **4**(2): p. 337-344.
58. Vaidya, V.S., M.A. Ferguson, and J.V. Bonventre, *Biomarkers of Acute Kidney Injury.* Annual review of pharmacology and toxicology, 2008. **48**: p. 463-493.
59. Silkensen, J.R., et al., *Temporal induction of clusterin in cisplatin nephrotoxicity.* Journal of the American Society of Nephrology, 1997. **8**(2): p. 302-5.
60. Ahmed, S.M. and F.E. Fouad, *Possible protective effect of platelet-rich plasma on a model of cisplatin-induced nephrotoxicity in rats: A light and transmission electron microscopic study.* J Cell Physiol, 2018.
61. Perše, M. and Ž. Večerić-Haler, *Cisplatin-Induced Rodent Model of Kidney Injury: Characteristics and Challenges.* BioMed research international, 2018. **2018**: p. 1462802-1462802.

62. Yu, X., et al., *Celastrol ameliorates cisplatin nephrotoxicity by inhibiting NF-κB and improving mitochondrial function.* EBioMedicine, 2018. **36**: p. 266-280.
63. Miller, R.P., et al., *Mechanisms of Cisplatin nephrotoxicity.* Toxins, 2010. **2**(11): p. 2490-2518.
64. Cao, X., et al., *Protective Smell of Hydrogen Sulfide and Polysulfide in Cisplatin-Induced Nephrotoxicity.* International journal of molecular sciences, 2019. **20**(2): p. 313.
65. Ishida, S., et al., *Ishida S, Lee J, Thiele DJ, Herskowitz IUptake of the anticancer drug cisplatin mediated by the copper transporter Ctr1 in yeast and mammals. Proc Natl Acad Sci USA 99: 14298-14302*. Vol. 99. 2002. 14298-302.
66. Navjotsingh, P., et al., *The copper transporter Ctr1 contributes to cisplatin uptake by renal tubular cells during cisplatin nephrotoxicity.* American Journal of Physiology-Renal Physiology, 2009. **296**(3): p. F505-F511.
67. Ludwig, T., et al., *Nephrotoxicity of platinum complexes is related to basolateral organic cation transport.* Kidney International, 2004. **66**(1): p. 196-202.
68. Filipski, K.K., et al., *Contribution of organic cation transporter 2 (OCT2) to cisplatin-induced nephrotoxicity.* Clin Pharmacol Ther, 2009. **86**(4): p. 396-402.
69. Vattimo, M.d.F.F., et al., *Polymyxin B Nephrotoxicity: From Organ to Cell Damage.* PloS one, 2016. **11**(8): p. e0161057-e0161057.
70. Zavascki, A.P. and R.L. Nation, *Nephrotoxicity of Polymyxins: Is There Any Difference between Colistimethate and Polymyxin B?* Antimicrobial Agents and Chemotherapy, 2017. **61**(3): p. e02319-16.
71. Manchandani, P., et al., *Role of Renal Drug Exposure in Polymyxin B-Induced Nephrotoxicity.* Antimicrobial agents and chemotherapy, 2017. **61**(4): p. e02391-16.
72. Dai, C., et al., *Colistin-Induced Nephrotoxicity in Mice Involves the Mitochondrial, Death Receptor, and Endoplasmic Reticulum Pathways.* Antimicrobial Agents and Chemotherapy, 2014. **58**(7): p. 4075-4085.
73. Hori, Y., et al., *Megalin Blockade with Cilastatin Suppresses Drug-Induced Nephrotoxicity.* Journal of the American Society of Nephrology : JASN, 2017. **28**(6): p. 1783-1791.
74. Udupa, V. and V. Prakash, *Gentamicin induced acute renal damage and its evaluation using urinary biomarkers in rats.* Toxicology reports, 2018. **6**: p. 91-99.
75. Randjelovic, P., et al., *Gentamicin nephrotoxicity in animals: Current knowledge and future perspectives.* EXCLI journal, 2017. **16**: p. 388-399.
76. Dursun, M., et al., *Protective effect of nebivolol on gentamicin-induced nephrotoxicity in rats.* Bratisl Lek Listy, 2018. **119**(11): p. 718-725.
77. Mohammed, M.A., B.E. Aboulhoda, and R.H. Mahmoud, *Vitamin D attenuates gentamicin-induced acute renal damage via prevention of oxidative stress and DNA damage.* Human & Experimental Toxicology, 2019. **38**(3): p. 321-335.
78. Burt, D., et al., *Application of emerging biomarkers of acute kidney injury in development of kidney-sparing polypeptide-based antibiotics.* Drug and Chemical Toxicology, 2014. **37**(2): p. 204-212.
79. Bjornsson, T.D., *Use of Serum Creatinine Concentrations to Determine Renal Function1.* Clinical Pharmacokinetics, 1979. **4**(3): p. 200-222.
80. Herrera, J. and B. Rodríguez-Iturbe, *Stimulation of tubular secretion of creatinine in health and in conditions associated with reduced nephron mass. Evidence for a tubular functional reserve.* Nephrology Dialysis Transplantation, 1998. **13**(3): p. 623-9.
81. Tomlanovich, S., et al., *Limitations of Creatinine in Quantifying the Severity of Cyclosporine-Induced Chronic Nephropathy.* American Journal of Kidney Diseases, 1986. **8**(5): p. 332-337.
82. Jenkinson, S.E., et al., *The limitations of renal epithelial cell line HK-2 as a model of drug transporter expression and function in the proximal tubule.* Pflügers Archiv - European Journal of Physiology, 2012. **464**(6): p. 601-611.

83. Kamiyama, M., et al., *The establishment of a primary culture system of proximal tubule segments using specific markers from normal mouse kidneys.* International journal of molecular sciences, 2012. **13**(4): p. 5098-5111.
84. Helbert, M.J., S. Dauwe, and M.E. De Broe, *Flow cytometric immunodissection of the human nephron in vivo and in vitro.* Exp Nephrol, 1999. **7**(5-6): p. 360-76.
85. Sakolish, C.M., et al., *Modeling Barrier Tissues In Vitro: Methods, Achievements, and Challenges.* EBioMedicine, 2016. **5**: p. 30-39.
86. Terryn, S., et al., *A primary culture of mouse proximal tubular cells, established on collagen-coated membranes.* Am J Physiol Renal Physiol, 2007. **293**(2): p. F476-85.
87. Bens, M. and A. Vandewalle, *Cell models for studying renal physiology.* Pflugers Arch, 2008. **457**(1): p. 1-15.
88. Glube, N., E. Closs, and P. Langguth, *OCTN2-Mediated Carnitine Uptake in a Newly Discovered Human Proximal Tubule Cell Line (Caki-1).* Molecular Pharmaceutics, 2007. **4**(1): p. 160-168.
89. Fauth, C., B. Rossier, and F. Roch-Ramel, *Transport of tetraethylammonium by a kidney epithelial cell line (LLC-PK1).* Am J Physiol, 1988. **254**(3 Pt 2): p. F351-7.
90. Lash, L.H., *Mitochondrial glutathione transport: physiological, pathological and toxicological implications.* Chem Biol Interact, 2006. **163**(1-2): p. 54-67.
91. Taub, M.L., I. Suk Yang, and Y. Wang, *Primary rabbit kidney proximal tubule cell cultures maintain differentiated functions when cultured in a hormonally defined serum-free medium.* In Vitro Cellular & Developmental Biology, 1989. **25**(9): p. 770-775.
92. Courjault-Gautier, F., et al., *Consecutive use of hormonally defined serum-free media to establish highly differentiated human renal proximal tubule cells in primary culture.* Journal of the American Society of Nephrology, 1995. **5**(11): p. 1949-1963.
93. Fulcher, M.L., et al., *Well-differentiated human airway epithelial cell cultures.* Methods Mol Med, 2005. **107**: p. 183-206.
94. Verhulst, A., P.C. D'Haese, and M.E. De Broe, *Inhibitors of HMG-CoA Reductase Reduce Receptor-mediated Endocytosis in Human Kidney Proximal Tubular Cells.* Journal of the American Society of Nephrology, 2004. **15**(9): p. 2249-2257.
95. Levey, A.S., R.D. Perrone, and N.E. Madias, *Serum creatinine and renal function.* Annu Rev Med, 1988. **39**: p. 465-90.
96. Kottgen, A., et al., *New loci associated with kidney function and chronic kidney disease.* Nat Genet, 2010. **42**(5): p. 376-84.
97. Koteff, J., et al., *A phase 1 study to evaluate the effect of dolutegravir on renal function via measurement of iohexol and para-aminohippurate clearance in healthy subjects.* Br J Clin Pharmacol, 2013. **75**(4): p. 990-6.
98. Ito, S., et al., *Relationship Between the Urinary Excretion Mechanisms of Drugs and Their Physicochemical Properties.* Journal of Pharmaceutical Sciences, 2013. **102**(9): p. 3294-3301.
99. Maeda, K., et al., *Inhibitory effects of p-aminohippurate and probenecid on the renal clearance of adefovir and benzylpenicillin as probe drugs for organic anion transporter (OAT) 1 and OAT3 in humans.* European Journal of Pharmaceutical Sciences, 2014. **59**: p. 94-103.
100. Burckhardt, G., *Drug transport by Organic Anion Transporters (OATs).* Pharmacology & Therapeutics, 2012. **136**(1): p. 106-130.
101. Shitara, Y., H. Sato, and Y. Sugiyama, *EVALUATION OF DRUG-DRUG INTERACTION IN THE HEPATOBILIARY AND RENAL TRANSPORT OF DRUGS.* Annual Review of Pharmacology and Toxicology, 2005. **45**(1): p. 689-723.
102. Ciarimboli, G., et al., *Proximal tubular secretion of creatinine by organic cation transporter OCT2 in cancer patients.* Clinical cancer research : an official journal of the American Association for Cancer Research, 2012. **18**(4): p. 1101-1108.

103. Weber, E.J., J. Himmelfarb, and E.J. Kelly, *Concise Review: Current and Emerging Biomarkers of Nephrotoxicity.* Current opinion in toxicology, 2017. **4**: p. 16-21.
104. Yin, J. and J. Wang, *Renal drug transporters and their significance in drug-drug interactions.* Acta pharmaceutica Sinica. B, 2016. **6**(5): p. 363-373.
105. Han, W.K., et al., *Kidney Injury Molecule-1 (KIM-1): A novel biomarker for human renal proximal tubule injury.* Kidney International, 2002. **62**(1): p. 237-244.
106. van Timmeren, M., et al., *Tubular kidney injury molecule-1 (KIM-1) in human renal disease.* The Journal of Pathology, 2007. **212**(2): p. 209-217.
107. Zappitelli, M., et al., *Urine neutrophil gelatinase-associated lipocalin is an early marker of acute kidney injury in critically ill children: a prospective cohort study.* Crit Care, 2007. **11**(4): p. R84.
108. Cruz, D.N., et al., *Plasma neutrophil gelatinase-associated lipocalin is an early biomarker for acute kidney injury in an adult ICU population.* Intensive Care Med, 2010. **36**(3): p. 444-51.
109. Ishii, A., Y. Sakai, and A. Nakamura, *Molecular pathological evaluation of clusterin in a rat model of unilateral ureteral obstruction as a possible biomarker of nephrotoxicity.* Toxicol Pathol, 2007. **35**(3): p. 376-82.
110. Pabla, N. and Z. Dong, *Cisplatin nephrotoxicity: Mechanisms and renoprotective strategies.* Kidney International, 2008. **73**(9): p. 994-1007.
111. Lieberthal, W., V. Triaca, and J. Levine, *Mechanisms of death induced by cisplatin in proximal tubular epithelial cells: apoptosis vs. necrosis.* Am J Physiol, 1996. **270**(4 Pt 2): p. F700-8.
112. Gao, H., et al., *Omeprazole protects against cisplatin-induced nephrotoxicity by alleviating oxidative stress, inflammation, and transporter-mediated cisplatin accumulation in rats and HK-2 cells.* Chemico-Biological Interactions, 2019. **297**: p. 130-140.
113. El Mouedden, M., et al., *Apoptosis in renal proximal tubules of rats treated with low doses of aminoglycosides.* Antimicrob Agents Chemother, 2000. **44**(3): p. 665-75.
114. Sassen, M.C., et al., *Dysregulation of renal sodium transporters in gentamicin-treated rats.* Kidney Int, 2006. **70**(6): p. 1026-37.
115. Sandoval, R.M. and B.A. Molitoris, *Gentamicin traffics retrograde through the secretory pathway and is released in the cytosol via the endoplasmic reticulum.* Am J Physiol Renal Physiol, 2004. **286**(4): p. F617-24.
116. Sikka, P.K. and K.E. McMartin, *Normal rat kidney proximal tubule cells in primary and multiple subcultures.* In Vitro Cellular & Developmental Biology - Animal, 1996. **32**(5): p. 285-291.
117. Vattimo Mde, F., et al., *Polymyxin B Nephrotoxicity: From Organ to Cell Damage.* PLoS One, 2016. **11**(8): p. e0161057.
118. Jin, Y., et al., *Urinary kidney injury molecule1 as an early diagnostic biomarker of obstructive acute kidney injury and development of a rapid detection method.* Mol Med Rep, 2017. **15**(3): p. 1229-1235.
119. Vinken, P., et al., *Tissue Kim-1 and Urinary Clusterin as Early Indicators of Cisplatin-Induced Acute Kidney Injury in Rats.* Toxicologic Pathology, 2012. **40**(7): p. 1049-1062.
120. Keirstead, N.D., et al., *Early prediction of polymyxin-induced nephrotoxicity with next-generation urinary kidney injury biomarkers.* Toxicol Sci, 2014. **137**(2): p. 278-91.
121. Luo, Q.H., et al., *Evaluation of KIM-1 and NGAL as Early Indicators for Assessment of Gentamycin-Induced Nephrotoxicity In Vivo and In Vitro.* Kidney and Blood Pressure Research, 2016. **41**(6): p. 911-918.
122. Hidaka, S., et al., *Urinary clusterin levels in the rat correlate with the severity of tubular damage and may help to differentiate between glomerular and tubular injuries.* Cell and Tissue Research, 2002. **310**(3): p. 289-296.

123. Mi, X.-J., et al., *The protective effects of maltol on cisplatin-induced nephrotoxicity through the AMPK-mediated PI3K/Akt and p53 signaling pathways.* Scientific reports, 2018. **8**(1): p. 15922-15922.
124. Peres, L.A.B. and A. Dantas da Cunha Júnior, *Acute nephrotoxicity of cisplatin: Molecular mechanisms.* Jornal Brasileiro de Nefrologia, 2013. **35**(4): p. 332-340.
125. Zhu, S., et al., *DNA damage response in cisplatin-induced nephrotoxicity.* Archives of toxicology., 2015. **89**(12): p. 2197-205.
126. Ciarimboli, G., et al., *Organic cation transporter 2 mediates cisplatin-induced oto- and nephrotoxicity and is a target for protective interventions.* The American journal of pathology, 2010. **176**(3): p. 1169-1180.
127. Katsuda, H., et al., *Protecting Cisplatin-Induced Nephrotoxicity with Cimetidine Does Not Affect Antitumor Activity.* Biological and Pharmaceutical Bulletin, 2010. **33**(11): p. 1867-1871.
128. Verdoodt, A., et al., *Do Statins Induce or Protect from Acute Kidney Injury and Chronic Kidney Disease: An Update Review in 2018.* Journal of translational internal medicine, 2018. **6**(1): p. 21-25.
129. Velkov, T., et al., *Pharmacology of polymyxins: new insights into an 'old' class of antibiotics.* Future Microbiol, 2013. **8**(6): p. 711-24.
130. Ball, T. and P.A. McCullough, *Statins for the prevention of contrast-induced acute kidney injury.* Nephron. Clinical practice., 2014. **127**: p. 165-71.
131. Kumar, N. and M.A. Perazella, *Differentiating HIV-associated Nephropathy from Antiretroviral drug-induced Nephropathy: A clinical challenge.* Current HIV/AIDS Reports, 2014. **11**(3): p. 202-211.
132. Longenecker, C.T., et al., *Rosuvastatin preserves renal function and lowers cystatin C in HIV-infected subjects on antiretroviral therapy: The SATURN-HIV trial.* Clinical infectious diseases : an official publication of the Infectious Diseases Society of America., 2014. **59**(8): p. 1148-56.
133. Qiao, B., et al., *Rosuvastatin attenuated contrast-induced nephropathy in diabetes patients with renal dysfunction.* International journal of clinical and experimental medicine., 2015. **8**(2): p. 2342-9.
134. Mishra, J., et al., *Neutrophil gelatinase-associated lipocalin: a novel early urinary biomarker for cisplatin nephrotoxicity.* Am J Nephrol, 2004. **24**(3): p. 307-15.
135. Nakanishi, T., et al., *Functional Characterization of Apical Transporters Expressed in Rat Proximal Tubular Cells (PTCs) in Primary Culture.* Molecular Pharmaceutics, 2011. **8**(6): p. 2142-2150.
136. Prozialeck, W.C., et al., *Expression of kidney injury molecule-1 (Kim-1) in relation to necrosis and apoptosis during the early stages of Cd-induced proximal tubule injury.* Toxicology and applied pharmacology, 2009. **238**(3): p. 306-314.
137. Ichimura, T., et al., *Kidney injury molecule-1: a tissue and urinary biomarker for nephrotoxicant-induced renal injury.* Am J Physiol Renal Physiol, 2004. **286**(3): p. F552-63.
138. Supavekin, S., et al., *Differential gene expression following early renal ischemia/reperfusion.* Kidney Int, 2003. **63**(5): p. 1714-24.
139. Mori, K., et al., *Endocytic delivery of lipocalin-siderophore-iron complex rescues the kidney from ischemia-reperfusion injury.* J Clin Invest, 2005. **115**(3): p. 610-21.
140. Quiros, Y., et al., *An Integrative Overview on the Mechanisms Underlying the Renal Tubular Cytotoxicity of Gentamicin.* Toxicological Sciences, 2010. **119**(2): p. 245-256.
141. Jones, A.T. and M. Wessling-Resnick, *Inhibition of in vitro endosomal vesicle fusion activity by aminoglycoside antibiotics.* J Biol Chem, 1998. **273**(39): p. 25301-9.
142. Ciarimboli, G., *Membrane transporters as mediators of Cisplatin effects and side effects.* Scientifica, 2012. **2012**: p. 473829-473829.

143. Harrach, S. and G. Ciarimboli, *Role of transporters in the distribution of platinum-based drugs.* Frontiers in pharmacology, 2015. **6**: p. 85-85.
144. Shen, D.-W., et al., *Cisplatin resistance: a cellular self-defense mechanism resulting from multiple epigenetic and genetic changes.* Pharmacological reviews, 2012. **64**(3): p. 706-721.
145. Qiu, X., et al., *An in vitro method for nephrotoxicity evaluation using HK-2 human kidney epithelial cells combined with biomarkers of nephrotoxicity.* Toxicology Research, 2018. **7**(6): p. 1205-1213.
146. Lee, D.W., S. Faubel, and C.L. Edelstein, *A pan caspase inhibitor decreases caspase-1, IL-1α and IL-1β, and protects against necrosis of cisplatin-treated freshly isolated proximal tubules.* Renal Failure, 2015. **37**(1): p. 144-150.
147. Sasaki, D., et al., *Comparison of the course of biomarker changes and kidney injury in a rat model of drug-induced acute kidney injury.* Biomarkers, 2011. **16**(7): p. 553-66.
148. Babic, J.T., et al., *Evaluation of Urinary KIM-1 for Prediction of Polymyxin B-Induced Nephrotoxicity.* Antimicrob Agents Chemother, 2017. **61**(11).
149. Mingeot-Leclercq, M.P. and P.M. Tulkens, *Aminoglycosides: nephrotoxicity.* Antimicrobial agents and chemotherapy, 1999. **43**(5): p. 1003-1012.
150. Mathews, A. and G.R. Bailie, *CLINICAL PHARMACOKINETICS, TOXICITY AND COST EFFECTIVENESS ANALYSIS OF AMINOGLYCOSIDES AND AMINOGLYCOSIDE DOSING SERVICES.* Journal of Clinical Pharmacy and Therapeutics, 1987. **12**(5): p. 273-291.
151. Moestrup, S.K., et al., *Evidence that epithelial glycoprotein 330/megalin mediates uptake of polybasic drugs.* Journal of Clinical Investigation, 1995. **96**(3): p. 1404-1413.
152. Antoine, D.J., et al., *Statins inhibit aminoglycoside accumulation and cytotoxicity to renal proximal tubule cells.* Biochem Pharmacol, 2010. **79**(4): p. 647-54.
153. Ishida, S., et al., *Uptake of the anticancer drug cisplatin mediated by the copper transporter Ctr1 in yeast and mammals.* Proceedings of the National Academy of Sciences, 2002. **99**(22): p. 14298-14302.
154. Katsuda, H., et al., *Protecting cisplatin-induced nephrotoxicity with cimetidine does not affect antitumor activity.* Biol Pharm Bull, 2010. **33**(11): p. 1867-71.
155. Kolb, R.J., A.M. Ghazi, and D.W. Barfuss, *Inhibition of basolateral transport and cellular accumulation of cDDP and N-acetyl- L-cysteine-cDDP by TEA and PAH in the renal proximal tubule.* Cancer Chemother Pharmacol, 2003. **51**(2): p. 132-8.
156. Lee, R.H., et al., *Cisplatin-induced apoptosis by translocation of endogenous Bax in mouse collecting duct cells.* Biochem Pharmacol, 2001. **62**(8): p. 1013-23.
157. McIlwain, D.R., T. Berger, and T.W. Mak, *Caspase functions in cell death and disease.* Cold Spring Harb Perspect Biol, 2015. **7**(4).
158. Dive, C. and J.A. Hickman, *Drug-target interactions: only the first step in the commitment to a programmed cell death?* British Journal of Cancer, 1991. **64**(1): p. 192-196.
159. Cepeda, V., et al., *Biochemical mechanisms of cisplatin cytotoxicity.* Anticancer Agents Med Chem, 2007. **7**(1): p. 3-18.
160. Oren, M., *Decision making by p53: life, death and cancer.* Cell Death Differ, 2003. **10**(4): p. 431-42.
161. Cummings, B.S. and R.G. Schnellmann, *Cisplatin-Induced Renal Cell Apoptosis: Caspase 3-Dependent and -Independent Pathways.* Journal of Pharmacology and Experimental Therapeutics, 2002. **302**(1): p. 8-17.
162. Jiang, M., et al., *Regulation of PUMA-α by p53 in cisplatin-induced renal cell apoptosis.* Oncogene, 2006. **25**(29): p. 4056-4066.
163. Salvesen, G.S. and V.M. Dixit, *Caspases: intracellular signaling by proteolysis.* Cell, 1997. **91**(4): p. 443-6.

164. Florea, A.-M. and D. Büsselberg, *Cisplatin as an anti-tumor drug: cellular mechanisms of activity, drug resistance and induced side effects.* Cancers, 2011. **3**(1): p. 1351-1371.
165. Ozkok, A. and C.L. Edelstein, *Pathophysiology of Cisplatin-Induced Acute Kidney Injury.* BioMed Research International, 2014. **2014**: p. 17.
166. Hsu, Y.H., et al., *Prostacyclin protects renal tubular cells from gentamicin-induced apoptosis via a PPARα-dependent pathway.* Kidney International, 2008. **73**(5): p. 578-587.
167. Wei, Q., et al., *Activation and involvement of p53 in cisplatin-induced nephrotoxicity.* American Journal of Physiology-Renal Physiology, 2007. **293**(4): p. F1282-F1291.
168. Han, X., J. Yue, and R.W. Chesney, *Functional TauT Protects Against Acute Kidney Injury.* Journal of the American Society of Nephrology, 2009. **20**(6): p. 1323-1332.
169. Herzog, C., et al., *zVAD-fmk prevents cisplatin-induced cleavage of autophagy proteins but impairs autophagic flux and worsens renal function.* American Journal of Physiology-Renal Physiology, 2012. **303**(8): p. F1239-F1250.
170. Kaushal, G.P., et al., *Role and regulation of activation of caspases in cisplatin-induced injury to renal tubular epithelial cells.* Kidney International, 2001. **60**(5): p. 1726-1736.
171. Zhou, Q., et al., *Interaction of the Baculovirus Anti-apoptotic Protein p35 with Caspases. Specificity, Kinetics, and Characterization of the Caspase/p35 Complex.* Biochemistry, 1998. **37**(30): p. 10757-10765.
172. Ferguson, M.A., V.S. Vaidya, and J.V. Bonventre, *Biomarkers of nephrotoxic acute kidney injury.* Toxicology, 2008. **245**(3): p. 182-93.
173. Fagerholm, U., *Prediction of human pharmacokinetics — renal metabolic and excretion clearance.* Journal of Pharmacy and Pharmacology, 2007. **59**(11): p. 1463-1471.
174. Jenkinson, S.E., et al., *The limitations of renal epithelial cell line HK-2 as a model of drug transporter expression and function in the proximal tubule.* Pflugers Arch, 2012. **464**(6): p. 601-11.
175. Cook, D., et al., *Lessons learned from the fate of AstraZeneca's drug pipeline: a five-dimensional framework.* Nat Rev Drug Discov, 2014. **13**(6): p. 419-31.
176. Giacomini, K.M., et al., *Membrane transporters in drug development.* Nat Rev Drug Discov, 2010. **9**(3): p. 215-36.
177. Schmitz, C., et al., *Megalin deficiency offers protection from renal aminoglycoside accumulation.* J Biol Chem, 2002. **277**(1): p. 618-22.
178. Suzuki, T., et al., *Megalin contributes to kidney accumulation and nephrotoxicity of colistin.* Antimicrob Agents Chemother, 2013. **57**(12): p. 6319-24.
179. Zhan, Y., et al., *The roles of caspase-3 and bcl-2 in chemically-induced apoptosis but not necrosis of renal epithelial cells.* Oncogene, 1999. **18**(47): p. 6505-6512.
180. Lash, L.H., S.E. Hueni, and D.A. Putt, *Apoptosis, necrosis, and cell proliferation induced by S-(1,2-dichlorovinyl)-L-cysteine in primary cultures of human proximal tubular cells.* Toxicol Appl Pharmacol, 2001. **177**(1): p. 1-16.
181. Cummings, B.S., J.M. Lasker, and L.H. Lash, *Expression of glutathione-dependent enzymes and cytochrome P450s in freshly isolated and primary cultures of proximal tubular cells from human kidney.* J Pharmacol Exp Ther, 2000. **293**(2): p. 677-85.
182. King, S.M., et al., *3D Proximal Tubule Tissues Recapitulate Key Aspects of Renal Physiology to Enable Nephrotoxicity Testing.* Frontiers in Physiology, 2017. **8**(123).
183. Soo, J.Y.C., et al., *Advances in predictive in vitro models of drug-induced nephrotoxicity.* Nature reviews. Nephrology, 2018. **14**(6): p. 378-393.
184. Morrissey, K.M., et al., *Renal Transporters in Drug Development.* Annual Review of Pharmacology and Toxicology, 2013. **53**(1): p. 503-529.
185. Edwards, I.R. and J.K. Aronson, *Adverse drug reactions: definitions, diagnosis, and management.* The Lancet, 2000. **356**(9237): p. 1255-1259.